QUANTIFYING THE PATTERNS OF FUNCTIONAL CONNECTIVITY WITHIN

THE BRAIN DURING IMAGINED AND OVERT MOVEMENT OF A FUNCTIONAL

TASK IN NON-DISABLED SYSTEMS

Alicia Gionfriddo

Submitted in partial fulfillment of the requirements

for the degree of Master of Science

at

Dalhousie University

Halifax, Nova Scotia

August 2014

TABLE OF CONTENTS

LIST OF TABLES

LIST OF FIGURES

ABSTRACT

This project was aimed at quantifying functional connectivity within the brain during motor imagery (MI) and the actual performance of a motor task, and comparing these networks using graph theory. Fifteen participants took part. Following three days of familiarization, brain activity was recorded using high-density electroencephalography during MI and actual performance of the motor task. After localizing source-level brain activity, functional connectivity and graph theory analyses were performed. Graph theory metrics included determining the number and density of connections in the network, as well as assessing network efficiency via small worldness. Findings of this study show that the network active during MI involved connectivity within prefrontal, premotor, and primary sensorimotor regions. During performance of the motor task, the network was characterized by sensorimotor and cerebellar connectivity. Both the MI and motor networks were efficient, exhibiting small world properties. This research contributes to our knowledge related to brain activity underlying movement.

LIST OF ABBREVIATIONS USED

ADL	Activities of Daily Living
ADHD	Attention Deficit/Hyperactivity Disorder
BOLD	Blood Oxygen Level-Dependent
BSR	Bootstrap Ratio
BEM	Boundary Element Modeling
CCo	Clustering Coefficient
CIMT	Constraint Induced Movement Therapy
CCC	Cortico-Cortical Coherence
CDR	Current Density Reconstruction
DL	Dorsolateral
DCM	Dynamic Causal Modeling
EEG	Electroencephalography
EMG	Electromyography
EOG	Electro-Occulogram
ERP	Event Related Potential
FFT	Fast Fourier Transform
FEF	Frontal Eye Fields
FC	Functional Connectivity
fMRI	Functional Magnetic Resonance Imaging
FFA	Fusiform Face Area
IPAQ	International Physical Activity Questionnaire
KVIQ	Kinesthetic Visual Imagery Questionnaire

MEG	Magnetoencephalography
MET	Metabolic Equivalent of Task
MI	Motor Imagery
M1	Motor Cortex (Primary)
MEP	Motor-Evoked Potentials
ND	Node Degree
PHG	Parahippocampal Gyrus
PC	Parietal Cortex
PLS	Partial Least Square
PL	Path Length
PFC	Prefrontal Cortex
PMC	Premotor Cortex
PCA	Principal Component Analysis
RTP	Repetitive Task Practice
S1	Sensory Cortex (Primary)
S2	Sensory Cortex (Secondary)
SWN	Small World Network
sLORETA	Standardized Low Resolution Brain Electromagnetic Tomography
SMA	Supplementary Motor Area
TC	Temporal Cortex
TMS	Transcranial Magnetic Stimulation
UL	Upper Limb
VL	Ventrolateral

V1   Visual Cortex (Primary)

Acknowledgements

I would like to take this time to first, and foremost, thank my supervisor Dr. Shaun Boe for his continued guidance during my masters studies. This work would not have been possible without his advice and in particular, without his patience and attentiveness for any (and all) questions I posed to him over the past two years. I cannot stress how grateful I am for Dr. Boe's role in positively shaping my graduate experience. In addition, I would like to thank my committee members, Dr. Tim Bardouille and Dr. Lori Dithurbide, for guiding me through the process of forming this project's procedures and performing the final analysis. I would also like to acknowledge the members of the Laboratory for Brain Recovery and Function, who I could always depend on for moral support, and a few laughs, throughout my graduate experience. A final thank you is extended to my friends and family, without whom I surely would not have made it this far.

CHAPTER 1 INTRODUCTION

Movement execution is controlled by the integration of information amongst various brain regions, which in-turn comprises a neural network. Neural networks are characterized by functional connectivity, which is defined as temporal relationships in activation between various neural substrates (Grefkes & Fink, 2011). To date, neuroimaging studies examining the neural substrates underlying movement execution have largely focused on uncovering spatial activation changes within the brain in non-disabled controls and after neurological insult. Locating brain areas involved in movement, and measuring their activity, does not provide enough information concerning the production of movement; yet, understanding how a specific brain region interacts with surrounding brain areas (i.e., those in the same neural network) will provide researchers with more insight as to how the brain produces movement. A systematic analysis of neuronal network patterns within the motor system is necessary to enhance our fundamental understanding of how spatially distributed brain areas are linked, and how these links are involved in motor processing. Thus, the objective of the research was to quantify patterns of functional connectivity within the brain, using imagined movement as a model to facilitate exploration of the underlying motor network in non-disabled individuals.

To address the research objective, high-density electroencephalography (EEG) was used to capture the electrical activity of the brain during real and imagined performance of a reach and grasp movement. The use of high-density EEG coupled with advanced source localization techniques to identify active brain regions permit functional connectivity analyses to be performed. Functional connectivity analyses allowed for

network maps to be derived that illustrate the reliability of information flow between nodes in the motor network (K. J. Friston, Harrison, & Penny, 2003). As research has yet to uncover the specific patterns of connectivity that are active within intact networks during imagined movement, non-disabled participants were recruited for investigation. In addition, the task paradigm used in this research had individuals make a real sandwich, followed by subsequent imagined sandwich making. The purpose of having individuals make a real sandwich was to enhance motor imagery (MI) vividness and to improve the applicability of study results to real-world scenarios. Quantification of network properties was achieved via the application of graph theory (Bullmore & Sporns, 2009). Specifically, network nodes were analyzed by comparing the density and strength of their connections to quantify which region is more heavily involved during MI in intact systems. It was hypothesized that nodes in the pre-motor and parietal cortices in intact networks would act as network 'hubs' (i.e., have a greater number of connections) during both overt and imagined (albeit at a lesser intensity) movement.

This study uncovered connectivity within premotor, parietal, and prefrontal regions for the performance of MI. In addition, the results uncovered that during a functional motor task, the connectivity network relies on primarily sensorimotor and cerebellar regions of the brain. A final finding of the current work was that there are distinct similarities (i.e., fronto-parietal, prefrontal regions) and differences (primary and premotor cortices) in the connectivity that governs these two tasks. In addition, this study uncovered the fact that both the performance of imagined and overt movements result in task-related networks that are characterized by small world parameters in non-disabled participants. The given research contributes to advancing our knowledge related to the

fundamental processes that produce and control movement. Importantly, the findings provide insight into the neural correlates of imagined movement by characterizing, in a quantifiable manner, the spatial and temporal aspects of network activation underlying movement.

CHAPTER 2 BACKGROUND AND RATIONALE

2.1 Recording and Analysis of Brain Activity

Advances in neuroimaging hardware and analysis techniques have permitted the investigation of brain networks; that is, multiple brain regions, or nodes, which demonstrate coherent patterns of activation both spatially and temporally (K. J. Friston et al., 2003; Grefkes & Fink, 2011; Roebroeck, Formisano, & Goebel, 2005). To date however, much of our understanding about how the brain controls movement, and how this is altered following injury, is based on neuroimaging studies examining *spatial* patterns of brain activation. These studies have greatly improved our understanding of the neural substrates underlying movement; however, they do not provide information about how brain regions *interact* to produce movement, and more importantly, how brain damage alters the pattern of interaction that produces movement. Currently, we lack an essential understanding of how neural networks control movement in the central nervous system.

Grefkes and Fink (2011) define the brain as a system of neuronal populations that interact in a spatial and temporal manner to achieve a task. Novel neuroimaging methodologies allow researchers to examine both spatial and temporal domains of brain activity. Examples of such methodologies include functional magnetic resonance imaging (fMRI), EEG, magnetoencephalography (MEG), and positron emission tomography (PET), each of which has advantages and disadvantages with regard to measuring brain activity.

The use of fMRI allows researchers to measure brain activity at rest or during a functional task via the blood oxygen level-dependent (BOLD) signal (for review see

(Ogawa, 1998); that is, fMRI is an indirect measure of brain activity. Neuroimaging

studies using fMRI infer that a region of the brain is active during a task based on

increased blood flow to the area. As a data collection agent, fMRI provides information

that is rich spatially (i.e., resulting in regions of the brain being elucidated on the order of

millimetres); however, the data has poor temporal resolution as the frequency with which

data are obtained is on the order of seconds. Unlike fMRI, EEG is a more direct measure

of brain activity. EEG involves the measurement of electrical potentials at the scalp

resulting from the synchronous activity of neurons underlying the EEG electrodes.

Analysis of EEG data is typically done using one of three approaches, including: [1]

examining voltage fluctuations over time (i.e., a change in the magnitude of the electrical

signal in relation to some cue or stimulus onset) that can be averaged to form event

related potentials (ERPs); [2] frequency-based analysis (i.e., oscillations occurring in

specific frequency bands, such as alpha, 8-13 Hz, or beta, 15-30 Hz); and [3] time-

frequency analysis (i.e., changes in frequency over time). Further analysis of the EEG

data can include examining coherence among brain regions; that is, temporally linked

firing of neurons in remote anatomical regions within the same frequency band implies

communication between these areas. This type of analysis is known as cortico-cortical

coherence (CCC) (Knyazeva, 2001). While advantages of using EEG include high

temporal resolution of the data obtained (on the order of milliseconds), the major

disadvantage is its poor spatial resolution due to the nature of measuring an electric

potential that has moved through the surrounding brain tissue, cerebrospinal fluid,

meninges and scalp to reach the electrode. This movement, termed volume conduction,

results in a smearing of the signal measured at the sensor (electrode) level (Nunez, 1997).

In addition, the data obtained via EEG can only allow for inferences regarding the source (or sources) generating the neural activity to be made; however, the accuracy of these inferences can be improved when advanced source localization techniques are employed. Even when advanced source localization techniques are applied, results need to be interpreted in the context of several limitations associated with solving the inverse problem. The inverse problem is an attempt to determine source generators within some 3D model (i.e., the brain) based on information collected at the level of the scalp. In an attempt to overcome this problem, novel mathematical approaches have been developed for the purposes of performing source reconstruction. To perform source localization, and in-turn the measurement of activity at particular regions in the brain, an individual's anatomical MRI can be co-registered with the functional EEG data based on the digital representations of the individual's scalp position and certain anatomical landmarks in space (A. Gevins, Smith, M.E., McEvoy, L., & Yu, D. , 1997). In cases where an anatomical MRI is not available, co-registration can be done with a template brain. This co-registration allows researchers a method of visualizing the source of the obtained EEG data. A more detailed description of limitations associated with source-localization using EEG are included in section 7.22.

The use of MEG allows researchers to obtain measures of neuronal activity via the magnetic fields generated from the synchronous activity of neurons within the brain. In particular, the movement of current (i.e., neuronal population activation) results in a net electric dipole, which, according to the right-hand rule, will produce a magnetic field that flows around the vector of the given dipole (Cohen, 2003). Similar to EEG, MEG data are obtained via an array of sensors overlying the surface of the scalp with high

6

temporal resolution (on the order of milliseconds). While MEG typically allows for data

collection from a larger number of sensors than EEG, researchers are still tasked with

making inferences regarding the source of the brain activity based on information

obtained at the sensor level. Source localization techniques (similar to those used with

EEG) can be applied to MEG data in an attempt to identify generators of neural activity.

Unlike EEG however, the magnetic fields recorded via MEG are not subject to spatial

smearing and thus spatial resolution tends to be higher in MEG source reconstruction

(Cohen & Cuffin, 1983). The need to constrain head movement and thus limit the amount

of movement during a MEG scan decreases its applicability for studies involving

movement. A final methodology to consider is PET, which uses nuclear tracers in order

to track metabolic processes in the body (Muehllehner & Karp, 2006). While advantages

of PET as an exploratory model include the ability to assess brain activity at the

biochemical level, obvious disadvantages include the potential harm to the individual,

and the short lived nature of the nuclear tracers, associated with the radioactive

component of PET.

2.2 Spatial Patterns of Brain Activity

Currently, much of the information available regarding the underlying

neurophysiology of motor control is from neuroimaging studies that have examined the

brain on a region-by-region basis (Ciccarelli et al., 2005; Colebatch, 1991). For instance,

Ciccarelli et al. (2005) compared regions of the sensorimotor network active during

passive and active dorsiflexion of the ankle in non-disabled individuals using fMRI. The

study findings outline that in both passive and active conditions, the brain regions active

included the primary motor cortex (M1), the primary sensory cortex (S1), and the

premotor cortex (PMC), albeit at higher intensities during active movement (Ciccarelli et al., 2005). Specifically, studies investigating spatial brain activation patterns outline that during an intended movement, areas such as M1, S1, and PMC are active in the brain, with little or no documentation of how these areas might be interacting. For example, Luft et al. (2002) documented that fMRI data obtained from non-disabled individuals uncovered a significantly greater amount of activation occurring in the supplementary motor area (SMA) during knee flexion and extension movements, as compared with elbow flexion and extension movements. Although this information is important, it does not provide researchers the necessary knowledge to further our understanding of how the brain plans and produces overt movement. The reason for this being that successful movement execution is the result of interactions across a combination of brain regions that are working together, which implies that the underlying neural correlates of movement should be investigated as an integrated unit (or network). Ideally, neuroimaging studies should apply connectivity-based approaches to data related to the spatial activation patterns underlying movement to further elucidate how these areas are working together to control motor function. This approach to examining network connectivity patterns in the brain will enhance our understanding of their spatiotemporal distribution, as well as how the links between nodes in the network are involved in the production and control of movement.

2.3 A Network Analysis Approach to Understanding Brain Activity

A network approach to examining brain function will provide greater insight into a fundamental area of human behaviour: how the brain produces and controls movement. Sporns, Tononi, and Kotter (2005) outline the three levels of network analysis used to

quantify brain activity: [1] Microscale (i.e., at the level of neurons and synapses), [2] Mesoscale (i.e., at the level of neuronal populations), and [3] Macroscale (i.e., at the level of specific anatomical nodes and their interacting pathways). The data obtained from non-invasive neuroimaging techniques (see above Section *2.1*) is most commonly quantified at the macroscale level during network approaches to understanding the brain. Approaches to analyzing functional connectivity in the brain can be further broken into functional specialization (or effective connectivity) and functional integration (or functional connectivity) methods.

Functional specialization (effective connectivity) allows researchers to elucidate brain areas that can be linked to a specific motor or sensory processing function (Grefkes & Fink, 2011). For example, functional specialization has been used in non-disabled adults in order to localize the specific areas of the visual cortex involved in the perception of colour, which was cued by assessing brain activity (via PET) while viewing a multicoloured abstract display in comparison to a standard grey scale display; the findings of this study outline that the perception of colour is associated with activation in the prestriate gyrus (Zeki, 1991). Additionally, links between specific brain regions can be examined via effective connectivity, which allows researchers to assess how much control one neural system exerts over another (K. J. Friston, Worsley, K.J., Frackowiak, R.S.J,, Mazziotta, J.C., & Evans, A.c., 1994). Effective connectivity analysis allows researchers to discern causality among brain region interactions (Grefkes & Fink, 2011). Several paradigms have been proposed for effective connectivity approaches to brain network analysis. In brief, common approaches include granger causality modeling (Gao, Duan, & Chen, 2011), structural equation modeling (Boucard, Marchand, & Nogues,

2007), and dynamic causal modeling (DCM) (Kiebel, Garrido, & Friston, 2007).

Roebroeck et al. (2005) used granger causality modeling in order to explore effective

connectivity influences among neuronal populations via fMRI in non-disabled adults

performing a dynamic visuomotor tracking and finger tapping response task. Specifically,

this method relies on the granger causality postulation (i.e., determining if one time series

can be used to predict another) in order to predict the influence of one brain node on

another. In the Roebroeck study, results showed that the lateral premotor area, as well as

the pre- and medial- supplementary motor area (SMA), had a strong influence on the

fusiform face area (FFA); additionally, the FFA had an influence over the bilateral infero-

temporal cortex, and parts of the bilateral posterior parietal cortex during the visuomotor

task. In comparison to granger causality methods, structural equation modeling requires

the formation of a statistical model to be tested once the neuroimaging data has been

obtained. Structural equation modeling outlines that the connection strength between two

nodes "indicates how the variance of area "X" depends on the variance of area "Y", if all

other influences on area "X" are held constant" (Penny, Stephan, Mechelli, & Friston,

2004). Finally, DCM is characterized by measuring changes in brain activity (assessed

via fMRI, for example) that are driven by some external cue resulting in changes in

patterns of activation amongst the neuronal populations of interest (K. J. Friston et al.,

2003). For instance, Kalberlah and colleagues (2013) applied an effective connectivity

analysis to fMRI data obtained while non-disabled young adults were asked to

discriminate between two vibro-tactile stimuli (i.e., low vs. high frequency) applied at

two different sites on the same finger. The researchers found that there were two

contralateral S1 nodes for location (i.e., cortical representation of the fingers), as well as

one secondary somatosensory cortex (S2) node for amplitude (i.e., only active at higher frequencies); further, analysis using DCM indicated that the vibro-tactile information was processed in series (i.e., passed directly from S1 to S2) with higher frequency stimulations (Kalberlah, Villringer, & Pleger, 2013).

In comparison to effective connectivity, it has been suggested that a functional integration (or connectivity) perspective is necessary to conceptualize the functional specialization of brain regions active in order to achieve some outcome (e.g., movement); that is, functional integration considers the reliance of specific brain areas on one another in relation to the integration of sensory, motor and cognitive information for successful movement execution (K. J. Friston, 2002). Further, a functional integration method assumes that areas within the brain are part of the same neural network if neuronal activity within these brain areas are temporally synched (Grefkes & Fink, 2011). The idea behind a functional connectivity (FC) approach is to elucidate neuroimaging data for a region of interest or node to be compared with other brain areas exhibiting activity related to this node. Specifically, data gathered from different regions of the brain is compared to the previously defined region of interest at a given time in order to assess coherence among the regions, as evidenced by activity within the same frequency band or power spectrum. By definition, the above analysis technique is non-linear FC, which is characterized by description of information from a node given the time frequency analysis of phase synchronization information in another area (Grefkes & Fink, 2011). For instance, Bardouille and Boe (2012) applied a CCC analysis to brain activity (obtained via MEG) during rest and a bilateral gripping task in non-disabled individuals. Results of the study showed that during the gripping task, as compared with rest blocks,

individuals exhibit greater CCC (i.e., functional connectivity) within M1, S1, PMC, SMA and prefrontal cortex (PFC). Functional connectivity approaches provide the basis for researchers to explore multiple brain networks at once, which ultimately furthers our understanding of how information from multiple systems (i.e., sensory, motor, etc.) is integrated to produce movement.

In order to quantify the relationships defined by FC, researchers have recently begun to employ a graph theoretical analysis (Dosenbach et al., 2007; Wang et al., 2010). Graph theory allows researchers to quantify links between temporal and spatial activation patterns within the brain that define network parameters (Bullmore & Sporns, 2009). Importantly, graph theory is a method of analysis that examines network nodes on the basis of communication efficiency (Grefkes & Fink, 2011). Specifically, researchers quantify connectivity based on node degree (ND), which measures how many connections with neighboring areas a node exhibits, and clustering coefficients (CCo), which are based on ND as a proportion of total possible connections. In addition, networks can be quantified on the basis of path lengths, which measure the distance between nodes that are participating in functional connections within the network (Figure 1).
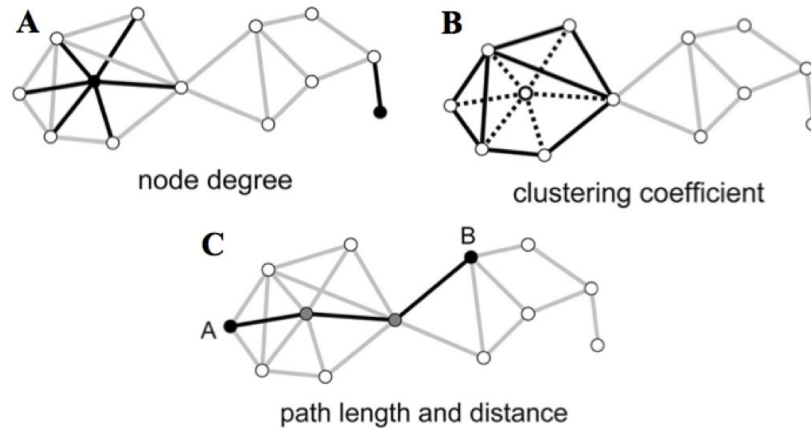
Figure 1 Depiction of Graph Theory Parameters: where nodes are depicted as circles and edges (or connections) are depicted as lines. 'A' shows a node with a ND of 6, 'B' depicts a cluster of interactions between neighboring nodes, and 'C' shows a node connection with a path length of 3 (i.e., A and B are connected by three edges).

In non-disabled young adults, graph theory has been used to quantify network properties of resting state MEG data. This particular study documented that these individuals demonstrated brain networks described as "optimally functioning", a distinction that was characterized by high CCo and shorter path lengths amongst active regions that comprised the network (Stam et al., 2009). The FC of particular brain regions can be further understood through analysis of the small world brain networks that graph theoretical methods attempt to quantify. Functional connectivity methods of investigation also provide an effective means for exploring how neurological insult (i.e., stroke) impairs multiple brain networks and how these networks may reorganize with recovery (Carter, Shulman, & Corbetta, 2012).

2.4 Small World Brain Networks

It has been proposed that efficient brain networks combine properties of both functional specialization and integration (Tonini, 1994). The specialization of these connections is characterized by the existence of short path length measures within the

task related network, and further, these connections are found between brain regions working together to achieve the given task (Rubinov & Sporns, 2010). The integration component of these ideal networks is explained as brain nodes of interest that have a large number of connections (i.e., greater clustering coefficient and node degree) via the specialized links mentioned above (Rubinov & Sporns, 2010). It is the combination of these particular properties (i.e., high clustering and short path lengths) that makes up what is known as a small-world network (SWN). More specifically, SWNs have been defined as those containing dense connections and short path lengths (Watts, 1998). It is the presence of these SWNs that infer a specific brain region is communicating efficiently in order to achieve a task or outcome. For example, in epileptic patients, research using event related analysis of MEG data obtained during a visual stimulus paradigm has uncovered that although brain activity changes over time and within frequency bands, the typical SWNs are maintained (Valencia, Martinerie, Dupont, & Chavez, 2008). After further investigation of the parameters (i.e., path length and clustering) that define these persistent SWNs, it has been theorized that an optimum network structure is characterized by equal concentrations of local (i.e., few brain regions involved) and global (i.e., wide spread neuronal involvement across the cerebral cortex) connections across brain nodes of interest (Ahmadlou, Adeli, & Adeli, 2012; Watts, 1998). The realization that SWNs are driven by some quantifiable measure has lead scientists to investigate potential use of these cortical topography patterns (i.e., topographical maps derived from sensor level data) in clinical settings. Recent research has documented that characteristics of SWNs can be used to define the common neural correlates specific to various brain pathologies (Bernhardt, Chen, He, Evans, &

Bernasconi, 2011; Liu et al., 2008; Murias, Webb, Greenson, & Dawson, 2007). This area of investigation provides an interesting model for clinicians looking to more effectively diagnose and treat particular neurological disorders. While the research in this area is promising, it should be noted that Stam et al. (2009) have documented similarities in path length between random and ordered networks, which indicates that this particular parameter may not be ideal for differentiating between non-disabled and pathological brains. Based on the potential for clinical application however, researchers have attempted to determine whether SWN parameters characteristic of specified brain interactions could be used to distinguish between intact and pathologic brains.

Small world network analysis has been used to further define the network parameters specific to a variety of behavioural deficits. Liu et al. (2008) used FC methodologies to distinguish the differential small world topographies characteristic of the brains of individuals with schizophrenia; the researchers produced correlation matrices and subsequent parameters measuring the degree of connectivity from resting state fMRI data to outline that patients with schizophrenia show disrupted small world properties, as compared with healthy controls. Similarly, an EEG study of patients with schizophrenia (as compared with non-disabled individuals) performing a working memory task displayed disruptions in small world topography within the alpha (8-15 Hz), beta (15-30 Hz), and gamma (32+ Hz) frequency bands (Micheloyannis et al., 2006). In addition, a resting state fMRI study documented poor communication across nodes within the prefrontal, temporal, and occipital cortices in participants with attention deficit disorder as compared with non-disabled individuals; that is, the global network

characteristics of attention deficit disorder shifts away from a more functional network (Wang et al., 2009).

The above findings indicate that SWN topographies can be used to distinguish disordered or pathologic brains from healthy ones. However, these general changes in cortical interactions need to be further defined to infer the importance of particular nodes in varying brain networks for achieving some goal. Ahmadlou et al. (2012) documented that graph theoretical analysis can be used on EEG data to find differences in left hemisphere long-distance (i.e., global networks) connectivity within the delta band of individuals with attention deficit disorder (ADHD), as compared with healthy controls. In further support for this concept, graph theory parameters such as path length and clustering coefficients have been used to distinguish individuals' brains with ADHD from those of healthy controls (Ahmadlou et al., 2012). These findings add to the notion that brain activation should be studied from a network perspective (see section 2.2), especially when investigating those individuals with some neurological disorder.

In an attempt to better define interactions amongst brain regions in individuals that have a neurological disorder, researchers have investigated the resting state activation present in patients with epilepsy between seizures (i.e., interictal activity). Graph theoretical analysis has been applied to cortical thickness data obtained via MRI to determine that path lengths are longer in patients with drug resistant temporal lobe epilepsy, as compared with healthy controls (Bernhardt et al., 2011). Graph theoretical analysis of EEG data within the alpha band has also shown that patients with epilepsy display increases in path length pre- and post-seizure, as compared with interictal state brain activity; although, the changes in path length are not large enough to indicate the

presence of global pathways (Ponten, Bartolomei, & Stam, 2007). In patients with Alzheimer's disease, graph theory methods have been used to distinguish the relative random global networks (vs. small world) characteristic of their resting state fMRI brain activity (Sanz-Arigita et al., 2010), which is further supported by documentation of the loss of SWN characteristics in EEG beta band brain activity in this population (Stam et al., 2009). The previously mentioned SWN research is focused on brain disorders related to behavioural or cognitive deficits, which may possess neuropathologies specific to brain regions that underlie higher-order cognitive processes. For the purposes of motor rehabilitation, it is important to investigate the SWN characteristics of those diseases that impact specific motor regions of the brain. Importantly, the above studies provide evidence that network analysis can be used to characterize and distinguish particular pathologies from both resting state and task related brain activation, lending to the potential for application in a clinical setting.

2.5 Cortical Reorganization and Stroke

The connectivity pattern amongst nodes comprising the motor system undergoes change based on experience (e.g., repetitive practice) and following neurological injury (Gerloff et al., 2006). Although the current project is focused on uncovering patterns of brain activation in non-disabled individuals, it is important to distinguish how this knowledge is relevant to improving neurorehabilitation techniques commonly used by clinicians. In stroke rehabilitation, a wide variety of therapies such as repetitive task-specific practice (RTP), constraint induced movement therapy (CIMT) and electrostimulation are commonly used in order to improve motor function via cortical reorganization (Longhorne, 2009). In particular, the beneficial impact of RTP has been

well documented in patient populations; that is, patients who have experienced a stroke undergoing RTP-based therapies exhibit functional gains (Arya, Pandian, Verma, & Garg, 2011; French et al., 2009; Kopp, 1999). The neurophysiology underlying functional improvements from RTP-based therapies is characterized by task-dependent brain plasticity, which is essentially the functional reorganization of the brain areas involved in the intended movement due to constant efferent and afferent pathway stimulation (Hodics, Cohen, & Cramer, 2006). Active and continuous stimulation of damaged brain regions via overt or induced peripheral muscle contractions can cause the motor system to "re-wire", a finding consistent with the principles of Hebbian plasticity (Butz, Worgotter, & van Ooyen, 2009). For instance, Liepert (1998) used transcranial magnetic stimulation (TMS) to map motor areas in the human brain, as evidenced by the presence of a motor evoked potential (MEP) in patients following a stroke during a single session of physical rehabilitation focused on the affected hand. The repetitive use of the paretic hand during therapy resulted in an expansion of the hand area of M1, as evidenced by the ability to evoke MEPs over a greater number of locations and larger amplitude MEPs. Similarly, electrical stimulation of the peripheral nerve in patients who have experienced a stroke also causes cortical reorganization. In particular, peripheral nerve stimulation after stroke produces functional improvements on grasp and reach tasks (Kimberley et al., 2004). Peripheral nerve stimulation impacts the central nervous system via afferent pathways in order to cause facilitative cortical reorganization. For example, in stroke patients, repetitive peripheral nerve stimulation leads to improvements in the strength of the paretic limb(s) (Conforto et al., 2002), as well as better performance on a sequential finger-tapping task (Ridding, 1997). Following a stroke, individual brain regions exhibit

axonal out growth, or sprouting, over both local and long distances (Carmichael, 2003).

Even in cases of severe brain injury where movement execution is not possible, plastic

changes can occur in the motor network (Butler & Page, 2006).

During movement, differential activity occurs in the motor network of an

individual who has experienced a stroke, as compared with a non-disabled system.

Neurological injury debilitates the motor system's ability to dynamically control the

necessary excitatory and inhibitory brain activity across hemispheres for proper

movement execution (Grefkes & Fink, 2011). Neuroimaging studies display that patient's

post-stroke exhibit contralesional patterns of brain activation during movements of the

affected hand (Ward, 2003). The result of the imbalance between excitatory and

inhibitory connections across hemispheres is competitive inhibition. Electrophysiological

data has contributed to our understanding of competitive inhibition by uncovering the

abnormally persistent inhibition of M1 in the lesioned hemisphere by the contralesional

M1 during paretic limb movements in patients after a stroke (Murase, 2004). A

systematic review of UL recovery after stroke documented that the motor network of

acute patients (i.e., one week after stroke) is characterized by over activation of both the

primary and association motor areas, as well as contralesional M1 activity (Buma,

Lindeman, Ramsey, & Kwakkel, 2010). Further, in patient populations who have

recovered well, these networks return back toward a healthy, or original, state in many;

however, in those patients who have recovered poorly, the motor network continues to

recruit contralesional M1 and other motor areas during movement of the paretic limb

(Buma et al., 2010).

In addition to neuroimaging studies reporting spatially focused region-by-region information about brain activity, some researchers have attempted to analyze motor areas in individuals who have had a stroke using network approaches. Gerloff et al. (2006) reported that in chronic stroke patients, EEG-based coherence analysis during a metronome paced finger extension and rest task displays reduced CCC in the lesioned hemisphere, in comparison to increased connectivity in the contralesional hemisphere. An effective connectivity approach in a system that had experienced a stroke uncovered that the decreased interaction between SMA and M1 in the ipsilesional hemisphere was correlated with individual motor deficit (Grefkes, Eickhoff, Nowak, Dafotakis, & Fink, 2008). The findings of Grefkes et al. (2008) outline that processing between the ipsilesional SMA and M1 is necessary for proper movement execution, which indicates the importance of considering lesion location within the motor network and its link to recovery. Wang et al., 2010 suggest that connectivity between ipsilesional M1 and key motor regions in the lesioned hemisphere increase with time during stroke recovery. Further, the increased connectivity of most of these nodes is correlated to the amount of motor recovery experienced (Wang et al., 2010). The findings of the above studies clearly outline the importance of balanced interaction between the two hemispheres, as well as increased connectivity among specific brain regions involved in motor processing for return to function after stroke.

2.6 Stroke and Adult Disability

The ability to control movement involves the integration of information from multiple brain areas. Damage to a given area of the brain from neurological injury impairs this ability to produce movement (S. C. Cramer, 2004). Stroke involves a

disturbance in the blood supply to the brain due to either ischemia (i.e., lack of blood flow due to a blockage in the circulatory system), or a hemorrhage (i.e., an internal bleed from the circulatory system) (Sudlow & Warlow, 1997). The result of the cerebrovascular accident is damage and death to the involved neuronal populations; consequently, stroke is a leading cause of adult disability. A large number of individuals who have experienced a stroke require ongoing care and struggle to independently complete activities of daily living (ADL). Upper limb dysfunction is a primary factor contributing to the inability to maintain function in patients post-stroke (S. C. Cramer, 2004). Individuals who have experienced a stroke exhibit varying levels of UL impairment, ranging from performance similar to that of a non-disabled individual to a completely flaccid (i.e., paretic) limb. Currently, therapies for individuals with a flaccid UL either do not exist, or are being implemented without knowledge of how the treatment drives brain repair, and how it might promote functional UL recovery. The result is that individuals with UL dysfunction spend time in therapy sessions that may, ultimately, be ineffective, and are left with long-term impairments.

The result of these negative changes in the motor network following stroke (as noted in section *2.5*) inhibit the individual's ability to perform functional tasks at a pre-morbid level. An inherent problem for researchers looking to explore the brain after neurological insult is that the investigation of the motor system is confounded by the injury. In particular, brain activity that is common in patients who have experienced a stroke (e.g., interhemispheric inhibition) makes it difficult to make sense of the underlying neural correlates that might be associated with the given task. Moreover, owing to the presence of physical impairment, the inability of individuals post-stroke to

perform a given movement in a manner similar to that of a non-disabled participant further confounds the interpretation of the movement-related brain activity. To produce more effective interventions for patient populations, researchers must possess a better understanding of the motor system's underlying connectivity. The research presented here uses imagined movement, termed motor imagery (MI), as a modality to explore specific patterns of brain activation related to movement execution. The use of MI allows the researcher to gain fundamental knowledge regarding the motor system in the absence of the complexities (e.g., altered movement patterns, larger network activation, sensory integration, etc.) that overt movement may introduce, thus providing a platform with which to study patients with neurological injury in future work

2.7 Motor Imagery

Motor imagery has been proposed as a primary rehabilitation approach for patients who have no or limited UL function (Sharma et al., 2006). During MI, physical tasks are mentally rehearsed in the absence of overt muscle contraction (M. Jeannerod, & Frak, V., 1999). J. Decety (1996) outlines two forms of MI: [1] First Person Perspective MI, which is based on motor-kinesthetic information processing (i.e., imagine reaching for a glass of water as if you were "behind your own eyes"), and [2] Third Person Perspective MI, which is based on visuospatial processing (i.e., imagine you are a spectator watching yourself reach for a glass of water). Although each type has strengths and weaknesses, Fery et al., (2000) found that the use of first person perspective MI (i.e., kinesthetic) led to better performance of a tennis serve during learning, as compared with the application of third person perspective MI (i.e., visual).

Motor imagery has been used in sport as a means of teaching novel motor skills and as a preparation tool for game-time mental toughness (Murphy & Corbett, 2009). The sports training literature separates MI types into the following subgroups: [1] cognitive MI, further broken into cognitive-specific and cognitive-general, or [2] motivational MI, further broken into motivational-specific, motivational-general-mastery, and motivational-general-arousal (Rogers, 2006). The cognitive subgroup of MI aims to use the activation of neuromuscular processes involved in actual movement execution in order to improve motor skill acquisition and automaticity of intended movements. Cognitive-specific MI involves the imagined learning of a specific task (i.e., shoot a basketball), while cognitive-general MI aims at imagining linking all of these specific tasks together (i.e., a play in basketball). The motivational subgroup of MI is meant to improve the athlete's ability to cope during competition and increase self-efficacy associated with performance skills. Motivational-specific MI has individuals imagine events tied to specific goal setting (i.e., winning the basketball game). Motivational-general-mastery MI involves picturing methods of coping during competition (i.e., being mentally tough and confident), while motivational-general-arousal MI has participants imagine how they will deal will feelings evoked by the game (i.e., relaxing and keeping calm while taking a foul shot). The application of these MI methods can result in improvements in sport performance; for example, weightlifters that used motivational-general-arousal and –mastery MI prior to lifting had significant improvements in their performance as compared with a baseline lift (Shelton, 1978). Similarly, cognitive MI in combination with physical practice results in improved accuracy and regularity of tennis serving as compared to just physical practice on its own in young adults (Guillot,

Genevois, Desliens, Saieb, & Rogowski, 2012). In addition to its application in sport, MI has been used in medical settings in order to aid in motor skill acquisition for novice surgeons (for a review see (Hall, 2002)). Arora et al. (2011) found that the use of MI prior to performance of a surgical procedure in a novice population of doctors resulted in significantly lower self-report stress and heart rate measures, as compared with a control group. In medical settings, motivational-general-arousal MI may be beneficial for teaching coping mechanisms for stress and anxiety during challenging surgical procedures.

The idea of MI as an intervention in patient populations is to activate regions of the brain that would normally produce overt movement in order to promote plastic changes to drive functional recovery (i.e., brain repair). Specifically, the type of MI applied in rehabilitation settings is typically first person (i.e., kinesthetic), cognitive-specific or cognitive-general imagery. Kinesthetic MI is most often used in rehabilitation settings owing to its capacity to activate a simulation of movement within the motor regions of the cerebral cortex, in the absence of overt muscle contraction. To better understand the impact of MI on neural populations, emerging motor control research has investigated the physiological outcomes associated with MI in non-disabled individuals. Studies examining the neural basis of MI show that the neural substrates activated during imagined movement are similar to those during actual movement, albeit at a different level of intensity (Gerardin, 2000). Researchers have quantified the spatial regions activated during a typical MI protocol. In non-disabled controls, activation during imagined movement occurs in M1, the PMC, and regions of the parietal lobe involved in the preservation and generation of a kinaesthetic model (J. Decety, & Jeannerod, M.,

1996). An fMRI study documented that when imagining the performance of a dynamic

balance task, non-disabled individuals display brain activity in the motor regions

responsible for control of the trunk and legs (Ferraye et al., 2014). Some researchers have

indicated that in non-disabled individuals the neural correlates of MI involve activation of

the SMA (Tanji, 1994). The SMA involvement indicates that brain activity during MI

may be associated with motor planning and movement initiation. A recent meta-analysis

of the neural networks underlying MI documented that imagery most commonly results

in activation of a large fronto-parietal network, as well as some subcortical and cerebellar

regions (Hetu et al., 2013). Importantly, Hetu et al. (2013) note that activity in M1 during

MI is variable across studies. An effective connectivity based study used DCM of fMRI

data to specify that during MI in non-disabled individuals, the SMA suppresses the

activation of M1 (Kasess et al., 2008), which may account for the variability in M1

activation seen across studies. Further, researchers have found that in keeping with actual

movement execution, a reduction in accuracy with increased speed (i.e., Fitt's Law) is

maintained during MI (J. Decety, & Jeannerod, M., 1996). In addition, it has been

documented that MI elicits similar autonomic responses in participants, such as increased

heart rate and respiratory rate, to actual movement execution (Oishi, 2000; Roure, 1999).

The similarities between the physiological responses elicited during actual movement

execution and MI provide the basis for using imagined movement as a viable tool to both

investigate, and to treat the motor system.

2.8 Motor Imagery and Stroke

The above noted similarities in brain function during both overt and imagined

movement have lead to the emergence of MI as a viable therapeutic method for clinicians

treating individuals who have experienced a stroke. Researchers have investigated the relationship between MI-based therapy and performance improvements on functional tests in patient populations. S. J. Page, Szaflarski, J.P., Eliassen, J.C., Pan, H., & Cramer, C. (2009) found that scores on functional tests (i.e., the Action Research Arm Test) improved in a cohort of chronic stroke patients following an MI intervention, as well as in a case study involving a patient in the subacute phase of rehabilitation (S. J. Page, Levine, P., Sisto, S.A., & Johnson, M.V., 2001). In addition, of ten acute stroke patients receiving MI as an adjunct therapy, eight had significant improvements in UL functional test scores pre-to-post intervention (Crosbie, McDonough, Gilmore, & Wiggam, 2004). Similarly, performance on a skilled, sequential foot movement task after stroke improves when physical practice is augmented by MI (P. L. Jackson, Doyon, Richards, & Malouin, 2004). As a consequence of the functional improvements seen with MI, researchers report that patients who are performing MI during their rehabilitation also display increases in affected limb use (Page et al., 2005). As a therapy, MI seems to promote functional improvements in patients after stroke, likely via activation of the regions of the motor system responsible for planning and production of the intended movement. If the patients who have experienced a stroke do not have lesions to either the posterior parietal (i.e., kinesthetic awareness) or left frontal (i.e., executive function) brain regions, they retain the ability to reinvent motor experiences that are overtly impossible (Johnson, 2000). Johnson-Frey (2004) suggests that MI of particular tasks that the individual can no longer perform after stroke may result in reorganization of the motor execution network (as evidenced by a pilot study); thus, MI may play a role in facilitating cortical plasticity after stroke.

While clinicians continue to administer MI in stroke populations based on study findings (e.g., Crosbie et al., 2004 & Page et al., 2009), there is still much research necessary in order to better understand the underlying neural correlates of MI. In particular, it is not clear which neural substrates active during imagined movement are driving functional improvements in patients after stroke, and how these neural substrates compare to a brain that has not been damaged. In addition, the quantification of brain activity during MI following neurological injury varies across studies. A study using fMRI to investigate brain activation during MI after subcortical stroke found increased bilateral activation in M1, superior and inferior parietal regions, and the globus pallidus (Sharma, Baron, & Rowe, 2009). Importantly, Sharma et al. (2009) demonstrated the resounding disorganization that is present in the motor network of patients who have had a stroke; specifically, more bilateral involvement across M1 during MI of the affected hand was evident in individuals who had experienced a neurological injury. Studies investigating the use of MI in combination with RTP also found increased activation in bilateral M1 and PMC (Butler & Page, 2006), as well as the orbitofrontal region (Philip L. Jackson, Lafleur, Malouin, Richards, & Doyon, 2003). The above findings are in keeping with research documenting the imbalance and relative network disorganization found between hemispheres in the brain during actual movement execution for an individual who has had a stroke (see section *2.5*). The evidence suggests that motor networks deemed responsible for actual movement are active during MI in patients following stroke, which validates MI as a tool to both investigate and treat the motor system. However, study findings also suggest that motor networks after a stroke, as compared with non-disabled networks, are characterized by disorganization. The nature

of these changing connections in patients suggests that we first need to better understand the communication among underlying motor regions that are active during a given task in a population that has not experienced some neurological insult (i.e., non-disabled individuals).

2.9 Electroencephalography and MI

There has been recent documentation that EEG data can be used to investigate source level brain activity related to MI in both non-disabled and pathological systems. Researchers have used real time EEG data to procure source level connectivity patterns among brain regions active at 8-30 Hz during a finger-tapping task in non-disabled individuals. This research shows that real-time source level coherence data can be used to track spatial patterns of activity in the cortex, as well as the strength of the connections across specific nodes of interest that underlie these patterns (Hwang et al., 2011). While this study was limited by the use of a template brain (in comparison to individual anatomical MRIs), the research adds to the literature outlining that source level information can be obtained from sensor level data acquisition (i.e., EEG). Badia (2013) found that when motor execution training followed a MI paradigm there was a greater amount of task-related activity in the beta frequency in motor-related brain areas, as compared with simultaneous motor execution and observation of an avatar in non-disabled individuals (as assessed using EEG). Similarly, Li (2013) found that there is a correlation between actual right hand task performance and beta band (8-30Hz) EEG brain activation in the hemisphere contralateral to imagined task performance in non-disabled individuals. The researchers documented that this relationship is deduced from measures of synchronization between brain regions, as well as models outlining causal

dependence across nodes assessed via granger causality methods (Li, 2013).

Pfurtscheller, Brunner, Schlogl, and Lopes da Silva (2006) found that MI of right-handed movements in non-disabled individuals elicits desynchronization in the mu rhythm of obtained EEG data. Further, during both right and left handed MI and motor execution tasks, fMRI-based brain activity in healthy controls is lateralized to the contralateral hemisphere. Effective connectivity analysis performed using granger causality methods however has shown that the strength of the connections is less during imagined, as compared with overt, movement (Gao et al., 2011). In keeping with previous research outlining the similarities in brain activity between imagined and overt movement (i.e, (J. Decety, 1996)), research has displayed that there are no significant differences in EEG beta or alpha oscillatory power between real and imagined reach and grasp movements performed by healthy controls (Kilner, 2004).

In further support of the use of EEG to investigate connectivity in the brain, it has been documented that BOLD activation patterns (i.e., fMRI) during imagined right hand movements in non-disabled individuals are co-localized with event related desynchronization obtained via EEG in the same cohort of participants (Yuan et al., 2010). The ability to distinguish brain activation patterns specific to MI in healthy populations has led researchers to use similar methodologies to investigate connectivity within the pathologic brain. Importantly, network analysis on patients who have experienced a stroke performing MI has been assessed via EEG to uncover global clustering coefficients and longer path lengths (Yan, 2013), as well as increases in inter-hemispheric inhibition across active brain regions (De Vico Fallani et al., 2013). This research outlines that EEG data can be used to distinguish particular brain networks that

29

are active during imagined movement tasks in pathological systems. It is important to note that while FC approaches to understanding brain activity have been used in the studies mentioned in this section, few studies have quantified these patterns using graph theoretical methods.

2.91 Research Rationale

Understanding the brain networks (i.e., areas of the brain that work together) that underlie MI is necessary to explain the functional outcomes of the intervention, and importantly provide the opportunity to optimize treatment based on our understanding of what impact MI has on brain repair. To realize this, baseline network activity during MI needs to be established via a functional integration approach. Specifically, there is a need for a more detailed understanding of the brain regions that are active during MI, and how these activation patterns compare to those involved in overtly performing the movement. In addition, much of the research in this area has limited their paradigms to including actual and imagined tasks that are not functional in nature; that is, the majority of the tasks used in past research has included simple finger movements (e.g., repeated finger tapping). Use of such simple paradigms is largely to facilitate consistent behavior (actions) across participants. While useful for simplifying the experiment and potentially interpretation of the resulting data, use of such tasks limits the degree to which findings can be transferred to real-world application. For instance, investigating simple tasks does not provide information about brain activity that underlies the actual or imagined execution of ADLs. To gather such information, it is necessary to carry out investigation of the neural correlates of MI during a task that is directly related to activities individuals typically carry out in their day-to-day lives. As mentioned previously, novel

methodological approaches in neuroscience now permit brain activity to be examined from a network perspective (Grefkes & Fink, 2011; Stam, 2004). It is possible to elucidate areas of the brain that 'work together' from a spatial and temporal perspective to characterize the pattern of connectivity amongst nodes that underlie movement production and control. To date, this approach has had limited application to the understanding of neural networks that underlie MI and the chosen motor tasks have not been typical of daily activities.

The underlying purpose of the project is to expand our basic understanding of brain networks. Functional integration between poly-sensory, motor and cognitive brain regions is mediated by specific path connections. Although some studies have attempted to analyze cortical topography relationships between neural substrates during MI (Butler & Page, 2006; Philip L. Jackson et al., 2003; Sharma et al., 2009), there is a need for quantification of the patterns of connectivity that modulate behaviour in order to facilitate further understanding of the motor system. Specifically, this research will aid in revealing patterns of connectivity within the neural networks in non-disabled participants during MI. Investigation regarding FC within the neuronal systems that are involved in movement processing will aid in uncovering the typical SWN patterns that govern motor control. Although not part of this thesis work, these functional neuronal systems have potential for application in clinical settings for distinguishing particular brain pathologies. In addition, the findings of this study will aid in outlining the neural mechanisms active during MI that might be driving functional improvements in patient populations who, for example, have experienced a stroke. This research will allow for a better understanding

of the FC that is characteristic of MI, and how these patterns compare to those brain

activation patterns specific to the overt performance of a functional task.

CHAPTER 3 OBJECTIVES AND HYPOTHESIS

3.1 Objectives

In a cohort of non-disabled participants, our objectives include:

1. To determine the pattern of FC within the sensorimotor network during the imagined (MI) performance of a functional task

2. To determine the pattern of FC within the sensorimotor network during the performance of a functional task

3. To quantify the pattern of FC, using graph theory, during the actual and imagined performance of a functional task

3.2 Hypotheses

1. The pattern of FC in non-disabled participants during MI will involve communication amongst a number of primary nodes, including M1, the PMC, as well as regions within the parietal lobe due to its involvement in kinaesthetic awareness.

2. The pattern of FC in non-disabled participants present during the functional task will involve regions of the sensorimotor network such as M1, PMC, and S1.

3. It is anticipated that a graph theoretical analysis will uncover significant dependence on connections within the sensorimotor areas (i.e., higher ND) in non-disabled participants during both overt and imagined movement; however, those networks characteristic of MI will be more heavily linked to pre-frontal cortex (PFC) and parietal cortex (PC) areas.

CHAPTER 4 METHODS

4.1 Participants

4.11 Non-Disabled Participants

Participants consisted of 15 non-disabled young adults (22.7 ± 2.1 years; 9 females) with no history of neurological insult. Participants were screened for suitability for MRI [i.e., metal in the face, head, or upper chest (e.g. metal implants, aneurysm clips, middle ear prosthesis, shrapnel or metal foreign bodies in the eye, artificial heart valve pacemaker) or if they are female and currently pregnant] by both a research team member and a registered MR technologist prior to initiating the scan. Exclusion criteria included having a terminal illness, life-threatening co-morbidity or concomitant neurological or psychiatric illness. In addition, any individual who was participating in other studies was precluded from study involvement.

4.12 Study Enrolment

Non-disabled participants were recruited by word of mouth within the academic environment of the principal investigator. The group consisted of colleagues and students with additional participants recruited using an advertisement posted within Dalhousie University and the Capital District Health Authority (see Appendix I). Potential study participants were free to decide if they wished to participate in the study. Non-disabled participants had the opportunity to respond voluntarily to the study investigator's to indicate their interest in the study. At that time, a written and verbal description of the study was provided and potential participants were given time to decide if they would like to participate. Prior to providing written informed consent, the study investigators addressed any questions the participants had.

4.2 Measures Regarding Participant Characteristics

The following measures were used in order to characterize the study participants. Each

measure was taken once only during the initial study session (see Table 1).

Table 1: Timeline for Collection of Measures

Measure	Orientation Sessions			Experimental Session
	Day 1	*Day 2*	*Day 3*	*Day 4*
Informed Consent	√			
Demographics	√			
Health & Physical Activity Information	√			
KVIQ	√	√	√	√
MI Orientation Protocol	√	√	√	
MI Experimental Protocol				√

**Anatomical MRIs were obtained for each participant at a later date following completion of study involvement

4.21 Demographic Information

Descriptive information pertaining to age, sex, handedness (via the Edinburgh

Handedness Questionnaire [Oldfield, 1971]) and medical history was obtained from the

non-disabled participants upon study enrolment.

4.22 International Physical Activity Questionnaire (IPAQ)

The short IPAQ was used in order to obtain physical activity information from all

participants. The IPAQ allows for quantification of Metabolic Equivalent of Task (MET)

via self-report measures of hours spent engaged in physical activity each week. Moderate

intensity exercise is defined as 3-6 MET and vigorous intensity exercise is defined as >6

MET, while one MET is in reference to energy expenditure at rest (Craig et al., 2003). It

has been documented that the IPAQ is a valid assessment tool when compared to actual activity logs in healthy adults (Hagströmer, Oja, & Sjöström, 2007). Information related to physical activity was obtained for two reasons: 1) to allow for characterization of potential differences in activity levels among participants at baseline; and 2) to allow the researchers to better characterize the non-disabled participant population for future comparison to a patient population.

4.3 Measure Regarding MI Ability

The following measure was taken at the beginning of each session of study enrollment. The results were used to assess MI vividness, and its progression, over the course of the research period.

4.31 Kinesthetic Visual Imaging Questionnaire (KVIQ)

The KVIQ is an adapted MI questionnaire intended for individuals who may need guidance in rating their imagery and who cannot perform complex movements (Malouin et al., 2007). The KVIQ was used to assess the vividness of both the visual and kinesthetic dimensions of MI. Within the visual dimension, a self-report rating of 5 indicates the individual imagines the movement as clear as seeing, while a score of 1 is reflective of seeing no image at all; within the kinesthetic dimension, a participant rating of 5 indicates the MI is as intense as actually executing the movement, where a score of 1 is representative of feeling no sensation (Malouin et al., 2007). The KVIQ includes gestures that are simple upper limb movements, such as elbow flexion/extension, thumb-fingers opposition, shoulder elevation, etc., which are easily performed. Procedurally, the examiner has the individual perform the assessment while seated comfortably. First, the examiner demonstrates the movement, followed by the patient's overt performance of the

movement, and finally, the patient performs MI of the particular movement. Once the patient has finished their MI, the examiner prompts the individual to provide a self-report rating in accordance with the above mentioned 5-point scale. Importantly, application of the KVIQ has shown reliability in both non-disabled controls and stroke patients (Malouin et al., 2007). The KVIQ was used in the present study despite not enrolling patients post-stroke in order to establish its use in the laboratory and generate control data for follow-up studies of patient populations.

4.32 Experience With Imagined Movement

Prior to any explanation of the imagery task, all participants were asked the following questions on day one of study involvement:

(1) "Do you have any experience with motor imagery?"

(2) "If you answered yes to question one, in these experiences did you mentally rehearse a task? Please explain."

(3) "Have you ever performed motor imagery of a task that did not have to do with a sport? Please explain."

This information was obtained in order to provide context for the potential individuals who may perform better on the MI task. In particular, the above questions were developed for the purposes of obtaining information pertaining to MI experience that involved explicit mental rehearsal of a skill during learning.

4.4 Neuroimaging and Muscle Activity

The following measures were obtained throughout the performance of MI during the experimental session (Day 4).

4.41 Electroencephalography (EEG)

Electroencephalography is the detection of electrical activity along the scalp produced by the discharge of neurons within the brain. The resultant EEG signal is the summation of the synchronous activity of the neurons that have a similar spatial orientation relative to a given scalp electrode location. In the present work, the EEG signal was detected using a *QuikCap* (Compumedics Neuroscan, Charlotte, NC) (see Figure 2). The *QuikCap* is an electrode placement system manufactured of highly elastic, breathable Lycra material that houses the electrodes used to detect the EEG signal.

Figure 2 QuikCap for EEG Data Collection

The electrodes consist of soft, neoprene reservoirs that house the electrode itself. The reservoirs are filled with gel to conduct the signal from the scalp to the electrode, as the electrode does not actually contact the participant's scalp. *QuikCaps* were cleaned following each use, and a number of sizes were available to ensure a comfortable fit as well as recording from consistent sites on each individual's head. At the onset of the experiment, the *QuikCap* was placed on the individual's head and the gel reservoirs were filled with the electrode gel. To accomplish this, large gauge, disposable, blunt needles

were used. The needle was inserted into a hole on the outside of the cap and placed gently against the scalp. The needle head was then moved in a circular motion to move the hair under the electrode out of the way and to allow for the electrode gel to reach the scalp, a process continued as the needle is removed from the hole. This process was then repeated at each of the electrode sites (128 on the cap in total were used in the study).

In addition to the *QuikCap*, additional individual electrodes were placed at locations on the head and face including the left and right mastoid process (i.e., behind the left and right ear), above, below and to the left of the left eye, and to the right of the right eye. The electrodes placed behind the ears act as reference electrodes for the EEG signal, and the ocular (eye) electrodes served to obtain the electrooculogram (EOG). The EOG channels are used in subsequent analysis to identify and remove ocular artifacts resulting from eye movements. These additional electrodes were held in place via an adhesive ring.

During data collection, the researchers ensured that impedances at all electrodes remained below 10 Ω. The EEG data was acquired continuously throughout each session at a sampling rate of 1000 Hz and a band-pass of DC-333 Hz (SynAmps RT, Compumedics Neuroscan, Charlotte, NC). Participants were cued to task-state based on visual cues (see Procedures below). Event markers corresponding to these visual cues (i.e., task-state) were marked on the continuous EEG file to facilitate data analysis. Auditory tones, visual stimuli and transmission of event markers were achieved via software programmed by the study investigator in the Labview environment.

4.42 Electrode and Head Digitization

To facilitate FC analysis, localization of source generators was performed. To facilitate this analysis the 3D position of the *QuikCap* electrodes with respect to the location of standard anatomical landmarks on the subjects' head (including the nasion and left and right pre-auricular points) were digitized using a 3D position monitoring system (Polhemus, Colchester, VT). This information is also used for co-registration of the functional EEG data with anatomical MRIs acquired in a separate session (see anatomical MRI below). Head and electrode digitization took approximately fifteen minutes to complete.

4.43 Electromyography (EMG)

In addition to EEG data, electromyography (EMG) was recorded to allow the researchers to ensure that no muscle activity was present in the limb during MI. EMG was recorded using self-adhering Ag/AgCl electrodes (3 x 3 cm; Kendall-LTP, Chicopee, MA) in a bi-polar configuration (inter-electrode distance of 2 cm) and located on the dorsal and ventral aspects of the anterior forearm. The electrodes were positioned to record activity of the extensor (i.e., extensor carpi radialis longus) and flexor (i.e., flexor carpi radialis) muscles of the wrist and digits. The EMG signal was collected using the parameters outlined above on the same hardware as the EEG signal and stored for offline analysis. In addition, the researcher monitored the EMG signal online and noted any potential movement during the MI blocks for each participant.

The following measure was obtained following study involvement.

4.44 Magnetic Resonance Imaging (MRI)

Standard high-resolution 3D anatomical images were obtained on the 1.5 T MRI in the IWK Health Centre following the EEG portion of the study. Full brain T1-

weighted spoiled gradient recalled acquisition in the steady state (GRASS) anatomical

images were collected using standard imaging parameters as follows: TE = 5 ms; TR =

25 ms; FOV = 256 mm X 256 mm; 1.5 x 1 x 1 mm voxels; 102 sagittal slices.

4.5 Procedures

4.51 Familiarization Sessions

Each participant took part in three familiarization sessions on successive days (see

Table 1). The sessions consisted of the same procedures with the goal of familiarizing the

individual with MI (see Figure 3).
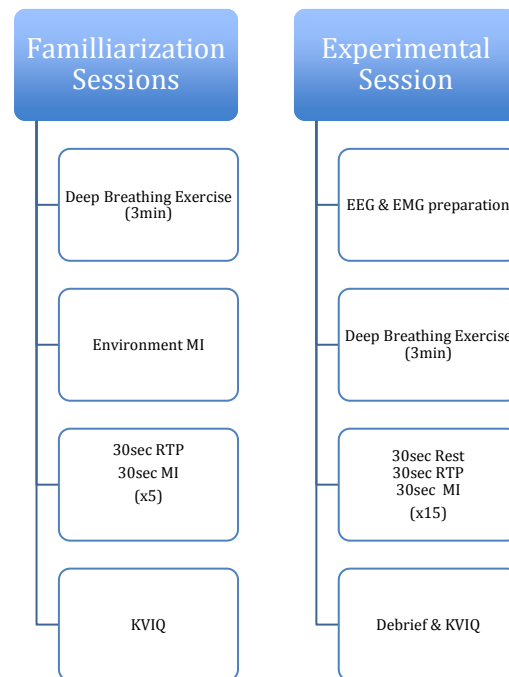
Figure 3 Timeline for Procedures: Familiarization sessions were repeated three days in a row, consisting of deep breathing, environmental imagery, coupled MI and RTP, and MI ability assessment. The experimental session included EEG during deep breathing, coupled rest, MI and RTP, and a final MI ability assessment.

Each session (i.e., both familiarization and experimental) included physical practice of

the task that would be imagined, description of the MI process, and practice of the MI

process. During the first familiarization session, the researcher explained the purpose and

procedures of the study and asked the participants to provide written and informed consent. Following consent, the participants were asked to provide the appropriate demographic, health history, physical activity, and past experience with MI information. At this time, the participants completed the KVIQ to obtain MI ability at baseline. The KVIQ was administered upon initial enrolment and at the end of each day of study involvement in order to track MI progress.

During each familiarization session, the training combined overt movement (via RTP) with MI in order to enhance vividness (Butler & Page, 2006; Philip L. Jackson et al., 2003). Custom software provided the participant with visual and auditory prompts for when to perform RTP, MI, or rest. The familiarization sessions lasted approximately thirty minutes based on the finding that this time frame or longer seems to elicit a learning effect for MI (S. J. Page, Murray, Hermann, & Levine, 2011). The researchers employed a 1:1 ratio of RTP to MI; specifically, participants engaged in thirty seconds of RTP, followed by thirty seconds of MI (see Figure 2). The short time blocks aided in facilitating MI ability, without losing participant attention to the task details. First person (kinaesthetic) cognitive-general MI was employed, whereby the participant was asked to picture the desired movement as though they were actually performing it (i.e., from "behind their own eyes") (Munzert, Lorey, & Zentgraf, 2009).

4.52 Deep Breathing and Environmental Imagery

At the beginning of each day of study involvement participants engaged in a three minute visually guided deep breathing exercise. The goal of the breathing exercise was to have the participants clear their body and mind of any built up tension or thoughts that might interfere with their ability to focus on the imagery task. The deep breathing video

was taken from a meditation practice and was simple to follow. Individuals were instructed to fixate on a flower oriented at eye level on the computer screen as the video began to play. The participants were told to breathe in as the flower became larger, and to breathe out as the flower shrunk back to its original size (see Figure 4).

Figure 4 *Screenshot of the guided deep breathing exercise video used to cue participants to either breath in or out, which resulted in their performance of a rhythmic breathing technique for three minutes.*

The use of the guided breathing video allowed for the participants to easily engage in three minutes of guided rhythmic breathing. Immediately following the guided rhythmic breathing, participants engaged in a thirty second MI block where they were asked to picture the environment that they were currently sitting in (i.e., the lab environment). On each day of study involvement, participants listened to an auditory script during environmental imagery (see Appendix II), which allowed for them to gain a more vivid mental picture of their surroundings. The researcher instructed participants to use any smells or noises that they could hear in order to better form the picture in their mind. The participants were told that they were to re-form this environmental picture during each of the MI blocks to follow. No analysis was done on the brain activity related to the deep breathing task or the environment imagery, as this was not the aim of the study.

4.53 Repetitive Task Practice (RTP)

As mentioned in the previous section the task selected for this project was making

a sandwich. The reason this task was chosen was that the researchers aimed to investigate

FC patterns during overt movement of a task that mimicked a real-world scenario. RTP

was used in the study during both the practice and experimental sessions, as RTP has

been shown to enhance vividness in MI ability (Butler & Page, 2006; P. L. Jackson et al.,

2004). To facilitate the RTP phase of the study, the researchers had all of the necessary

components required to make a sandwich on the table in front of the participant.

Figure 5 *The figure shows the paradigm set up for participants during the sandwich-making task. All sandwich-making materials were oriented within arm's reach, and were chosen based on the preferences of each individual participant.*

During the RTP phase, participants went through the five steps of making a real

sandwich, with a primary focus on using their right arm (with assistance from the left arm

where required). The five blocks included: [1] picking up the bun, [2] cutting the bun, [3]

putting condiments on the bun, [4] putting meat or a meat substitute on the bun, and [5]

adding any final toppings (i.e., lettuce, tomato, etc.) to complete the sandwich. Each of the five RTP blocks were matched in the subsequent MI blocks, such that participants engaged in the mental performance of making a sandwich in the same five step sequence. Participants were asked to repetitively perform the task to the best of their ability for 30 seconds until an auditory cue signaled for them to turn their attention to the computer for further instructions. Specifically, the participants were instructed to continue to repetitively practice the sandwich-making step (e.g., picking up the bun) for the entirety of the 30s block.

4.54 Motor Imagery (MI)

At the start of the first familiarization session, the researcher had the participant read a set of instructions (see Appendix III). The researcher then ensured that the participant understood the task and further described the nature of the MI. The researcher explained that the participants would be imagining the process by which they would make a sandwich. This task allowed each individual to tailor their sandwich to their particular taste, thereby maintaining interest and, importantly, attentiveness to the imagined reach and grasp movements. Prior to the performance of MI, individuals were asked to provide a verbal explanation of the individual steps they associate with the task (i.e., making a sandwich). This process aids in establishing whether or not the participant knows the appropriate sequencing and timing of the task (Braun et al., 2008).

The MI protocol emphasized poly-sensory aspects of the movement, and as such asked participants to not only concentrate on the actual movement, but also other sensory information associated with the experience (e.g., environment). For instance, the study investigator facilitated poly-sensory involvement with statements such as "Think of how

the bread feels in your hands" and "Be aware of the things you may smell when performing this movement"; emphasizing poly-sensory involvement through the use of statements such as these aids in enhancing MI ability (Braun et al., 2008). It was imperative that the participants were fully engaged in their MI practice, meaning participants were instructed to not only focus on the limb involved in the desired movement, but rather on all aspects of the movement. As such, the study investigator encouraged individuals to focus on more inclusive aspects of the movement, such as stabilizing the trunk when reaching (Braun et al., 2008). See Appendix IV for the transcribed scripts. In addition, for individuals who preferred not to eat meat, the meat component of the imagined sandwich-making task was substituted with vegetables (see Appendix V).

4.55 Experimental Session

Following the familiarization sessions involving the training of MI and RTP, participants took part in one experimental session, which included recording brain activity associated with MI, RTP, and rest via EEG. As described above, participants were fitted for the appropriate *QuickCap* and prepped for the experiment. The researcher explained that the participant was to maintain their focus on the computer screen positioned in front of them at eye level while waiting for the appropriate cue (see Figure 6).

Figure 6 *Display screen on the computer oriented at eye level during all days of study involvement for cueing task-relevant actions. The current screenshot depicts the count down that occurred before the participant was to engage in the three minute deep breathing exercise at the start of each day of study involvement.*

For analysis purposes, the EEG data collection was broken into appropriate blocks corresponding to task state (relaxation, RTP, and MI). The EEG session was separated into individual components, including breaks in which the participants cleared their minds and rested, RTP blocks where overt performance of the task occurred, and MI blocks where the individuals performed the MI task learned in the orientation sessions (see Figure 3 for the standard protocol employed during the experimental session). First, participants engaged in a rest period for 30 seconds where they were instructed to close their eyes and maintain a clear mind. Next, participants were prompted by the computer screen to begin RTP (for 30 seconds) of the sandwich task until cued by a tone to stop. Finally, the participants began the MI blocks lasting 30 seconds, with cessation of the block cued for the participant by a tone sounding from the computer. During the experimental session the participants completed fifteen cycles of rest, RTP, and MI (i.e.,

three repetitions of each MI five block segment). To cue the onset of the intended task (i.e., rest, RTP or MI), the computer screen counted down from three and then displayed a written instruction (i.e., "close your eyes and rest", "begin picking up the bun", "begin imagined movement", etc.). During the MI blocks, the written cue was followed by an auditory script, which indicated the participant was to close their eyes and begin the MI task. At the end of the experimental day, participants completed the session by filling out the KVIQ (see Figure 3 for further details).

4.6 Data Analysis

4.61 Kinesthetic Visual Imagery Questionnaire (KVIQ)

To determine whether MI vividness (via the KVIQ) improved during the first familiarization session, a Wilcoxon signed rank test was performed. Where significant main effects were found, appropriate post-hoc tests (i.e., Dunn multiple comparison test) were conducted in order to establish changes within specific domains of the KVIQ data over time. To determine whether MI vividness (via the KVIQ) significantly improved over the course of the study, a Friedman two-way ANOVA was performed (study day X imagery ability). If statistical significance was found, a follow up Spearman correlation was performed to determine the effectiveness of the test pairing. An a priori alpha of $p < 0.05$ was used to denote significance. Significant improvements in MI ability were tested in order to validate the familiarization session in it's ability to teach imagery, as well as to ensure that participants were truly engaged in the imagined task on the experimental day of study involvement.

4.62 Co-Registration

Anatomical MRIs were manually co-registered with the EEG data using the 3D digitization data acquired before the EEG component. The cortical surface reconstruction, and boundary-element modeling (BEM), as well as Talairach-Tournoux transformation of the individual anatomical MRIs was achieved automatically using software available in the Laboratory for Brain Recovery and Function (Curry 7; Compumedics Neuroscan, Charlotte, NC). The use of BEM methods allows for cortical surface reconstruction to aid with source estimation (M. Fuchs, Kastner, J., Wagner, M., Hawes, S., Ebersole, J.S., 2002). Specifically, the BEM segments the scalp, skull, cerebrospinal fluid, and brain tissues from the anatomical MRI data. From the extracted tissue volumes, BEM meshes (i.e., triangle meshes) were generated to better define compartment surfaces by closed triangles in Curry7, which improves the accuracy of source estimation (M. Fuchs, Kastner, J., Wagner, M., Hawes, S., Ebersole, J.S., 2002). The use of Talairach-Tournoux coordinates transforms all of the participants' MRI data to the same 3D space, which allows for the source data to be merged across participants (for group level connectivity analysis). After importing the anatomical MRI data, manual checks were performed to ensure that the following markers were distinguished for co-registration purposes: (1) the nasion, as well as the left and right pre-auricular points were established for co-registration with the functional EEG data via the 3D Polhemus structure, and (2) the anterior commissure, the posterior commissure, and the mid-sagittal point were selected in order to establish the appropriate Talairach-Tournoux grid space to be used for source localization purposes. These methods allowed for 72 cortical brain areas, as well as 8 cerebellar regions (i.e., 80 nodes or "seed" locations), to be established for source analysis (see 4.63.2 below).

4.63 Electroencephalography (EEG)

4.63.1 Pre-Processing and Artifact Reduction

The continuous data files were first baseline corrected and the continuous data were scanned for any artifacts that might interfere with the obtained signal (i.e., eye blinks on the EOG channels). To remove ocular artifacts first an average template was generated from the signals exceeding $360\mu V$ and $-360\mu V$ respectively. A principal component analysis (PCA) was then used in order to reduce the ocular artifacts from the EEG continuous signal. The PCA retains variation in the data so that no relevant information is lost, while reducing the dimensionality of the data so that irrelevant data (i.e., eye blinks) is removed (Ringner, 2008). The EEG data was then broken into relevant epochs to facilitate a state related analysis on a block-by-block basis with respect to task condition (rest, RTP, and MI). For each condition, all of the trial epochs (i.e., 15 epochs x 30s duration) were concatenated to produce one block of data (450 s duration) for each task for each participant. For the MI blocks, the nature of the data collection produced epochs that were 40 seconds long due to the environmental and sensory imagery occurring in the first 10 seconds; these 10 seconds were removed before concatenating to preclude this sensory information from being used in the final analysis. Finally, an interleave of 10 (i.e., every tenth data point that was sampled) was applied to the 450 s task relevant data files in order to down sampled the data to 100Hz. This interleave was applied to facilitate the source estimation in Curry 7.

4.63.2 Source Estimation Using Current Density Reconstruction

The source generators of the sensor level data were estimated using current density reconstruction (CDR). Specifically, the standardized Low Resolution Brain

Electromagnetic Tomography (sLORETA) method was utilized. This particular CDR is a linear method that does not use a Laplacian smoothing component to gain a smooth solution. Instead, the sLORETA computation estimates source variances based on noise present in the data (Wagner, 2004). The location maps are derived by sLORETA using a location-wise inverse weighting of the results of a minimum norm least squares regression (via the estimated variances) (M. Fuchs, Wagner, M., Kohler, T., & Wischmann, H.A., 1999). The use of the sLORETA method was chosen over minimum norm estimate (for example) due to its lack of localization bias (Wagner, 2004). In addition, it has been documented that sLORETA methods are less likely to over-estimate the source of the data obtained at the sensor level (M. Fuchs, Wagner, M., Kohler, T., & Wischmann, H.A., 1999; Wagner, 2004). The CDR was performed on each 450 s block of task relevant data (i.e., rest, RTP, and MI) for each participant using the BEM for calculation of the forward solution (i.e., a realistic model for use in determining source locations). The CDR analysis was constrained to 80 pre-determined "seed" locations (Figure 7) (Bardouille & Boe, 2012). The use of this constrained model allows the researchers to isolate particular regions of interest, including those shown to be involved in motor planning and execution. Additionally, owing to the number of source locations possible in an unconstrained model, the spatial precision of the source estimates may not be as accurate (Diaconescu, 2011).
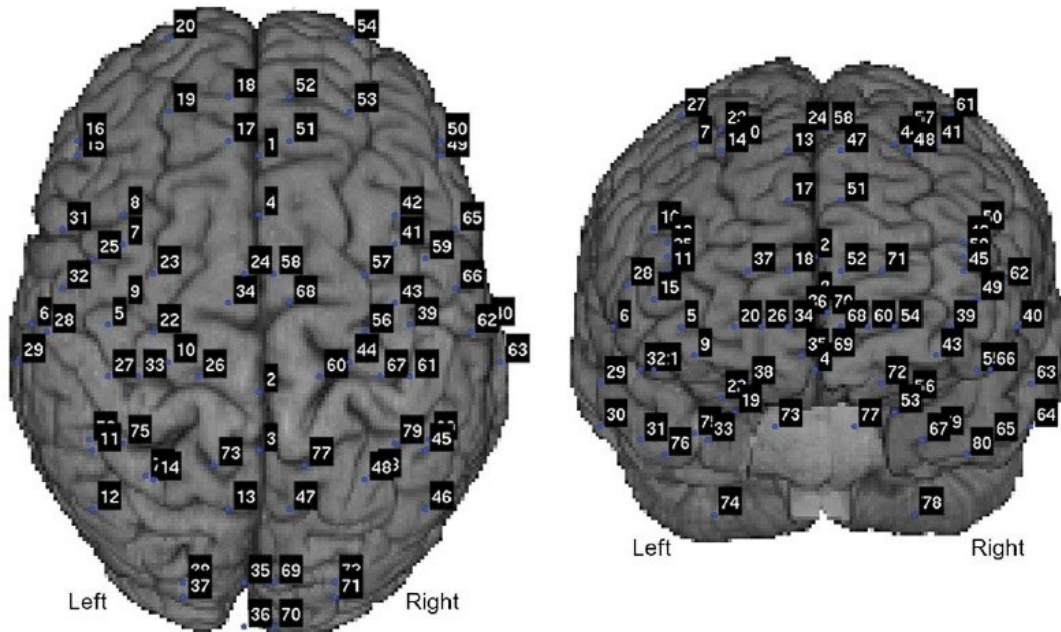
Figure 7 *Node positions overlaid onto a template brain. The figure on the left depicts the node locations from a top view of the cortex. The figure on the right shows the node positions used for source estimation as viewed from the back of the brain (Bardouille & Boe, 2012).*

For a complete list of the node names and coordinates, please see Appendix VI.

Following the CDR analysis, the CDR dipole information (position, strength, and orientation) was exported to Matlab (Mathworks, Natick, Massechussets, USA) for further analysis.

4.63.3 Beta Band Functional Connectivity Analysis

The CDR dipole data was used to calculate coherence across all possible node pairs (3160) for each condition (i.e., rest, RTP, and MI). Following the application of a Hanning window, complex Fast-Fourier transforms (FFT) were performed. The FFT is used to estimate the spectral information from the EEG signal (Thakor & Tong, 2004). The FFT contained 128 frequency bins, however, only the 19 bins from the beta band (15-30Hz) were carried forward for further analysis. A complex coherence analysis was

then performed via magnitude-square CCC for each node pair and frequency bin. Magnitude-square CCC uses time-frequency data to quantify functional coupling across seed locations via pair-wise comparisons (Gross, 2001).

4.63.4 Conditional Partial Least Squares (PLS) Analysis Within the Beta Band

Between-condition comparison in FC between nodes in the motor network was achieved by non-parametric statistical testing of changes in coherence (Bardouille & Boe, 2012; Hipp, Engel, & Siegel, 2011). Mean-centered partial least square (PLS) analysis was applied to the resultant 4D data structure (i.e., conditions X participants X frequency bins X node pairs), with the p value set to 0.05. The latent variables to be assessed were CCC during MI compared to rest, and CCC during RTP, compared to rest. The latent variables ask the questions: 1) is CCC different in MI compared to rest; and 2) is CCC different in RTP compared to rest. In both of these cases, the null hypothesis was that the conditional networks (i.e., MI or RTP) were not different from rest, which indicates that there are no significant differences between the CCC conditions across subjects. The PLS allowed for elucidation of the latent variables, which represent the conditional differences present in the CCC findings (McIntosh & Lobaugh, 2004). These inter-condition differences were established via 512 permutations to test for significant differences among latent variables. Further, the reliability of these latent variables was tested via bootstrap ratios (BSR). The BSR used 512 iterations measuring the reliability of the CCC across each possible node pair and frequency bin combination. The BSR is used to determine which elements show reliability in terms of the intended experimental effects (McIntosh & Lobaugh, 2004), which reflects node connections that are reliable during the task state as compared to rest. Once calculated, the BSR measures sign (i.e., positive or

negative) reflects the relative coherence across conditions; that is, greater or less coherence in one task state compared with the other. Within the relative latent variable (i.e., MI or RTP), all BSR values were assessed to calculate the 99.9th percentile, which represented the BSR threshold value for each condition. From this BSR threshold, task-positive networks consisting of only significant (i.e., reliable) node interactions were derived for both MI and RTP in the beta band. The BSR data were also used to create weighted (i.e., unthresholded) matrices showing the reliability of node connections for each condition.

4.64 Graph Theory

Graph theory analysis was applied to the task positive network (Bullmore & Sporns, 2009) to allow for a more powerful and discriminating analysis between conditions, facilitating the characterization of the sensorimotor network in the non-disabled participants. In particular, the PLS analysis allowed the researchers to determine whether or not the conditional network connections were significant, but it did not allow for direct comparisons across conditions. In order to achieve this comparison, graph theoretical parameters for each network were derived. At this point, the researchers created a binary coherence matrix for each condition within the beta frequency band. Within this binary matrix, all significant node connections (i.e., those exceeding the BSR threshold) were represented as a "1", and all non-significant node connections (i.e., those below the BSR threshold) were represented as a "0". From this binary matrix, connection probabilities in the forms of ND, CCo, and path lengths (PL) were calculated. Finally, SWNs were calculated for both the MI and RTP task-positive networks. In order to calculate SWNs, two sets of 20 random networks with the same number of nodes (i.e.,

80) and significant connections (i.e., number of reliable node pairs for each condition) for comparison to the MI and RTP networks were formed. From these random networks, average CCos and PLs were derived. Finally, the SWN calculation was performed via the following equations:

1) $SWN_{MI} = (CCo_{MI} / CCo_{rand[MI]}) / (PL_{MI} / PL_{rand[MI]})$

2) $SWN_{RTP} = (CCo_{RTP} / CCo_{rand[RTP]}) / (PL_{RTP} / PL_{rand[RTP]})$

The null hypothesis was that the conditional networks were not different from the generated random networks, which would be indicated by a SWN value < 1. In addition, both the MI and RTP small world parameters (i.e., CCos and PLs) obtained from the aforementioned analysis were compared to small world parameters derived from using values related to both the best (i.e., high CCo, short PL) and worst (i.e., small CCo, long PL) randomly generated networks in order to obtain a measure of variability pertaining to small worldness. All of the graph theoretical parameters were calculated via the use of the Brain Connectivity Toolbox, which is a Matlab toolbox that contains datasets used in the literature for calculating network measures (Rubinov & Sporns, 2010). The obtained parameters allowed for the efficiency of connections among various neuronal populations, and across multiple neural networks, to be compared. Further, the communication efficiency (i.e., ND, CCo, etc) of connections among secondary (i.e., PMC, SMA, etc.) and primary motor, as well as planning (i.e., PFC, parietal cortex) areas were compared between RTP and MI in order to highlight FC differences within the motor execution networks during imagined and overt movement.

4.65 Electromyography (EMG)

Online monitoring of the EMG signal was done by the researcher during all experimental trials, where any large movements during rest or MI blocks were noted. EMG signals were analyzed off-line to quantify muscle activity during MI. EMG signals were band-pass filtered for 25-100 Hz to isolate the envelope of muscle activity. To determine if muscle activity was present, EMG flexor activity during MI was compared to EMG activity during rest for each participant. An FFT was used to extract frequency information from the MI and rest block (450 s each) time series data. Absolute squared values of the FFT data were taken to calculate spectral power within the EMG signal for each MI and rest state for each participant. A qualitative evaluation of the power graphs between conditions was done in order to ensure there were no large differences in muscle activity between the two states.

CHAPTER 5 RESULTS

5.1 Participants

Due to technical issues, two of the fifteen participants had to be excluded from further analysis for the following reasons: (1) a functional data file was corrupt; and (2) the data contained constant noise artifacts occurring throughout the file that exceeded 500μV. In addition, software failures prevented the further analysis of 3 participants (see Section 7 for full explanation of limitations), further reducing the number of participants. The final analysis included 10 non-disabled young adults (23.1 ± 1.9 years; 5 females). Nine of the participants were right hand dominant and one individual was ambidextrous, as assessed via the Edinburgh Handedness Questionnaire (Oldfield, 1971). All participants had the ability to perform MI, and had little-to-no previous experience with imagined movement. Participants were all moderately active, as evidenced by participants reporting engaging in moderate physical activity ~3 days a week on the IPAQ.

5.2 Motor Imagery Experience and Ability

5.21 Motor Imagery Experience

Among the participants, only five of the included ten reported having experience with MI in the past. In addition, only two of these five stated that they had performed some form of imagined movement outside of a sport context. The remaining six participants reported never having had any previous experience with MI.

5.22 Kinesthetic Visual Imagery Questionnaire (KVIQ)

There were significant differences in kinesthetic imagery KVIQ scores pre- to post-familiarization session on day one of study involvement (W = 98, sum of positive =

109, sum of negative = -11, p = 0.0034). The pairing for the Wilcoxon signed rank test was significantly effective (Spearman = 0.7590, p = 0.0007).
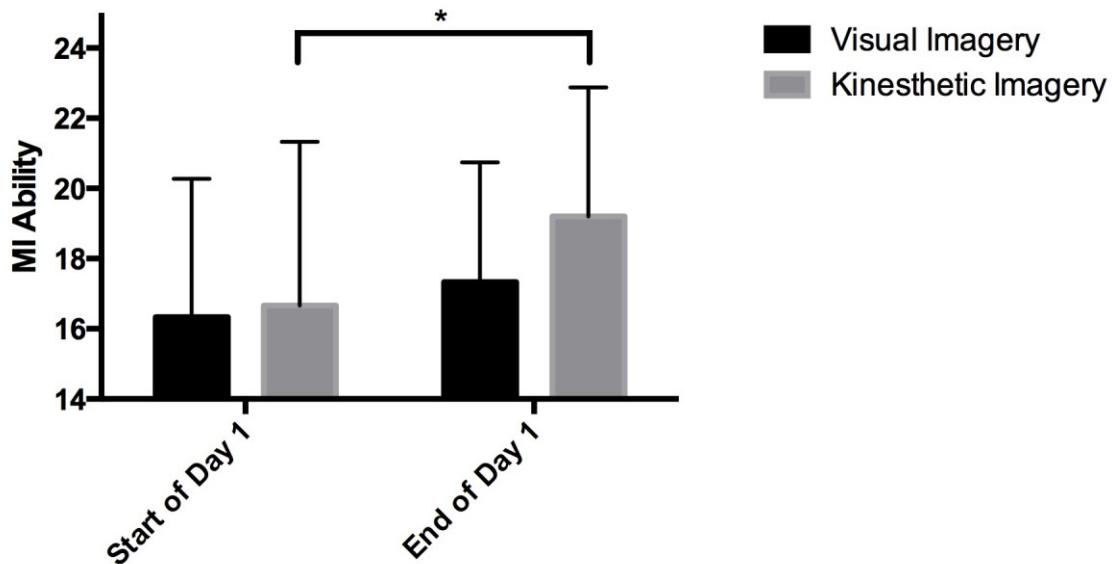
Figure 8 *MI ability in study session 1. Visual (black bars) and kinesthetic ability are shown for the start and finish of day one study involvement. While both increase over the single session, a larger increase is noted in the kinesthetic domain. Bars denote standard deviation. * denotes statistical significance, p < 0.05.*

There were no significant differences between KVIQ scores within the kinesthetic imagery domain across study days (F = 3.553, p = 0.3140). There were significant differences between KVIQ scores within the visual imagery domain across study days (F = 11.23, p = 0.0105). Follow up tests showed that the significant result was due to rank sum difference (-19.5) between visual imagery scores on day one and day four.
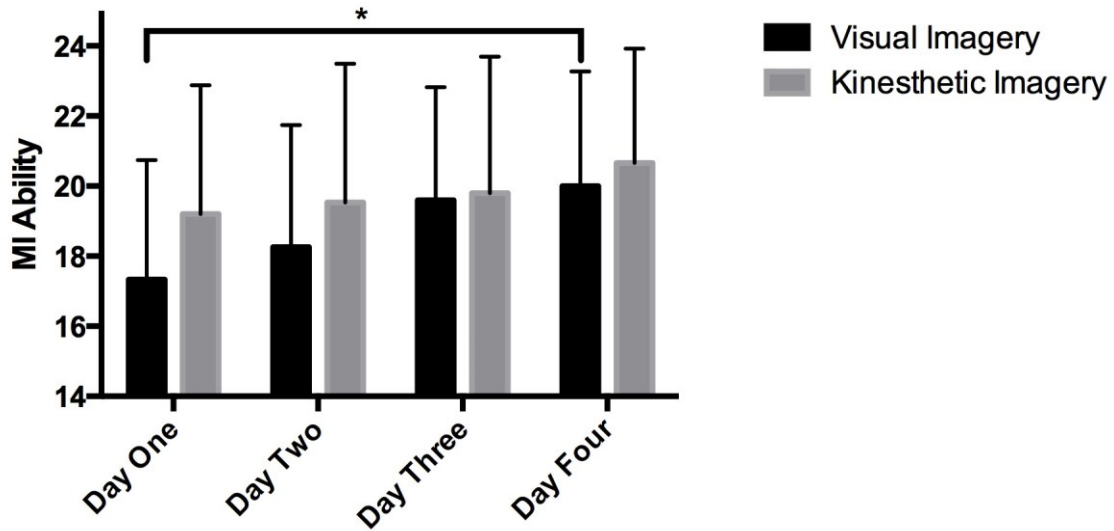
Figure 9 *MI ability over the course of the study. Visual (black bars) and kinesthetic (grey bars) ability increase over the four study days, with a larger increase noted for the visual domain. Bars denote standard deviation. * denotes statistical significant difference, p < 0.05.*

5.3 Electromyography During the Imagery Blocks

No overt movements of the right hand were noted during any rest or MI block during online monitoring of the EMG data on the experimental day of study involvement. Owing to an undetermined issue with either data collection or offline storage, the EMG data was not suitable for analysis. As a result, the intended FFT, and power spectrum calculations could not be performed (see section 7.1 for limitations).

5.4 Electroencephalograpy (EEG)

5.41 Motor Imagery Beta Band Network

5.41.1 Partial Least Square Regression for MI Within the Beta Band

The PLS analysis applied to determine differences in coherence between the task relevant network during MI and rest was significantly different ($p < 0.05$) within the beta band. To be explicit, the first latent variable (i.e., MI compared to rest) was statistically significant, indicating that there was a pattern of connectivity present during MI that was different from resting state connectivity.

The reliability of the connections present in the MI network was then investigated using the BSRs. The BSRs allowed for the calculation of a threshold to determine the task positive node pairs. The threshold BSR value for MI was -4.1238, and the maximal BSR was 7.9399. This threshold allowed the researchers to derive the task positive network consisting of only node pairs that possessed BSRs exceeding the threshold. For the MI condition, the analysis uncovered 59 significant node pairs (see Appendix VII for full list). Amongst these 59 significant node pairs, the researchers identified the pairs shown in Table 2 as being of interest for exploration. The node pairs in Table 2 were selected based on their known contribution to the sensorimotor network (Ciccarelli et al., 2005), and their involvement in MI (Hetu et al., 2013).

Table 2*: Node Pairs Within the MI Network*

Significant Node Pairs During MI				
Node	*Hemisphere*	*Node*	*Hemisphere*	*BSR Value*
Inferior Parietal Cortex	Left	Ventral Temporal Cortex	Right	-5.306369781
Superior Parietal Cortex	Left	Medial Prefrontal Cortex	Right	-5.063730717
Medial Premotor Cortex	Left	Superior Parietal Cortex	Right	-4.992370605
Medial Premotor Cortex	Left	Ventrolateral Premotor Cortex	Right	-4.599886417
Primary Motor Cortex	Right	Dorsolateral Prefrontal Cortex	Right	-4.439273834
Primary Sensory Cortex	Left	Ventrolateral Prefrontal Cortex	Right	-4.318048477

The node pairs shown in Table 2 reflect the involvement of the fronto-parietal network,

as well as regions of the motor and sensory systems in the performance of MI.

5.41.2 Cortico-Cortical Coherence for MI Within the Beta Band

Figure 10 shows the CCC within the beta band found across all possible node pairs (3160) for the 80 preselected nodes during MI. More specifically, the following matrix depicts the weighted BSR data, which allows for the interpretation of reliability information. Due to the orientation of the MI latent variable as negative (see Appendix VIII for graph showing significance), all task related coherence was shown as negative, which is pictured as blue within the matrix. Node connections that expressed high reliability are shown in darker blue.

Figure 10 Weighted Coherence Matrix for CCC During MI Within Beta: The above matrix shows the significant node pairs involved in the MI task where node connections with higher reliability (assessed via BSRs) are pictured in deeper shades of blue. This figure depicts the 80 nodes along both the vertical and horizontal aces, and as such, the matrix is mirrored along the diagonal.

Figure 11 shows the thresholded CCC within the beta band found across only significant node pairs for the 80 preselected nodes during MI. The BSR threshold of 4.1238 was applied to include only those node pairs that were within the 99.9[th] percentile. Task related increases in connectivity are pictured in Figure 11 as blue nodes.

Figure 11 *Thresholded Coherence Matrix During MI for Beta: This coherence matrix shows only those node connections that fall within the threshold set based on the BSR calculations. The boxes shaded in blue on this graph depict those connections within the 99.9[th] percentile of the possible node pairs. This figure depicts the 80 nodes along both the vertical and horizontal aces, and as such, the matrix is mirrored along the diagonal.*

Figure 12 is a representation of the task-positive network associated with MI as viewed from the top of the brain. The red lines are the BSR values that connect significant nodes and indicate the reliability of each connection. For those node pairs with the most reliable connection (i.e., higher BSR) the red line appears thicker.

Left   Right

Figure 12 *Task-Positive Network During MI: This figure shows the network underlying MI. The nodes are depicted as blue circles, while the connections are shown as red lines. The thicker red lines indicate a more reliable connection, as evidenced by the BSR values. Of particular interest are connections that occur during MI between the right parietal and left prefrontal regions. The relative dispersion of node connections in the MI network should also be noted.*

5.42 Repetitive Task Practice Beta Band Network

5.42.1 Partial Least Square Regression for RTP Within the Beta Band

The PLS analysis applied to determine differences in coherence between the task relevant network during RTP and rest was significantly different ($p < 0.05$) within the beta band. To be explicit, the first latent variable (RTP compared to rest) was statistically significant, indicating that there is a pattern of connectivity present during RTP that is different from resting state connectivity.

The researchers then investigated the reliability of the connections present in the RTP network via BSRs; in particular the BSR allowed for the calculation of a threshold to determine the task positive node pairs within the beta band. The threshold BSR value for RTP was -2.5871, and the maximal BSR was 3.1379. This threshold allowed for the researchers to derive the task positive network consisting of only node pairs that possessed BSRs exceeding the threshold. For the RTP condition, the analysis uncovered 58 significant node pairs (see Appendix IX for full list). Amongst these 58 significant node pairs, the researchers identified the pairs shown in Table 3 as being of interest for exploration. The node pairs in Table 3 were selected based on their known contribution to the sensorimotor network (Ciccarelli et al., 2005; Gerardin et al., 2000).

Table 3*: Node Pairs Within the RTP Network*

Significant Node Pairs During RTP				
Node	*Hemisphere*	*Node*	*Hemisphere*	*BSR Value*
Primary Motor Cortex	Right	Primary Visual Cortex	Right	-2.642186403
Primary Motor Cortex	Right	Medial Prefrontal Cortex	Left	-2.603501558
Frontal Eye Fields	Right	Superior Parietal Cortex	Right	-2.738321304
Dorsomedial Prefrontal Cortex	Right	Primary Sensory Cortex	Right	-2.569637775
Ventrolateral Prefrontal Cortex	Right	Medial Premotor Cortex	Right	-2.590708017
Contralateral Prefrontal Cortex	Left	Parahippocampal Cortex	Right	-2.74141264

The node pairs shown in Table 3 implicate the motor areas, as well as some prefrontal,

parietal and parahippocampal regions in the successful performance of a functional task.

5.42.2 Cortico-Cortical Coherence for RTP Within the Beta Band

Figure 13 shows the CCC within the beta band found across all possible node pairs (3160) for the 80 preselected nodes during RTP. More specifically, the following matrix depicts the weighted BSR data, which allows for the interpretation of reliability information. Due to the orientation of the RTP latent variable as negative (see Appendix X for graph showing significance), all task related coherence was shown as negative, which is pictured as blue within the matrix. Node connections that expressed high reliability are shown in darker shades of blue.
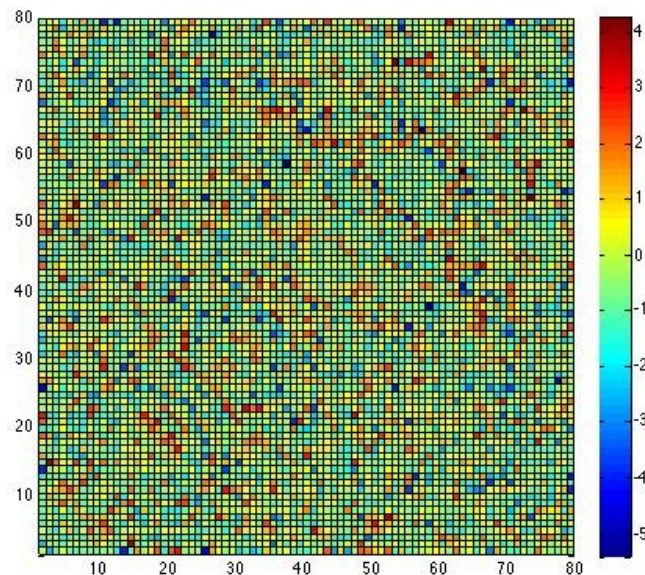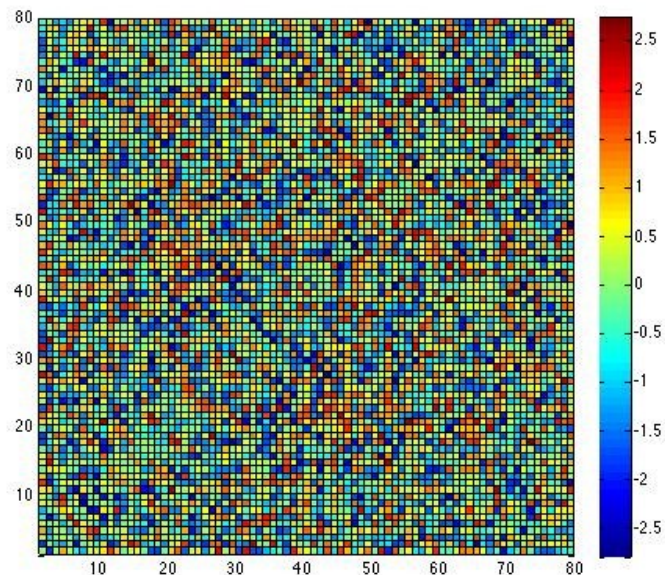

Figure 13 *Weighted Coherence Matrix for CCC During RTP Within Beta: The above matrix shows the significant node pairs involved in the RTP task where node connections with higher reliability (assessed via BSRs) are pictured in deeper shades of blue. This figure depicts the 80 nodes along both the vertical and horizontal aces, and as such, the matrix is mirrored along the diagonal.*

Figure 14 shows the thresholded CCC within the beta band found across only significant node pairs for the 80 preselected nodes during RTP. The BSR threshold of 2.5871 was applied to include only those node pairs that were within the 99.9^{th} percentile. Task related increases in connectivity are pictured in Figure 14 as blue nodes.
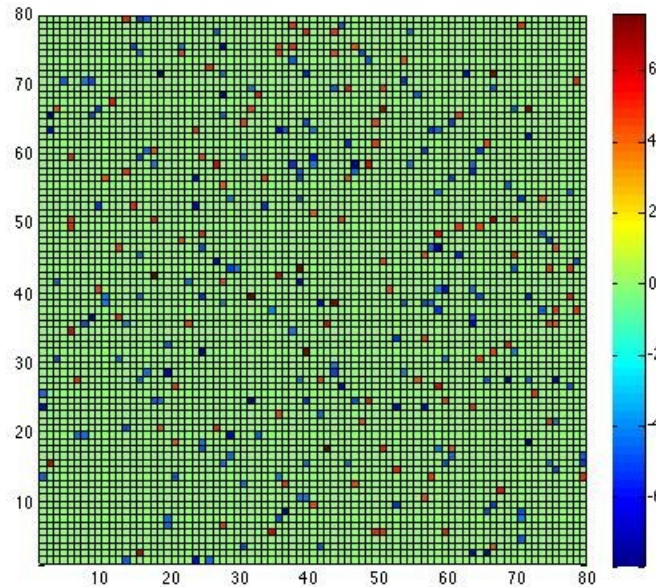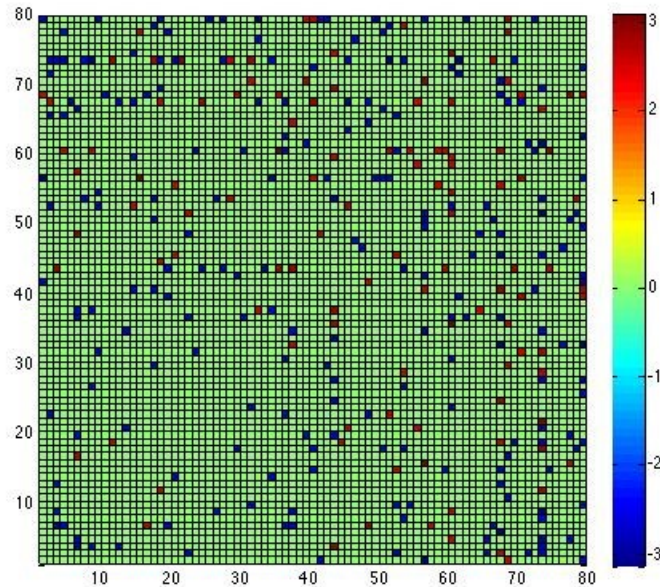

Figure 14 *Thresholded Coherence Matrix During RTP for Beta: This coherence matrix shows only those node connections that fall within the threshold set based on the BSR calculations. The boxes shaded in blue on this graph depict those connections within the 99.9^{th} percentile of the possible node pairs. This figure depicts the 80 nodes along both the vertical and horizontal aces, and as such, the matrix is mirrored along the diagonal.*

The following is a representation of the task-positive network associated with RTP as viewed from the top of the brain. The red lines are the BSR values that connect significant nodes and indicate the reliability of each connection. For those node pairs with the most reliable connection (i.e., higher BSR) the red line appears thicker.
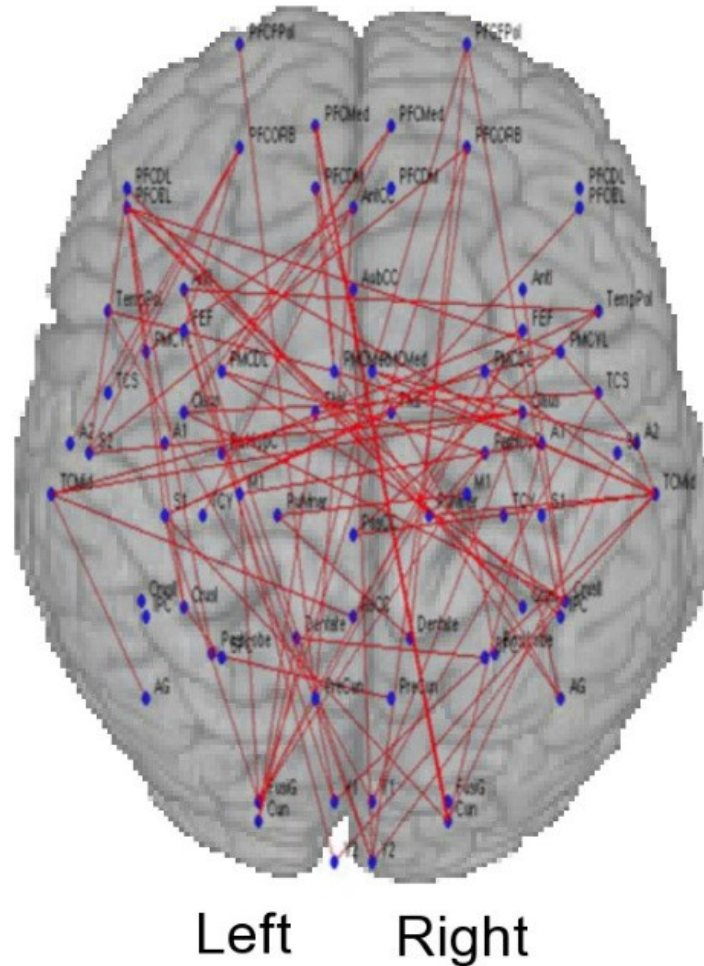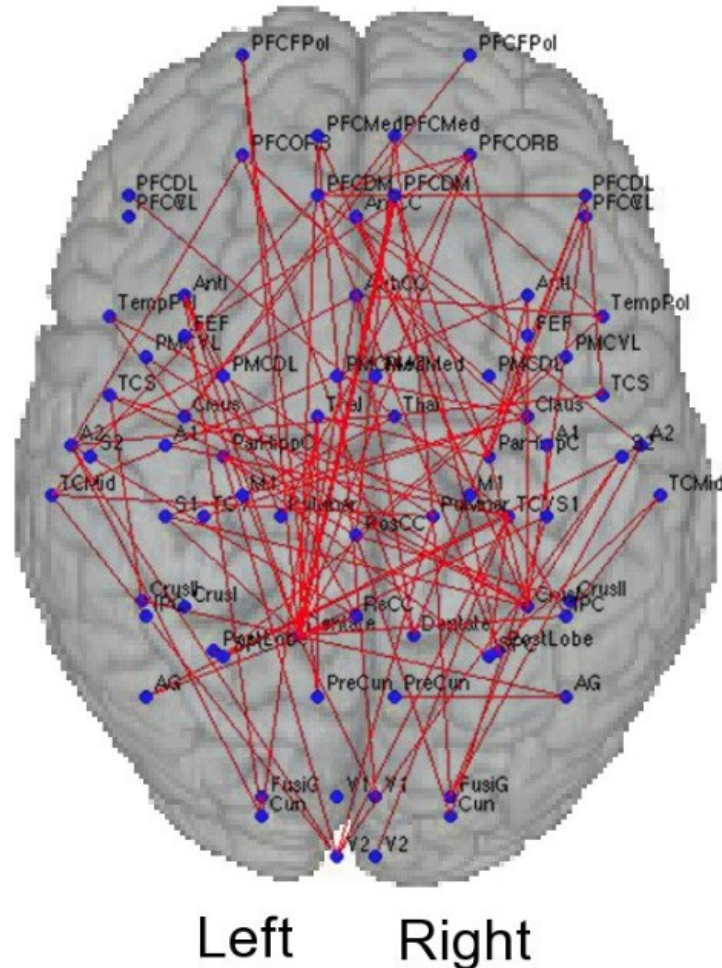

Figure 15 Task-Positive Network During RTP: *This figure shows the network underlying MI. The nodes are depicted as blue circles, while the connections are shown as red lines. The thicker red lines indicate a more reliable connection, as evidenced by the BSR values. Of particular interest is the greater amount of connections in the left hemisphere. The relative dispersion of the connectivity within the RTP network appears lesser than that of the MI network.*

5.43 Graph Theoretical Analysis

5.43.1 Node Degree

Figures 16 and 17 show the binary matrix data thresholded to only include task-positive node pairs for both the MI and RTP conditions respectively. The task positive node connections (i.e., those that fall within the relevant threshold) are represented in black. All node pairs that are not task positive (i.e., those that do not fall within the relevant threshold) are white. Node degree can be calculated from these binary matrices by counting a given nodes connections (represented by the white squares) along its repesentative row or colum.
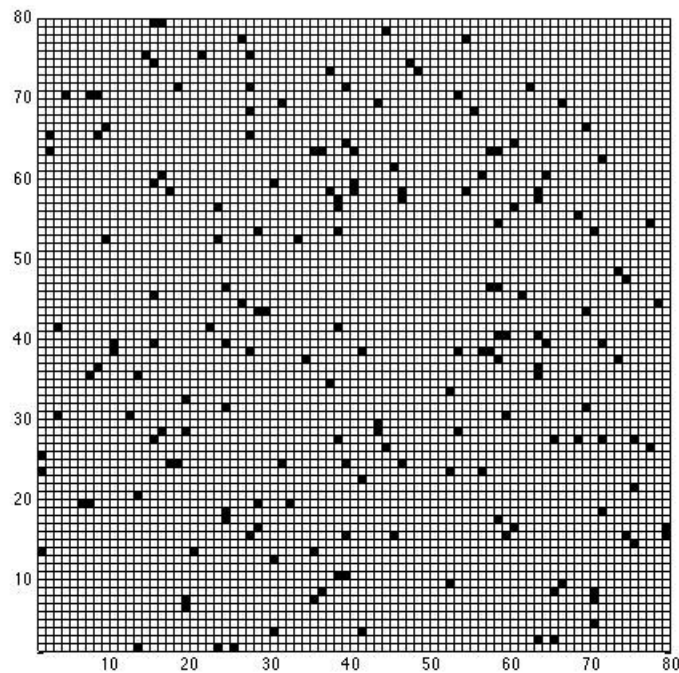
Figure 16 *Binary Matrix for CCC During MI: This matrix shows only task-positive node connections during the performance of MI, which are depicted by the black boxes.*

70
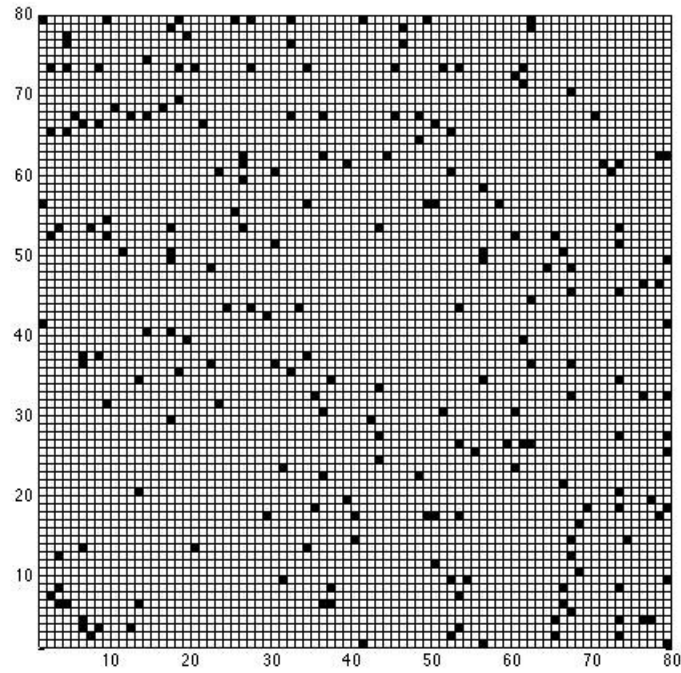
Figure 17 *Binary Matrix for CCC During RTP: This matrix shows only task-positive node connections during the performance of MI, which are depicted by the black boxes.*

The binary matrices allowed the researchers to investigate the network on the

basis of whether or not a node was involved in the performance of the task. These binary

measures of node involvement are used to derive graph theoretical parameters.

Table 4 contains the ND for pre-defined nodes in Talairach space possessing

connectivity during MI. These measures of node degree have been derived from FC data

found within the beta band during MI.

Table 4: *Node Degree for the Task Positive Network During MI*

Node	ND
Contralateral Prefrontal Cortex - Left	6
Primary Sensory Cortex - Left	6
Medial Premotor Cortex - Right	6
Middle Temporal Cortex - Right	6
Medial Premotor Cortex - Left	5
Dorsolateral Premotor Cortex - Left	4
Secondary Sensory Cortex - Left	4
Frontal Eye Field	3
Claustrum - Left	3
Precuneus - Left	3
Dorsolateral Prefrontal Cortex - Left	3
Primary Visual Cortex - Left	3
Frontal Eye Field - Right	3
Ventrolateral Prefrontal Cortex - Right	3
Parahippocampal Cortex - Right	3
Primary Motor Cortex - Right	2
Inferior Parietal Cortex - Right	2
Superior Temporal Cortex – Right	2
Ventrolateral Prefrontal Cortex –Left	1
Primary Motor Cortex - Left	1
Precuneus - Right	1

The ND measures shown in Table 4 only include a subset of the task-positive

nodes for MI (see Appendix XI for the entire list of NDs). The brain regions listed here

have been chosen for their known contribution to the performance of MI (Hetu et al.,

2013). Of note, areas in the premotor cortices displayed the greatest relative ND during

the task, as compared with areas such as M1 for example. In addition, areas located

within the medial temporal cortex (TC), as well as large portions of the PFC had high

NDs within the task positive network present during MI. Finally, it is of importance to

note that regions within the parietal cortex, which has been implicated in MI performance in the past, did not have the largest ND with respect to the entire network.

Table 5 contains the ND for the pre-defined nodes possessing connectivity during RTP. These measures of node degree have been derived from FC data found within the beta band during RTP.

Table 5*: Node Degree for the Task Positive Network During RTP*

Node	ND
Dentate - Left	11
Ventral Temporal Cortex - Left	8
Secondary Auditory Cortex – Left	6
Dorsomedial Prefrontal Cortex - Left	6
Parahippocampal Cortex - Left	5
Secondary Sensory Cortex - Left	5
Medial Prefrontal Cortex - Left	4
Claustrum - Left	4
Primary Sensory Cortex - Right	4
Superior Temporal Cortex - Right	4
Precuneus - Left	3
Primary Sensory Cortex – Left	3
Superior Parietal Cortex - Left	3
Frontal Eye Field - Left	2
Ventrolateral Premotor Cortex - Left	2
Primary Visual Cortex - Left	2
Primary Motor Cortex - Right	1
Medial Premotor Cortex - Right	1

The ND measures shown in Table 5 only include a subset of the task-positive nodes for RTP (see Appendix XII for the entire list of NDs). The brain regions listed here have been chosen for their known contribution to the performance of a goal directed overt movement task (Gerardin et al., 2001). Of note, areas in the cerebellar and temporal cortices displayed the greatest relative ND within the network. In comparison, areas such as the M1 had small measures of connectedness. Brain regions located within the prefrontal, and parahippocampal cortices had high NDs within the task positive network

present during RTP, indicating their heavy involvement in the task. In comparison to the

MI network, parietal regions exhibited relatively similar involvement in the RTP

network. Finally, brain areas responsible for sensory integration were also implicated as

being necessary for completion of the functional task

Tables 6 and 7 show the brain regions that expressed the highest ND for both the

MI and RTP tasks. The brain regions involved differed greatly across the two states. For

example, planning regions such as the PFC and PMC seem to be vital to the performance

of MI, as compared to RTP execution, which appears to rely more heavily on

connectivity within the cerebellum.

Table 6: *Brain Regions With the Highest ND for MI*

Highest ND During MI		
Node	*Hemisphere*	*ND*
Contralateral Prefrontal Cortex	Left	6
Primary Sensory Cortex	Left	6
Medial Premotor Cortex	Right	6
Middle Temporal Cortex	Right	6
Medial Premotor Cortex	Left	5

Table 7: *Brain Regions With the Highest ND for RTP*

Highest ND During MI		
Node	*Hemisphere*	*ND*
Dentate	Left	11
Ventral Temporal Cortex	Left	8
Secondary Auditory Cortex	Left	6
Dorsomedial Prefrontal Cortex	Left	6
Parahippocampal Cortex	Left	5

5.43.2 Small World Networks

Within the beta band, the task positive network that exists during the MI blocks exhibits a CCo of 0.005833. Within the task-positive MI network, the characteristic PL was 4.5438. In comparison, the task positive network characteristic of RTP shows a CCo of 0.024513. The higher CCo during RTP is an indication of a more ordered network. Within the task-positive RTP network, the characteristic PL was 3.7101. Following calculations of conditional CCo and PL, small worldness was calculated. The results show that both the MI and RTP networks exhibit small world properties (i.e., are SWNs) when compared to a randomly generated network possessing the same number of nodes and edges (SWN_{MI} = 1.1048; SWN_{RTP} = 6.0169), where small worldness was defined as a SWN statistic greater than 1. Importantly, the degree to which the RTP network was a SWN (as compared with random) was greater (i.e., 6.0169) than that of MI (1.1048). In order to explore variability in the SWN statistics obtained, the researchers compared the MI and RTP small world parameters to those of both the best (i.e., high CCo, small PL) and the worst (i.e., small CCo, high PL) random networks. The researchers found that as compared to the best random networks, neither of the task-positive networks were considered small world (SWN_{MI_Best} = 0.1866; SWN_{RTP_Best} = 0.6932); however, of note is the observation that the RTP network was approaching 1. Further, when compared to the worst random networks, both of the task-positive networks were considered small world (SWN_{MI_Worst} = 1.3280; SWN_{RTP_Worst} = 9.6908). Importantly, as compared with the worst random network, the RTP condition expressed a greater degree of small worldness as compared with the MI, which is in keeping with the average SWN statistic findings.

CHAPTER 6 DISCUSSION

6.1 Key Findings

The primary aim of this project was to quantify the patterns of functional connectivity underlying MI in non-disabled participants and compare these patterns to those active during the overt performance of a functional motor task (i.e., making a sandwich). Importantly, statistically significant differences were found between the task-positive networks active within the beta band during both the MI and RTP blocks, as compared to resting state connectivity. In addition, the significant node pairs established within both the MI and RTP beta task-positive networks provide interesting insight into the underlying neural correlates of these two conditions. During MI, FC was characterized predominantly by interactions that existed between parietal and prefrontal regions, as well as coherent activity signifying FC between motor areas including the right M1 and medial PMC in the left hemisphere (see Appendix VII for other connections). Further, graph theory measures uncovered the medial PMC as being a node with high degree, indicative of its role as a 'hub' for communication during MI. During overt performance of the functional task, FC was characterized by interactions between the primary visual cortex (V1), as well as the PFC and the M1 (see Appendix IX for full list of node pairs). Similar to the network observed for MI, functional connections were noted between parietal and prefrontal cortical areas. Further, graph theory analysis uncovered that the PFC and regions of the cerebellum in the left hemisphere were hubs for the performance of the functional task as evidenced by their high ND. Importantly, the current study found that a familiarization protocol coupling RTP and MI can be used to improve imagined movement ability in non-disabled participants both within one

session, and across four days of study involvement. The above findings as well as the study limitations will be discussed in full in the following sections.

6.2 Effectiveness of the Familiarization Protocol

The findings of this study outline that participants experienced a significant improvement in MI ability following one familiarization session, and across all study days. On the first day of study involvement, participants showed improvements in MI ability within the kinesthetic imagery domain. This is in keeping with the research aims and hypothesis as the instructions provided to participants encouraged first person kinesthetic imagery. In support of this notion, familiarization protocols have been used in the past to teach first person MI to non-disabled individuals (Gentili, Papaxanthis, & Pozzo, 2006). In addition, MI practice coupled with RTP has been shown to improve the ability to perform imagined movement and the functional movement itself in those with neurological insult (S. J. Page, Levine, P., Sisto, S.A., & Johnson, M.V., 2001). These findings support the claim that a familiarization protocol can be used to increase the vividness of MI performance. Based on the finding of improved KVIQ scores (and thus better MI), it can be inferred that the participants were actively engaging in the RTP and MI protocol on day one of study involvement. The improvements seen in MI ability most likely would result from the MI-based practice that comprised part of this first session, which in-turn leads us to the conclusion that the participants were attending to the MI task when prompted. The success seen across participants on day one might reflect the benefits of using auditory-guided imagery. The auditory script successfully guided the participants' attention in focusing on the task to be imagined. Holmes and Collins (2001) propose that successful MI scripts should include reference to the following

characteristics: physical, environment, task, timing, learning, emotion and perspective. The auditory scripts used in the current study attempted to include all of the above characteristics, and, in addition, the researcher provided all of the participants with explicit instructions regarding maintaining focus on such characteristics. The improved MI performance on day one of study involvement support the notion that the auditory script used possessed the appropriate properties for teaching first person imagery.

While improvements were seen on day one in the kinesthetic domain, these results were not replicated when MI ability was compared across all study sessions. Instead, participants displayed a significant improvement in MI ability within the visual domain between day one and day four. This finding suggests that by day four, participants were no longer engaging in first person, but rather third person MI (i.e., imagining watching themselves perform the movement as a bystander). This finding could be a result of the particular wording used in the auditory script for guiding the MI. While participants were instructed to imagine themselves performing the task from "behind their own eyes", there is the potential that these cues were lost once participants began the self-initiated MI task. In particular, the scripts used were meant to highlight motor aspects of the movement (e.g., focusing on the way the arm moves through the air), which may have incidentally led individuals to picture watching their arm movement as a bystander instead of imagining themselves generating the movement. This improvement in MI ability seen between day one and day four however reflects the success of the familiarization protocol as a whole in teaching the basic skills necessary for MI. These findings are further supported by literature stating that when mental

practice is augmented by physical practice, improvements are seen in MI ability (P. L.

Jackson et al., 2004; S. J. Page, Levine, P., Sisto, S.A., & Johnson, M.V., 2001).

The improvements seen in MI ability in both the kinesthetic and visual domain

verify that the state related brain activity data collected via EEG on the experimental day

was indeed a reflection of the performance of MI.

6.3 Functional Connectivity During Motor Imagery

The following section will address the first objective of this thesis:

(1) to determine the pattern of FC within the sensorimotor network during the

imagined (MI) performance of a functional task.

The results of the PLS analysis found that the network active during MI was significantly

different from that of rest, indicating that the node-node interactions present within the

network are reflective of the FC specific to the relevant condition (i.e., MI). These MI-

based interactions are discussed in the following section(s), and while reflective of the

results obtained, the findings need to be considered in the context of the limitations

imposed by source level analysis of EEG sensor level data (discussed in detail in Section

7.2), in addition to the loss of EMG data (see Section 7.12). The node-pairs chosen for

discussion involved structures known for their involvement in MI (i.e., PC), or those that

expressed high ND within the task-positive network.

6.31 The Role of the Prefrontal Cortex

In addressing the first study hypothesis, the results of this project display

significant interaction between PFC and regions of the PMC as well as the PC within the

beta band network during MI. In brief, the PFC is responsible for executive function,

which allows individuals to make judgments and decisions, as well as goal directed

movements. In more detail, the PFC is involved in taking information from other brain regions in order to produce coordinated, purposeful behaviour, such as successful manipulation of objects in the environment (Miller, 2001). Given that the intent of this work was to examine networks related to actual and imagined movements, for the purposes of this project, the role of the PFC will be discussed in the context of its motor functions.

When looking at the node pairs that express significant interaction within the beta band during MI, there is an important connection between the dorsolateral (DL)-PFC and M1 in the right hemisphere. Functional connectivity amongst these two brain regions could be a result of the role that the PFC is thought to play in both the initiation and inhibition of movements (Knight, 1999; Konishi, 1999). More specifically, the PFC contributes in part to inhibition of incorrect responses to stimuli in the environment. In support of this notion, Leung and Cai (2007), using fMRI, found that the ventrolateral (VL)-PFC, in both the right and left hemispheres, becomes active when subjects respond to a "go-no-go" task paradigm. The "go-no-go" task involves correctly responding to visual stimuli based on the congruency between the current trial and the previous trial target. The "go-no-go" task paradigm has individuals respond via a motor response (e.g., a button press when the stimuli presented are congruent) in order to assess inhibition of incorrect responses. The results of the study show that the VL-PFC becomes active during motor response inhibition when task cues are incongruent. These findings are in keeping with previous research done by Garavan (1999) showing that when non-disabled individuals are asked to inhibit motor responses (in the form of a button press) to incongruent targets, activity measured via fMRI occurs in the PFC (Garavan, 1999). In

addition, M. Jeannerod (2001) suggest that the DL-PFC might intervene during mental simulation states (i.e., MI) before the overt movement can start, further supporting the PFC's potential role in response inhibition. Taking these findings together, the connectivity between the DL PFC and M1 may well represent the inhibition during the imagined movement task. It should be noted that in the current study however it was the DL-PFC (and not VL as mentioned above) identified as being functionally connected to M1. It is likely that the source localization techniques used do not have the spatial specificity to tease apart the dorsal and ventral portions of the lateral PFC (see Section 7.2), which may account for why the current project found DL-PFC activity.

In addition to the PFC's role in response inhibition, research using effective connectivity to investigate neural activity via DCM has found that the SMA may play a roll in the inhibition of overt movement during MI (Kasess et al., 2008). The function of the SMA will be considered in more detail in Section 6.32, however it should be stated at this point that inhibition of motor activity during MI might be a result of this premotor structure and not the PFC. While other brain regions work to produce a virtual image and the related motor plan during MI, the PFC is part of the network in order to prevent the incorrect response (in this case overt movement) from occurring. As such, it can be understood that during MI, a network that exists in the lateral portion of the PFC, in part, mediates response inhibition.

A final consideration in the FC present between the DL-PFC and the M1 is the fact that this connection occurred in the right hemisphere (i.e., ipsilateral to imagined movement). Other FC was found between areas in the left M1 and surrounding brain regions (to be discussed later), however given that the MI task focused on right hand

movements, the researchers expected isolated left hemisphere (i.e., contralateral) M1 activity. The reason for this finding might be the simple fact that the imagined task used was a simulation of UL movement. More specifically, research has shown that overt UL movements might include both contralateral and ipsilateral M1 activation (Chen, 1997; Jankowska & Edgley, 2006). In addition, the functional task participants engaged in required bimanual coordination, which could account for the ipsilateral M1 activity seen during MI of this task. Finally, recent research by Boe et al. (2014) has documented significantly greater activity in ipsilateral sensorimotor cortex (compared to contralateral) early in the learning of MI, which may explain the increased connectivity seen in ipsilateral M1 during this study.

Further investigation of the network during MI shows that the left hemisphere PFC is coherent in the beta band with regions as diverse as the right S1, the left superior PC, as well as the left inferior and superior temporal cortices (TC). It is clear that the PFC functions within the beta band during MI to contribute to the planning of movement through interactions with S1 for integration of sensory feedback, and the PMC for movement planning. The FC between the PFC and S1 may be a reflection of sensory integration. The PFC takes relevant task related information in the form of visual, auditory, or tactile feedback from the sensory cortices, and then works to plan an appropriate motor response (Knight, 1999). In the context of this project, the PFC likely receives sensory information from S1 related to the MI task. This sensory information is then incorporated into the motor plan, which is relayed to relevant motor areas, in this case the PMC. The current literature has suggested that this internal simulation of kinesthetic sensations in S1 seems to be necessary for successful performance of MI

(Mulder, 2007). In addition to prefrontal interactions with S1, connectivity derived from the PFC within the beta band plays a role in acquiring both a concept of self (via interactions with the parietal cortex: see Section 6.33.1) as well as the environment (via interaction with the TC) during MI. The CCC exhibited between prefrontal and temporal areas is best understood in the context of the TC's role in the integration of visual and auditory information (Beauchamp, 2004; Belin, 2002). In particular, the TC has been implicated in the successful identification of objects in the environment, lending to this cortical region's role in visual perception (Miyashita, 1993). As such, it can be inferred that during MI, FC between the PFC and TC might reflect understanding of objects in the physical world.

6.32 Activation of Sensorimotor Regions During MI (The PMC, SMA and M1)

The results of this study revealed CCC among regions of the PMC in the beta band, which is in keeping with the current literature regarding brain activity during MI (J. Decety, 1996; Gerardin, 2000). The PMC is commonly broken into the lateral and medial premotor cortices for analysis purposes, as function in this part of the cortex is region specific. The lateral PMC is well documented to be involved in coding for the intention to move (i.e., motor planning) (G. Rizzolatti, Fogassi, L., & Gallese, V., 2002). The medial PMC consists of a region known as the supplementary motor area (SMA), which is known to play a role in the self-regulated initiation of movement (Cunnington, Windischberger, Deecke, & Moser, 2002). It should be noted that differentiating the two premotor regions is difficult with the current analysis (see section 7.2).

When considering important node pairs present during MI within the beta band, the present study found an interesting connection between the left DL-PMC and the right

middle TC. It is possible that the lateral PMC expresses coherence with the middle TC during MI for the purposes of further incorporating visual perceptual information into the intended motor plan, or in this case imagined movement. This notion is in keeping with documentation that production of the appropriate visuomotor associations for contribution to the motor plan occurs respective to connectivity between temporal and premotor areas, and is importantly mediated by the PFC (Toni, Ramnani, Josephs, Ashburner, & Passingham, 2001) (see Section 6.31). Within the beta band during MI, PMC-TC interactions occur in order to associate visual patterns with motor responses and produce a visuomotor representation of the intention to move. This finding should be interpreted in the context of the relative importance of the TC to the task positive network. In particular, the right hemisphere middle TC is only involved in CCC during MI, and not overt movement. This context infers that the right middle TC is a brain region that is vital to the performance of an imagined, and not overt, movement task. As such, one could conclude that connectivity between the TC and the PMC is necessary for the execution of MI based on its contribution to the formation of visuomotor associations.

The MI task-positive network generated in this study displayed a significant node pair within the beta band between the right VL-PMC and the left medial PMC (i.e., the SMA for the purposes of this discussion). The FC found across these regions was anticipated as it has been documented in the past that during MI, right hemisphere SMA is coupled with left hemisphere lateral PMC activation assessed via fMRI in healthy adults (Porro, 2000). Further, it has been suggested that the PMC has a part in action observation and imitation (G. Rizzolatti, Fogassi, L., & Gallese, V., 2002). Based on this idea, within the current study FC between the left lateral PMC and the right SMA might

be involved in representing the spatial constructs of the imagined action. The researchers hypothesize that this spatial representation of movement mechanics within the premotor areas is based on the previous observation of the RTP movement. More specifically, in the experimental paradigm participants engaged in the reach and grasp sandwich-making task, and then immediately after closed their eyes and performed guided MI of the same task. The result may be that a form of action-observation occurred, which preserved the movement mechanics and used this to represent the intended imagined movement within the premotor cortices. The above hypothesis is based on evidence documenting the similarities of action-observation and MI. In brief, action-observation refers to the activity seen in motor areas when individuals watch others performing movement, and this brain activity is thought to represent an attempt at replicating and simulating the observed action without the intended movement (i.e., similar to MI). Further, G. Rizzolatti, Fadiga, L., Gallese, V., & Fogassi, L. (1996) documented that areas in the PMC become active during observation of hand movements, which are brain regions similarly activated consistently in the literature during the performance of MI (Hetu et al., 2013). In the current project, the hypothesis that MI performance has resulted in properties of brain activity that overlap with those of action-observation cannot be explicitly stated, but simply inferred. More research is necessary in order to tease out these two neural networks.

In this study, M1 in the right hemisphere was found to have significant interaction with other nodes. More specifically, there was a functional connection during MI between the right lateral PFC and M1 during MI in the beta band. While the role that the PFC may have in impacting ipsilateral (i.e., right hemisphere) M1 has been discussed

above (see Section 6.31), this section will address the involvement of contralateral (i.e., left hemisphere) M1 in the task-positive network during MI. It is important to understand that while the overt performance of the functional task was bilateral in nature, instructions for the MI explicitly asked participants to focus on imagining right hand reach and grasp movements. This context is critical in assessing the fact that there was CCC found that involved the left hemisphere M1 (contralateral to the imagined active hand) during MI. This finding reflects the fact that the MI script was successful in guiding individuals to engage in MI that caused representations of the imagined movement within the contralateral sensorimotor network. The involvement of M1 in neuroimaging studies investigating the neural correlates of MI has been heavily debated (Kosslyn, 2001). A study by Dechent (2004) investigated M1 involvement in imagined sequential thumb and index finger opposition tasks; the researchers found that fMRI can be used to uncover activation in the contralateral M1, as well as regions of the PMC and SMA during MI. This finding has been replicated in the current study, as well as in other MI literature (Ehrsson, Geyer, & Naito, 2003; Porro, 2000). In contrast, some researchers suggest that during MI the SMA might inhibit activity in the contralateral M1. In support of this concept, Kasess et al. (2008) found that DCM could be used to determine that the SMA is in fact having an effect on the M1 during an imagined movement protocol, which was interpreted as inhibition of the motor cortex. In contrast to claims by Kasess et al. (2008), a previous review by M. Jeannerod (2001) has stated that the presence of M1 activity at all implies that the SMA does not exhibit an inhibitory cortico-cortical connection with M1 during MI. Instead, the researcher suggests that the neural mechanism inhibiting overt movement during MI might exist somewhere downstream

(i.e., within the corticospinal tract, for example) (M. Jeannerod, 2001). In the current study, it is impossible to tease out exactly what brain regions (if any) might be having an inhibitory impact on M1. However, it is important to consider the implications of MI being able to induce sensorimotor activity within the primary motor cortices in this project. The involvement of M1, as well as areas such as the PMC and S1, indicate that MI of a functional task successfully simulates the sensorimotor network in non-disabled participants, which lends the potential for the use of this type of MI paradigm in treating patients with neurological insult resulting in motor impairment.

6.33 Parietal Cortex Involvement

During MI, the task-positive networks for the beta frequency band expressed a large number of connections involving various parts of the PC. The posterior PC is considered to be involved in preserving kinesthetic awareness and spatial aspects of movement (S. T. Grafton, & Arbib, M.A., 1996). As a result of this, it is not surprising that the performance of MI in this study resulted in considerable FC between the PC and other brain regions. This concept is supported by research showing that in healthy controls the bilateral parietal cortices are active during imagined tasks (Fleming, Stinear, & Byblow, 2010; Lorey et al., 2010).

6.33.1 Parietal Cortex

In the current study, the network activated during MI in the beta band was characterized by a number of connections between the PFC and regions in the PC. It has been suggested that MI activates areas associated with movement planning and ideation (Gerardin, 2000), which may explain why in the current experiment (and much of the literature) the network patterns characteristic of MI consist of fronto-parietal interactions.

Sack et al. (2008) suggest that the active network during MI might be similar to that which is active in humans during typical perceptual visuo-spatial tasks (i.e., widespread activation of fronto-parietal regions). Further, these researchers have stated that there is a predominately fronto-parietal network specific to imagined movement (Sack et al., 2008). The suggestions by Sacks and colleagues are supported by much of the literature, which consistently reports robust activation occurring within fronto-parietal regions when performing MI (Gerardin, 2000; Hanakawa et al., 2003; Sack et al., 2008). The predominant role of this fronto-parietal interaction in performing MI might be associated with the brain's capacity to produce a representation of the conscious self. That is, in order to perform an imagined movement, the participant must first possess a kinesthetic concept of him/herself, which is done through the process of self-monitoring. For instance, when healthy controls are asked to produce a representation of themselves in their mind, data obtained using PET shows that the fronto-parietal network is highly activated (Lou et al., 2004). In the current study, it is thus likely that FC found between fronto-parietal regions was a result of the participant working to create a kinesthetic image in their mind during MI. While in this experiment significant node pairs between the PFC and PC only existed between the right precuneus (discussed below)-left VL PFC and the left superior PC-right medial PFC, the majority of the node pairs involved in the network in general consisted of connectivity with one of either the PFC or PC. The lack of direct fronto-parietal node connections is not consistent with the current literature (Gerardin, 2000; Ishai, 2002; Lorey et al., 2011) and may well reflect cognitive processes unrelated to the performance of MI.

The beta band network during MI displayed a significant interaction (i.e., node pair) between the left inferior PC and the right ventral TC. As mentioned previously the TC is the site of visual and auditory perception; this, in combination with the role of the PC in maintaining a concept of self, leads to the conclusion that this functional connection has a large role in reproducing an accurate depiction of one's physical surroundings and being during MI. The interaction between parietal regions and the TC reflects the network working to integrate task related information in order to form the most vivid MI possible. When considering node pairs within the beta band, the right superior PC exhibits connectivity with the right medial PMC (i.e., SMA). The activity exhibited here is an additional reflection of the integration of polysensory information. It has been documented that connectivity between the parietal lobe and the PMC is involved in polymodal motor processing in response to visual, tactile, or auditory cues (Bremmer, 2001). This notion is further verified by the nature of the MI task. The imagined movement was guided by an auditory script, which would act as a sensory cue, accounting for the parietal-premotor interaction found within the task-positive network. In support of this concept, researchers have suggested that during MI, top-down processes exist within the brain that begin at the superior parietal cortex and influence sensorimotor regions in order to create a mental image (Mechelli, Price, Friston, & Ishai, 2004). This was found through the use of DCM during fMRI to determine the directional activation found among parietal node hubs during the imagining of faces and places (Mechelli et al., 2004). The above findings clearly outline the importance of the parietal cortex in sensory integration during imagined movement tasks. In contrast to the findings of this project, Gerardin (2000) found that greater amounts of connectivity during MI, as

compared to overt movement, occur only within the left parietal cortex. Results of the same study would suggest that right hemisphere parietal cortex activation instead demonstrates levels of activity that are on par with actual motor performance (Gerardin, 2000). The results of this study are not consistent with these findings, but rather reflect the relative involvement of bilateral parietal cortices in MI. This current result is consistent with more recent documentation stating that fMRI uncovers that the bilateral parietal cortices are activated during an imagined upper limb task in healthy controls (Fleming et al., 2010).

6.33.2 Precuneus Activation

In the current study, FC was found between the precuneus and premotor, as well as prefrontal, brain areas. The precuneus is located in the medial portion of the parietal cortex along the medial longitudinal fissure and has a role in executing visuo-spatial imagery, episodic memory retrieval, and self-processing (i.e, taking on first person perspectives) (Cavanna & Trimble, 2006). In addition, projections from the precuneus connect with the dorsal PMC and the SMA, making this parietal brain region of particular importance in terms of motor related network activation in this study.

The results of this study uncovered that during MI there is a functional connection present within the beta band between the precuneus in the left hemisphere and the right DL-PMC. While regions of the superior PC are involved in maintaining first person perspective, it has been suggested that activation of the precuneus during MI only occurs when individuals take on a third person perspective (Vogeley, 2004) (i.e., imagining watching yourself make a sandwich) as apposed to a first person perspective (i.e., imagining making a sandwich from behind your own eyes). This point lends to the idea

that the familiarization sessions used in this study were not successful in teaching

kinesthetic, but instead visual, MI (see Section 6.2). An alternative reason for FC

involving the precuneus and premotor areas during MI could be the role of the precuneus

in visuo-motor processing. Movement production requires the transformation of the

visual representation of what a task should look like into a proper motor plan to be

carried out by primary motor cortices. It has been stated that the precuneus might have a

role in these visuo-motor transformations (Dohle et al., 2011). As such, it could be

speculated that the CCC seen between the precuneus and the PMC during MI within the

beta band reflects the process of altering visual cues into motor plans.

The current project also uncovered CCC within the beta band task-positive

network during MI between the right precuneus and the left VL-PFC. It has been

documented that in terms of anatomical architecture, the main cortico-cortical

connections projecting from the precuneus are with the PFC (Cavanna & Trimble, 2006).

In addition, during imagined movement, the precuneus is thought to be involved in

directing attention in space (Dohle et al., 2011). Taken together, these two findings add to

the notion that the PFC-precuneus CCC seen during MI reflects processes involved in the

"what and where" of MI. The "what" is the concept of space that exists due to

consciousness in the PFC, while the "where" is in reference to the perceptual

understanding of said space that occurs through the precuneus. The above findings

implicate the fronto-parietal network in the successful performance of MI.

6.34 The Formation of an Environmental Model During MI

The following section investigates the influence of the parahippocampal gyrus

(PHG) on the task-positive network during MI. It should be noted that source localization

techniques might have been inaccurate in depicting the PHG as a source generator during the task due to this structure's deep brain location; however, at this time the PHG will be discussed based on its potential for contributions to the MI network, and the limitations of source localization techniques will be reviewed elsewhere in this thesis. The PHG plays an important role in the recognition of environmental scenes (i.e., landscapes, rooms, etc.). In particular, a region of the PHG known as the parahippocampal place area (PPA) is thought to be involved in retrieval of this environment related information. Due to the high degree of connectivity present in the PHG within the network, it is likely that this brain region was involved in producing and maintaining the appropriate image within the mind during imagined movement. In particular, the beta band task-positive network outlines that there is CCC between the PHG and the TC. In this context, information from the TC is again likely related to the perception of incoming auditory and visual information during the MI blocks. This perceptual information might be integrated within the PPA in order to procure a more vivid picture of the environmental surroundings (O'Craven, 2006). This notion is in keeping with work by O-Craven & Kanwisher (2000) documenting that activation in the PPA (assessed via fMRI) in healthy controls occurs during visual imagery of an environment (i.e., home, etc.). The role of the PHC-TC interaction in creating vivid images is further explained by the concept of visual path integration. Wolbers, Wiener, Mallot, and Buchel (2007) found that right hemisphere fMRI hippocampal activity was correlated with pointing accuracy during a visual path integration task. This study guided individuals through a virtual reality across two sides of a triangle, at this point the virtual environment stopped moving and asked individuals to use a joystick in order to point towards the direction of their start point (i.e.,

completing the triangle). The importance of this study is not regarding the hippocampal capacity for memory, but in the process of visual path integration for forming a conception of physical space. In the current study, the findings of Wolbers et al. (2007) infer that the PHG involvement in MI reflects that of conceptualizing the structural confines of the environment within the mind. This notion is supported by the fact that significant node pairs were found between TC and the PHG within the task-positive network in the beta band during MI. Another explanation for the FC across the PHG and TC found in this study might be the TC's role in the representation of complex features such as global shape. The concept of global shape is concerned with recognition of the physicality and dimensions of environmental objects (Schwartz, 1983). Based on the functionality of the TC, it can be inferred that connectivity within this area during MI is aimed at producing and maintaining a concept of the physical world within the mind. It should also be noted that TC involvement in FC during imagined movements is in keeping with the current literature (Lacourse, Orr, Cramer, & Cohen, 2005).

A final brain region to consider in exploring the underlying neural correlates of MI is the V1. The predominant role of the V1 is to process the incoming visual information to be relayed to association brain areas (for example, the PC) for conceptualization. In the current project, the beta band network derived suggests there is FC between the V1 and PHG. Connections with the PHG may reflect the retrieval of surrounding environment information or task sequencing from memory (Lehn et al., 2009). Importantly, the large extent of CCC seen within the V1 during MI (supported by a ND of 5) is not what the researchers expected given the nature of the imagined task. The performance of MI is meant to produce a mental simulation of movement from the

kinesthetic perspective. This mental simulation has been found to activate the sensorimotor brain network in some form when individuals are performing MI. In comparison, the performance of visual imagery has been documented to activate brain regions in the occipital cortex (i.e., V1), in the absence of involvement of the primary motor and sensory cortices (Solodkin, Hlustik, Chen, & Small, 2004). It has been stated in the current discussion that the participants might have been engaging in visual imagery (see the KVIQ results, and precuneus involvement in the network), as opposed to kinesthetic first-person imagery. While the degree of connectivity observed for V1 adds to this notion, the presence of connectivity within motor areas (i.e., M1, SMA, PMC) suggests that participants were engaged in kinesthetic imagery. In response to this, it has been proposed that the brain network underlying visual imagery and that of MI are likely parallel to a degree. While the similarities in these two networks has been documented in parietal and premotor areas (Solodkin et al., 2004; Stinear, Byblow, Steyvers, Levin, & Swinnen, 2006), more research is necessary to better understand the extent to which they may differ.

6.4 Functional Connectivity During Repetitive Task Practice

The following discussion will address the second objective of the thesis:

(2) to determine the pattern of FC within the sensorimotor network during the performance of a functional task.

Similar to the findings for MI, results of the PLS analysis showed that the network active during RTP was significantly different from that of rest, indicating that the significant node-node interactions are reflective of the FC specific to the performance of the functional task. As indicated previously (and outlined in detail in section 7.2),

results regarding network activation patterns should be interpreted in light of the potential for inaccurate determination of source generators via EEG-based source localization. The node-pairs chosen for discussion involved structures known for their involvement in the sensorimotor network (i.e., M1, PMC, S1), or that expressed high ND within the task-positive network.

6.41 The Role of the Sensorimotor Regions

6.41.1 Motor Execution

During the overt performance of a functional task (i.e., making a sandwich), the RTP network within the beta band includes connections with M1. This pattern of connectivity is consistent with expected results when performing network analysis on brain activity obtained during a motor task. Specifically, the current study found coherence between the right M1 and both the right V1, and the left medial PFC. Prior to exploring the nature of the connections between the above mentioned regions, it must first be stated that M1 activity in the right hemisphere was not anticipated. Based on what is known regarding contralateral limb control via the crossing of the corticospinal tract in the brain stem (Woolsey et al., 1979), right hemisphere M1 activity is reflective of left hand movement(s). This pattern of contralateral control is incongruent with the study paradigm wherein participants were instructed to use their right hand, which should result in left hemisphere M1 activity. The presence of M1 activity in the right hemisphere may in part be explained by the role of M1 in ipsilateral limb control, which has been documented in motor control research (Chen, 1997; S. C. Cramer, Finklestein, S.P., Schaechter, J.D., Bush, G., & Rosen, B.R., 1999; Jankowska & Edgley, 2006; Wassermann et al., 1991). In more detail, the results of Wassermann and colleagues

(1991) show that rTMS can be used to induce right-handed MEPs via stimulation of both the contralateral and ipsilateral hemisphere of non-disabled individuals. In addition, another rTMS study found that timing errors in successful right-handed performance of a piano sequence task occur during stimulation of both the contralateral and ipsilateral primary motor cortices of non-disabled individuals (Chen, 1997). Taken together, these findings imply that the formation of right-handed movements might involve activation in both hemispheres, which may account for the activity seen in this study within the right M1. An additional explanation for right M1 activity (especially in the absence of left M1) might be the nature of the functional task. The instructions provided to participants regarding the RTP stated they were to perform the majority of the movement using their right hand, with the understanding that successful completion of the functional task would require the use of both arms. The result of this being that the task itself was bimanual (not unimanual) in its execution, which helps to explain why a distinct pattern of contralateral network activation was not found during the RTP. As indicated above, this study shows functional connections with M1 ipsilateral to the *intended* dominant hand, in the absence of functional connections involving the contralateral M1 (i.e., M1 in the left hemisphere). The finding of ipsilateral M1 (i.e., right hemisphere) activity in the absence of contralateral M1 activity may also be due in part to the unstructured nature of the functional task, which is discussed in Section 7.3.

6.41.2 Motor Planning

As the sandwich making procedure was a goal directed movement, it was expected that the task positive network during RTP would include V1. The significant node pairing of the right M1 and V1 is likely a reflection of the transfer of visual

processing information to the motor areas for formation of a task relevant movement plan. This notion is supported by research investigating the neural activity specific to the performance of visuomotor tasks (Classen, 1998; Culham, Cavina-Pratesi, & Singhal, 2006; Floyer-Lea & Matthews, 2004). It has been documented that increases in FC (assessed via EEG) are exhibited between V1 and M1 when healthy controls perform visual tracking tasks, as compared with rest (Classen, 1998). More specifically, in the Classen (1998) study, the visuomotor task required individuals to apply a force on a strain gauge with the index finger in order to manipulate a horizontal line into a sinusoidal output. While the current study did not include a structured visuomotor task, the process of choosing toppings (for example) for the sandwich required participants engage visual areas within the brain in order to integrate visual information into the movement plan, which may account for connectivity between the V1 and M1 during RTP.

The second node pair within the task positive network for RTP was between the right M1 and the left medial PFC. The FC found between these regions in the present study should be considered in the context of the role PFC plays in motor planning and execution. Lesion studies in humans show that when the PFC is damaged, individuals have difficulty not only with inhibiting incorrect responses (as discussed in Section 6.31), but also with the performance of correct responses (Goldman-Rakic, 1987). This finding indicates that the functional connection between the PFC and M1 might reflect the process of selecting the correct movement to be executed during the RTP task. This notion is easy to conceptualize given that the participants were required to perform motor tasks that were associated with a particular goal during each RTP block. For example, if

the instruction asked participants to "cut the bun", the process of responding correctly to the cue in order to successfully perform this task would require the coherence seen across the PFC and M1. This is further supported by suggestions within the literature that the PFC may have a role in object directed grasping (Pool, Rehme, Fink, Eickhoff, & Grefkes, 2013). In addition, the process of the three-day familiarization phase that occurred prior to the experimental session required participants to learn the intended movements for each step associated with the sandwich-making task. The result was that by the experimental day, the participants had acquired the procedural information necessary to carry out the sequential sandwich-making task from memory. In further support of the present findings, when a sequential motor skill is already learned, fMRI research has found that there is greater coherence between frontal regions and M1 in non-disabled individuals performing a bimanual button-pressing task (Sun, Miller, Rao, & D'Esposito, 2007).

The PFC must also be considered in the framework of its interaction with the PMC during RTP. During RTP, a functional connection between the right VL-PFC and the right medial PMC (i.e., SMA) was observed. Previous work using fMRI has documented that the SMA plays a role in the production of lateralized hand movements in healthy controls (Pool et al., 2013). Specifically, DCM showed that SMA expresses an influence over M1 during lateralized fist closures (Pool et al., 2013), implicating the SMA as a key structure involved in initiating movement. Further, the connectivity expressed between SMA and other brain regions during RTP might be related to the complex nature of the functional task. It has been documented that there is a positive correlation between the firing rate of neurons in SMA and the complexity of the intended

hand movement (Padoa-Schioppa, Li, & Bizzi, 2004). The RTP in the current study required a dynamic sequencing of the appropriate motor procedures in order to successfully complete the goal directed behaviour, which can be interpreted as a complex movement and may account for the involvement of the SMA.

In addition to task complexity, the actual sequential characteristics of the task might be adding to premotor connectivity. In keeping with this notion, fMRI studies have shown that when performing a previously learned sequential button press task, healthy adults express greater activity in the SMA as compared with the performance of a novel sequence (Hikosaka, 1996). In contrast to findings of Hikosaka (1996), Sun et al. (2007) document that fMRI uncovers that performing a novel sequential skill results in increased connectivity in the PMC and SMA, as compared with learned. This finding would indicate that in the current project, SMA involvement in the network might reflect that the functional motor task is not a learned sequence. The results of this project do not allow the researchers to distinguish whether the sequencing of the motor task was truly learned, as this was not the aim of the study. Instead, the presence of the SMA in the active network during RTP might be better understood in the context of its interaction with the PFC. In particular, a fMRI study used a "go-no-go" paradigm to investigate PFC interactions with other prefrontal structures and found coupling of PFC and SMA during conflict monitoring (Fassbender et al., 2004). The researchers suggest that this PFC-SMA interaction is reflective of task set maintenance, where task set refers to the procedures involved in a given task (Fassbender et al., 2004). In the current study, FC between the PFC and the SMA could reflect online monitoring of the correct sequencing associated with the functional task.

6.41.3 Sensory Integration

A final consideration in the planning and execution of movement is the integration of polysensory feedback into the motor plan via connections with the sensory cortices. The results of the current project show that there are functional connections present during RTP between the right DM-PFC and the right S1. Generally, S1 activity reflects the processing of sensory information (Gerardin, 2000). The process of carrying out a functional sequence of movement requires feedback regarding task-relevant information in order to form the appropriate motor plan. In the current study, the RTP blocks required participants to engage in a sequence of movements continually in order to achieve a specified goal (for example, pick up the bun). Due to the nature of this continuous task, the participants had to process online sensory feedback regarding visual, tactile, or proprioceptive cues in order to select the appropriate motor plan, which accounts for S1's high degree of involvement in the overt movement task. This notion of integrating sensory feedback into the intended motor plan was reflected in the CCC seen during RTP between prefrontal and S1 regions. This prefrontal-sensory cortex interaction is further supported by significant interaction between the right orbitofrontal cortex and the left secondary somatosensory cortex (S2).

In regards to sensory integration, of interest is the functional connection found between the right hemisphere claustrum and VL-PMC during RTP. It should be re-iterated that source localization techniques are not without limitations, and as such, the understanding of how the claustrum contributes to the sensorimotor network should be done within this context. The main role of the claustrum in motor control is polysensory integration (Crick & Koch, 2005). The functionality of this brain region aids in

explaining its contribution to the task-relevant motor network, and connectivity within this region during goal directed movements is in keeping with the current literature (Baugh, Lawrence, & Marotta, 2011). This project uncovered FC between the claustrum and the VL-PMC, which can be interpreted as the network integrating poly-sensory information into the intended movement motor plan. The relative importance of this interaction is supported by research stating that in comparison to other premotor-M1 interactions, the VL-PMC has the most dominant connection with the M1 hand-area (Dum & Strick, 2005). As such, it can be concluded that the VL-PMC plays a large role in planning the intention to perform hand movements via information regarding sensory integration obtained from the claustrum.

6.42 Influence of the Parietal and Temporal Cortices

As outlined previously, the PC plays a role in the direction of attention in space. For the purposes of this section, the following finding should be understood in the context of this particular PC function. The beta band RTP network during the functional task uncovered FC between right superior PC and the right frontal eye fields (FEF). During motor tasks, the FEF function to perform non-tracking, voluntary eye movements via the integration of visuospatial information from varying brain regions (Paus, 1996). The connectivity between the FEF and parietal regions indicates that spatial perceptual information from the PC was integrated into the ocular motor plan; this integration of visuo-spatial information allows the participants to actively scan their environment during the RTP in order to successfully complete the task. In addition to connections with the FEFs, the RTP network also showed connections between the parietal and prefrontal cortices. A review by Corbetta and Shulman (2002) outlined that the fronto-parietal

network might carry information about the preparation of hand movements. More specifically, the authors state that the PC contributes to the motor plan by helping to map hand-coordination in the form of pre-shaping hand conformation (Corbetta & Shulman, 2002). As such, in the current project the fronto-parietal involvement in the RTP task-positive network may be reflective of the integration of hand shaping information into the motor plan for goal-driven movements. This idea is in keeping with the findings of PC lesion studies, which have shown that the execution of visually guided, goal-directed hand movements break down in this population (Karnath & Perenin, 2005).

The general functions of the TC include visual and auditory information integration, as well as global shape recognition (Miyashita, 1993). The current project found that there were significant node interactions between the right ventral TC and the left medial PMC during RTP. This temporal-premotor connection was also observed in the MI condition, and reasons for activation across these regions were discussed in full above (see Section 6.32). In brief, integration of visual and auditory information in the temporal cortices allows for the formation and maintenance of a visuomotor representation regarding the task within the PMC (Matsumoto et al., 2003). Further, when individuals are performing overt (and not imagined) movement, FC within the temporal and premotor areas has been documented in the past (Jiang, He, Zang, & Weng, 2004). In addition to the connectivity between the temporal and premotor regions, research has documented that the temporal lobe is associated with recognition of object properties, such as size and shape during reach and grasp movements (Culham et al., 2003). The role of the TC in object recognition aids in explaining this regions involvement in the functional motor task. Specifically, making the sandwich required participants to

recognize objects in the environment and conceptualize how to reach out and grasp them. It has been well documented that the process of judging object boundaries is controlled by activity within the ventral stream (i.e., TC), while aspects of the grasping movement such as hand pre-shaping are a result of brain activity in the dorsal stream (i.e., PC) (Milner & Goodale, 2008). The FC between the TC and PMC in this study can be inferred as the integration of object boundary information into the motor plan for the successful performance of the reach and grasp movements necessary during RTP.

6.43 Motor Task Recall and Movement Coordination

As previously stated, it should be outlined that the involvement of deep brain structures such as the PHG might not be a true reflection of the task network due to limitations associated with the source localization techniques used; however, the PHG's role in the RTP network will be briefly discussed for exploratory purposes. The PHG plays a role in memory encoding and retrieval of task related information. The nature of the study paradigm required participants to retrieve the motor task sequencing and dynamics from memory, which accounts for the large amount of connectivity seen between the PHG and surrounding brain regions during the RTP in the beta band. Of particular interest is the CCC found within the beta band during the functional task between the right PHG and the left contralateral-PFC. The PFC has been identified as a key structure active in the replication of a learned sequential movement in non-disabled individuals performing a button press task assessed via PET (Destrebecqz et al., 2003). As such, the contribution of the PFC to the motor task here might be in reference to this brain regions involvement in retrieving procedural information from memory.

A final brain region for consideration in its contribution to the RTP task-positive network is the cerebellum, and in particular the left hemisphere dentate nucleus, which plays a large roll in the coordination of bimanual tasks. Again, this is a deep brain structure whose involvement in the network should be interpreted in the context of limitations associated with source localization methods. In the current study, the functional task required the participants to coordinate limb movements in both arms for successful completion of sequences such as cutting the bun (for example). It has been documented that performance of a bimanual coordination task results in increases in cerebellar activation assessed via fMRI (Debaere, Wenderoth, Sunaert, Van Hecke, & Swinnen, 2004). Additional work by Debaere et al. (2004) showed that activity in the cerebellum is greater during bimanual coordination tasks, as compared with the performance of one limb movement in isolation.

6.5 Comparing the Task Positive Networks Using Graph Theory

The following discussion points will address objective three;

(3) to quantify the pattern of FC, using graph theory, during the actual and imagined performance of a functional task.

The following discussion compares ND calculations between task-positive networks for MI to those of RTP in order to characterize important similarities and differences between the two conditions.

6.51 Brain Regions Expressing the Highest ND During MI and RTP

Through the investigation of graph theoretical parameters it is possible to infer which regions are of most importance for the successful completion of the given task (i.e., MI vs RTP). In particular, initial inspection of the brain regions that expressed the

highest NDs (see Tables 6 and 7) uncovers obvious differences in the cortical areas involved across the two conditions. The MI network requires the greatest connectivity across motor programming areas such as the premotor and prefrontal cortices. This finding is in keeping with documentation above outlining the potential contributions these brain regions may have had during MI in terms of M1 inhibition by PFC (Garavan, 1999) and action observation in the PMC (Rizzolatti et al., 2002). In addition, the findings regarding the highest NDs during MI are in keeping with the researchers' hypothesis that the MI connectivity would rely more on regions of the PFC; although, the current study did not find that the MI network expressed greater connectivity within the PC, which is not in line with the researchers' hypothesis. In comparison, the two brain areas expressing the highest ND in the RTP network were both located within the cerebellum, which further implicates the role of this structure during overt bimanual coordination (Debeare et al., 2004). An unexpected result was the high degree of involvement seen in the auditory cortex during RTP. It is most likely that this finding is due to source estimation error (see Section 7.2). In more detail, the auditory cortex is located within the superior TC, which is positioned in close relation to S1. As such, the great amount of connectivity found within the auditory cortex during RTP might actually reflect S1 involvement, particularly when this finding is considered in the context of the potential for poor spatial specificity due to source estimation error. Similar to the MI network, the RTP condition also relied on interactions with regions of the PFC, which might have occurred due to the involvement of prefrontal regions in both the selection of correct and incorrect responses (Goldman-Rakic, 1987) during the imagined and overt movement tasks.

6.52 The Role of the Parietal-Prefrontal Network

The derived task-positive networks active during both MI and RTP within the beta band exhibit high degrees of connectivity across fronto-parietal regions. It has been well documented that an extensive network exists across PFC and parietal cortex regions (Gerardin, 2000; Hanakawa et al., 2003; Lorey et al., 2011). In the current study, the degree of connectivity seen directly between the PFC and the PC was less than what would be expected during MI based on current literature. It should be noted that we anticipated higher ND values in parietal regions during MI as compared with RTP. In this project, parietal regions expressed relatively similar (or lesser) ND values to those found within the RTP network. For both the right and left hemisphere superior PC, the task-positive network during MI exhibited a ND of 1 in comparison to a ND of 3 for RTP. The greater number of connections found for the superior PC during RTP may be explained by the parietal region's involvement in reaching movements. Specifically, literature has highlighted the PC as being involved in pre-shaping of the hand in visuomotor control (S. T. Grafton, 2010). While the lesser degree of involvement shown in the superior PC during MI is not consistent with neuroimaging results from prior MI studies (Fleming et al., 2010; Hanakawa et al., 2003; Sack et al., 2008), this might be explained by the more noted role of the inferior (vs superior) PC in the performance of MI. In particular, the inferior parietal lobe (within the PC) has been implicated in the internal recruitment of motor representations during MI (Hetu et al., 2013). The differential involvement of the superior PC found in this study could be explained by the idea that it is actually the inferior regions (not superior regions) of the PC that are more involved in the performance of MI. It should be noted however that in this study the inferior PC only

expressed a ND of 2 in the right hemisphere, which could simply indicate that participants were not as actively involved in reproducing the motor representations as the researchers had anticipated. Consistent with the notion that other parietal cortex regions are involved in MI, our analysis did reveal other regions within the PC necessary for the MI component of the study.

In comparison to superior PC findings, the ND value for the precuneus expresses both similarities and differences between the MI and RTP networks. When considering the left hemisphere, ND for the precuneus during MI and RTP are both 3. Graph theory analysis for precuneus in the right hemisphere however uncovers differences between the two networks; in particular, ND in this region for MI is 1, while within the RTP network the precuneus was not shown to have any significant connections (i.e., it had a ND of 0). While this finding indicates that the right precuneus was not involved in the execution of the RTP, it also uncovers an important point in the way that the MI fronto-parietal network differentiates from RTP. In more detail, the connection derived from the right precuneus in the MI network is with the left VL-PFC; while the ND is not high in the context of the entire network, the relative importance of this connection to proper execution of the MI task cannot be ignored. In contrast to the differential parietal structure involvement found between MI and RTP, the current project uncovered task positive networks for both MI and RTP predominantly characterized by FC between the PFC and other brain regions. The similar importance of the PFC within both the MI and RTP networks is further explained by the relative NDs derived in the present study. Specifically, within the left hemisphere, the MI network exhibits a ND of 6 for the contralateral-PFC; in comparison, the left DM-PFC expressed a ND of 6 during the RTP

state. While it is clear that the PFC is vital to the performance of both the MI and the RTP tasks, it is likely that this brain region is differentially involved in either task. During MI, the PFC has been linked to activation during preparation states (M. Jeannerod, 2001), implying that this brain area might be involved in the MI network based on its contribution to motor planning and programming. In comparison, activity within the DM-PFC has been identified in the literature as necessary for the control of correct responses (Narayanan & Laubach, 2006), which accounts for the high degree of connectivity documented within this region during the RTP component of the study.

6.53 The Role of Sensorimotor Regions

It has been shown that there is increased activity in brain regions such as S1 during overt, as compared with imagined movement (Gerardin, 2000). In the current project, distinct differences are seen between the graph theory parameters of the left S1 during MI (ND=6), and RTP (ND=3). In comparison, the right hemisphere S1 was found to have a greater degree of connectivity during RTP (ND=4) as compared with MI (ND=1). The differences seen here across conditions in graph theory parameters imply that the two sensory cortices are differentially involved in imagined and overt movement of the same task. This finding might be understood in the context of M1 involvement in the RTP task. During the functional task, the right hemisphere M1 was active in the absence of left hemisphere activation. The high ND found for the right hemisphere S1 in the RTP network simply adds to the notion that participants were engaged in more left handed movements than had been intended by the researcher. In the MI network, a high degree of S1 activity implies that the participants were successful in representing

kinesthetic simulations of the imagined movement within the contralateral sensory brain regions.

Interestingly, in the present study the ND expressed for M1 in the right hemisphere was higher during MI (i.e., 2), as compared with RTP (i.e., 1). Further, in the left hemisphere a ND of 1 was found for M1 during MI, and a ND of 0 for M1 during RTP. These are not the expected findings in terms of FC and prove difficult to understand in the context of comparing an imagined to an overt movement. Simply, it can only be inferred that the participants were more actively engaged in the MI task than the functional motor task, which might be a consequence of the state-related analysis (see Section 7.3 for limitations). Another region to consider when investigating conditional differences in ND is the left dentate nucleus of the cerebellum. As previously stated, interpretation of this finding concerning a deep brain structure should be done in the context of limitations associated with source localization techniques. Graph theory analysis uncovered that within the left hemisphere, the dentate nucleus of the cerebellum expresses a ND of 2 during MI, and a ND of 11 during RTP. This large difference outlines the reliance of the sensorimotor system on cerebellar input when performing overt, as compared with imagined, movements. (Miall & Reckess, 2002) Based on the current research (Bastian, 2006), it can be stated that the performance of a functional motor task requires online monitoring by regions of the cerebellum in order to successfully coordinate the movement. In comparison to the RTP network, the cerebellum might not be as vital to the performance of the imagined task, or may merely be differentially involved. This notion is supported by the fact that while the cerebellum

was active during the imagined movement, the ND was lower as compared with that of the RTP network.

A final consideration for comparison between the two conditions is the PMC. The results of this project showed that the PMC expresses a higher ND during MI relative to RTP. Most notably, in the left hemisphere the medial PMC (i.e., SMA) expresses a ND of 5 during MI, and only 1 during RTP. This finding is replicated in the left DL-PMC, wherein the ND is 4 during MI, and only 2 during RTP. These findings support recent speculation in the literature that MI might be more heavily dependent on engaging brain areas associated with planning, as opposed to engaging primary sensorimotor cortices in general (Sharma, Pomeroy, & Baron, 2006). More specifically, in the review cited by Sharma et al. (2006), the authors speculate the brain activity underlying MI might be more closely linked to regions whose function is aimed at planning, programming, and memory. In the current project, it is evident that connectivity within premotor areas responsible for planning and initiating intended movements is vital to the successful performance of MI of a functional task. An additional role of the SMA (i.e., PMC) during the imagined movement might be this brain structure's potential function in inhibiting M1 activity to prevent overt movement during MI (Kasess et al., 2008). While this is an important study, the findings of Kassess and colleagues are only speculative at this point as their results have yet to be replicated in the literature. More research is necessary in this area in order to better define the influence of the SMA on the M1 during an imagined movement protocol, and how this interaction compares to FC between these regions during overt movement.

6.54 Small World Networks During MI and RTP

The task positive network for the MI condition was characterized by a lower CCo (0.005833) relative to that of the RTP network (0.024513). From this information we can infer that the task-positive FC present during the performance of the functional task required more clusters of interacting brain regions, as compared with the network present during MI. In more detail, the higher CCo reflects greater efficiency for local information transfer (Bullmore & Sporns, 2009). The second property to consider is the characteristic PL present within the network during MI (4.5438) and RTP (3.7101). These PL values indicate the following: 1) during MI, for all possible connections the average number of shortest paths between node pairs was 4.5438, and 2) during RTP, for all possible connections the average number of shortest paths between node pairs was 3.701. Taken together, the higher CCo and the smaller path length present in the RTP network indicates that this is a more ordered, and thus more efficient, network as compared to that of MI.

The graph theoretical properties described above are those that are characteristic of a SWN. In further support of this, a SWN statistic was calculated which found that both the MI and RTP task positive networks were SWNs ($SWN_{MI} = 1.1048$; $SWN_{RTP} = 6.0169$). In order to obtain this statistic, the CCo and PL of the MI and RTP networks were compared to graph theor y parameters of randomly generated networks. The SWN statistics above are each greater than one, confirming that there is a degree of small worldness present in both of the task positive networks (Watts, 1998). Of note, the MI network expresses a SWN statistic that is only slightly greater than 1 (i.e., 1.1048), which could indicate that this network may have properties closer to that of a random, as opposed to ordered, network. The notion that both of these conditions resulted in SWNs

in non-disabled participants suggests that these networks are communicating efficiently, which is especially obvious in the RTP condition based on the size of the SWN statistic obtained (i.e., 6.0169). In particular, Rubinov and Sporns (2010) indicate that SWNs are highly integrated in terms of their functional connections, as compared with those connections of a random network. In addition, it should be noted that the degree to which the RTP network parameters (i.e., SWN of ~6) differed from that of the randomly generated network measures was much greater than that observed for the MI network (i.e., SWN of ~1). As such, it can be inferred that the RTP network exhibits a greater degree of small-worldness, reflecting the greater efficiency of functional connections within this network, as compared to that of the MI network. This large difference also reflects the possibility that the MI network found was actually random, and not small world. As documented in the results section, the researchers explored the variability in these SWN statistics when compared to both the best (i.e., high CCo, short PL) and worst (i.e., small CCo, long PL) possible randomly generated networks. Importantly, while neither condition was small world compared with the best possible network, the RTP network had a SWN statistic approaching 1 (i.e., 0.6932) as compared with the much lower measure in the MI network (i.e., 0.1865). A second comparison to the worst possible random network uncovered that both MI and RTP were small world, although again the degree to which the RTP condition expressed small worldness was greater (i.e., 9.6908) as compared with the MI condition (i.e., 1.3280). Taken together these findings regarding variability imply that the average SWN statistic for MI falls somewhere between 0.1865 and 1.3280, which further suggests that the connectivity found in this study during MI may have been a random network. In contrast, these findings clearly

outline that the connectivity during the RTP condition was ordered, as evidenced by an average small world statistic that falls somewhere between 0.6932 and 9.6908. An explanation for the greater small worldness seen in the RTP condition might be that reach and grasp movements are a well-learned and practiced task for non-disabled young adults, which would infer that the underlying motor network is well developed. As networks change and become more efficient with practice over time (i.e., the concept of neuroplasticity), it is more likely to display greater SWN characteristics. In comparison, the MI task was only learned for the purposes of the study, and as such we could speculate it was not as efficient as the RTP network and thus had a lower degree of small worldness.

CHAPTER 7 LIMITATIONS

7.1 Technical Issues

7.11 Down Sampling

To facilitate the source localization analysis using Curry 7, the epoched data (for each 450 s task state) was down sampled to 100Hz. The EEG data from which these epochs were derived was initially sampled at 1000Hz, with the intention of down sampling to 250Hz (an interleave of 4). Technical issues with the Curry 7 software would only allow for the CDR to be performed with an interleave of 10 (i.e., a sampling rate of 100Hz). The result of this down sampling was that the data carried forward to the CCC and PLS analysis was not as rich temporally in that there were 45000 data points for each participant (as opposed to the intended 112 500 data points). It is unfortunately not within the scope of the current project to determine the effect this down sampling had on the results obtained, but it is reasonable to conclude given the results that the 100 Hz data was sufficient for the analysis performed.

7.12 Lost Data

In addition to the need for down sampling, technical issues with the software led to the removal of three participants from the CDR analysis. The inability to perform the CDR analysis on these three participants resulted in the FC analysis being performed on ten participants only.

A final consideration regarding technical issues encountered during data analysis includes the inability to perform a quantitative analysis on the EMG data. Although the quantitative EMG analysis would have been ideal for explicitly stating that the FC findings were associated with imagined (and not overt) movements, we believe that the

114

online monitoring of muscle activity was sufficient to determine that no overt movements of the ULs occurred during the MI blocks. It should be noted that much of the literature reports the underlying neural correlates of MI in the absence of data related to muscle activity detected using EMG (Hetu et al., 2013).

7.2 Source Level Analysis with Electroencephalography

Perhaps the greatest limitation of the current work is the fact that the source level data was obtained using source localization based on sensor level data. In more detail, the electrical activity collected at a particular electrode might not necessarily indicate that the source generator of this signal was located directly below said electrode (Michel et al., 2004). This issue is referred to as the inverse problem. A consequence of the inverse problem includes associating activity at a particular electrode with the brain region below it, when the real source might exist in some deep brain location (Michel et al., 2004). The goal in solving the inverse problem involves locating the active source with as much precision as possible (Bailet, 2001), by attempting to reduce the impact of factors such as spatial smearing and specificity. Spatial smearing refers to the effect of collecting a signal that has traveled through brain tissue, meninges, skull, and skin (i.e., volume conduction), which might result in data collected at the sensor level that no longer possesses distinct spatial characteristics (Szava, 1994). Spatial specificity refers to the issue of parsing out particular source generators from one another, when their orientation within the brain may be too close for determining differential activity across said nodes at the sensor level. Addressing the inverse problem involves computation of the forward solution, which refers to determining the best possible model for the calculation of the source generators.

In order to address these potential issues, the current research employed a source localization technique that allowed for the estimation of the sources of relevant brain activity via complex mathematical algorithms. The technique, sLORETA, has been used extensively for localization of source generators in EEG data (Cao, 2010; Pascual-Marqui, 2002). Briefly, the sLORETA model estimates source generators by taking a location-wise inverse of a minimum norm least squares analysis via estimated variances (Wagner, 2004). In particular, the CDR method used in the current study, when coupled with BEM geometry for segmentation purposes, improves the probability that the obtained source information is accurate. More specifically, the combination of CDR and BEM methods aimed to address both the inverse problem and forward solution. Details related to the mathematics underlying said operations are beyond the scope of this project.

In terms of electrode configuration, it has been proposed that an inter-electrode distance of 2-3 cm is necessary to avoid distortions in the obtained scalp potential (A. Gevins, Brickett, P., Costales, B., Le, J., & Reutter, B., 1990). In addition, it has been documented that there is a linear increase in the precision of source localization of a single dipole between the use of 20, up to the use of 100 electrodes for EEG data collection, and then this precision plateaus (Michel et al., 2004). In response to these findings, the current study used an EEG cap consisting of 128 electrodes in order to improve the accuracy of the obtained source results. It should also be noted that there is some debate as to the accuracy of source level analysis on EEG data due to its poor spatial resolution (i.e., high volume conduction). In terms of spatial resolution, Cuffin (2001) have documented that the absolute EEG source localization error is 10.5 ± 5.4

116

mm. This infers that source localization methods used on EEG data can only determine spatial differences in source dipole locations if said dipoles are located ≥ ~l cm of one another. The result of using a measure such as EEG for source localization is the potential merging of signals from different (albeit anatomically close) regions in the brain. As stated above, the current project attempted to overcome this (in part) through the use of methodologies for source reconstruction such as the CDR approach, allowing for more discrete information regarding brain activation locations to be collected. Laplacian smoothing techniques are commonly used to counter volume conduction during source localization of EEG data. Instead of Laplacian methods however, the current project applied sLORETA, which relies on the use of signal to noise data present within the EEG signal itself for smoothing, which has shown to be effective in the past (M. Fuchs, Wagner, M., Kohler, T., & Wischmann, H.A., 1999). Further, there has been a great amount of support in the literature for the application of source localization techniques on sensor obtained data due to the emergence of such methodological approaches (Bardouille & Boe, 2012; Grech et al., 2008; Schoffelen & Gross, 2009).

It is important to note that the literature has documented some potential limitations related to source reconstruction methods (Michel et al., 2004; Thakor & Tong, 2004). The CDR used in this study in particular (sLORETA) can only distinguish sources active simultaneously if the signal is spatially distinct and of similar intensity (Wagner, 2004). Based on this idea, it should be noted that there is the potential for error when interpreting source level results that have been constrained to the 80 pre-specified nodes. Of the 80 nodes used in this study, many have coordinates that are somewhat close together in three-dimensional space. Due to the lower spatial resolution of EEG source

localization (i.e., 10.5 ± 5.4 mm), it is possible that relevant data is lost or indistinguishable. More specifically, there is the potential for data from two distinct brain regions to be considered as one, thus leading to the inaccurate interpretation of the findings.

7.3 Implications of the Task Choice

The use of a functional task was intended to permit the investigation of network patterns applicable to real-world scenarios. The use of the selected task however introduces considerable variability into the data obtained during the motor blocks. The research paradigm attempted to control for the variability that would result from using the sandwich task by instructing individuals to continue actively engaging in reach and grasp practice during all RTP blocks. More specifically, the participants were told to repeat the movement for the entire 30 s, even if the intended task (for example, pick up the bun) did not take the entire 30 s. However, there is the chance that these movements were performed in an uncontrolled manner that resulted in time points wherein no motor activity was being executed. The result of this could be that when collecting the EEG data on the experimental day, large portions of data within the RTP blocks were not reflective of actual overt movement, which may explain the lack of left hemisphere M1 involvement in the derived network. The nature of the functional task complicates the analysis further in that each RTP trial was aimed at completing a different component of the sandwich-making task. Specifically, the participants were each asked to engage in 30 s blocks of RTP 15 times, where each of these blocks was a different component of the task (i.e., picking up the bun, cutting the bun, putting condiment on the bun, putting meat or substitute on the bun, or putting toppings on the bun). When all of these blocks were

concatenated, the result was a 450 s block of data consisting of the performance of motor tasks, however each of these tasks differed in their execution. The use of the full 30 s time block of RTP for a FC analysis is much longer than what has previously been performed. For instance, previous work examining FC in the sensorimotor network used 5 s blocks, wherein each block used in analysis included brain activity related to the same movement (Bardouille & Boe, 2012). With the current project, it must be stated that activity in the beta frequency band likely fluctuated considerably over these 30 s blocks, leading to greater variability in the data (particularly when compared to the previously cited work). While we attempted to control for this variability, it must be noted that the nature of this functional task might have resulted in the collection of some data unrelated to overt movement during the RTP blocks.

CHAPTER 8 CONCLUSION

8.1 Future Directions

Future research is necessary in order to differentiate distinct portions of the task positive network for MI. In particular, it would be of interest to investigate the differences and similarities between the underlying neural correlates active during visual and kinesthetic MI tasks. These findings may guide clinicians in attempting to create MI protocols that are engaging the intended, and potentially region specific, sensorimotor brain networks. A final direction for future research would be the investigation of the neural correlates underlying MI in patients who have experienced a neurological insult (e.g., stroke), and the subsequent comparison of this task-positive network to that of a non-disabled individual. In addition, the functional task component of the current study would likely uncover explicit differences in the patterns of connectivity between non-disabled and patient populations. These differences would be a result of the differential, and relatively random, brain networks active during movement present after some neurological insult, and would aid researchers and clinicians in better characterizing how the motor network changes after injury.

8.2 Implications of the Research

This research contributes to advancing our knowledge related to fundamental processes that produce and control movement. Importantly, the findings provide insight into the manner in which the brain plans and executes movement by characterizing, in a quantifiable manner, the spatial and temporal aspects of network activation underlying overt and imagined movement. This study compared brain networks active during MI and overt movement in non-disabled participants. This comparison allowed for a better

understanding of how regions in the brain that comprise the motor system interact in order to perform motor simulations (i.e., imagery) in the absence of actual movement. More specifically, this study uncovered FC within premotor, parietal, and prefrontal regions for the performance of MI. In addition, the results uncovered that during a functional motor task, the FC network relies on primarily sensorimotor and cerebellar regions. A final finding of the current work was that there are distinct similarities (i.e., fronto-parietal, PFC) and differences (M1, PMC) in the FC that governs these two tasks. In addition, this study uncovered the fact that both the performance of imagined and overt movements result in task-related networks that are characterized by small world parameters in non-disabled participants.

This more detailed investigation of FC and network characteristics in the brain has the potential for application in clinical settings. In particular, patterns of FC underlying the performance of the functional motor task may be used to aid clinicians for diagnostic and treatment purposes. The acquired knowledge regarding the node pairs underlying imagined movement may aid in forming treatment plans for patients in the future by using MI more effectively to drive activity in specific brain regions. The establishment of an MI-specific network provides researchers and clinicians with fundamental information regarding how the brain simulates movement. In addition, the finding that the FC underlying MI exhibits small world properties distinguishes the networks governing MI from those of resting state connectivity, which adds to the notion that MI can be used in patient populations to engage specified brain connections for rehabilitation purposes. The continual investigation regarding FC within the neuronal systems that are involved in movement planning and execution is essential for uncovering

the typical network patterns that govern motor control.

Appendix I: Recruitment Advertisement

Capital Health

VOLUNTEERS NEEDED

Investigators at Dalhousie University and Capital Health are studying brain activity during imagined movement using electroencephalography (EEG).

We are looking for healthy volunteers 18 years of age and older to help us better understand how brain areas work together to create movement. The research study will be performed at the Laboratory for Brain Recovery and Function and will consist of three 60 minute and one 120 minute session.

If interested please contact:

A.M. Gionfriddo

MScPT(RR) Candidate

School of Physiotherapy

Dalhousie University

alicia.gionfriddo@dal.ca

(902) 494 1446

DALHOUSIE
UNIVERSITY
Inspiring Minds

Appendix II: Environment Script

"Imagine you are about to make a sandwich. Picture the space around you right now in your mind. Focus on the feel of the chair underneath you. Do you hear any noises? Use these to picture where you are about to make a sandwich. Get an image of all of the things you need to make a sandwich on the table in front of you."

Appendix III: Task Instructions

Instructions

First I want to orient you to the TV screen in front of you. During every day of study involvement you will be provided with both visual and auditory cues from this computer. The computer will display a visual written instruction for you and then count down from 3 for you to begin the given task. Any time that you hear a beep during the study you are to stop what you are doing and look to the screen for further instructions.

The first thing that you are going to do is a deep breathing exercise. The purpose of this is to relax your mind before you begin imagery. The deep breathing will last about three minutes. The breathing exercise will be guided for you visually by a video on the computer screen. The video will tell you when to breathe in and out. During this, I want you to focus on releasing any built up tension you might have in your body. I also want you to focus on taking deep, full breathes, and then releasing all of this air slowly and deliberately.

During this study you are going to be performing actual movements. The practice of real movement is when you will be making your sandwich. The buttons on the left side of the screen will let us take breaks in between each task. The buttons also allow me to explain to you what the next practice section will include. Specifically, the sandwich making will be broken up into the following parts: picking up a bun, cutting the bun, putting on condiment, putting on meat, and putting final toppings on.

In addition to real practice, I will also ask you to engage in imagined movement, or what we call motor imagery. When I ask you to perform motor imagery today I want you to imagine that you are performing the task yourself – or from "behind your own eyes". This is known as first person imagery. During all of the imagined tasks I want you to close your eyes and focus on how you would perform the movement yourself. An auditory script will guide each of the imagery blocks you will perform.

Appendix IV: Motor Imagery Scripts

Picking Up the Bun

"Take a deep breath. Imagine you are about to pick up the bun for your sandwich. Focus on reaching out your right arm to pick up the bun. Imagine how your arm extends at the shoulder, the elbow, and finally, the wrist so that you can stretch out and grasp the bun. Now think of bending your arm so that you can place the bun on the plate in front of you. Focus on how your arm moves as you grasp and carry the bun."

Cutting the Bun

" Take a deep breath. Imagine reaching out your right arm and picking up the knife on the table in front of you. Now focus on picking up the bun on your plate with your left hand so that you can cut it in half. Imagine yourself using the knife in your right hand to slice back and forth. Focus on the movement of your right arm controlling the knife to cut back and forth, back and forth, until the bun is in two pieces. Place the bun on the plate."

Putting Condiment on the Bun

"Take a deep breath. Imagine your favorite condiment. Picture your right arm reaching out to grab the sauce. Focus on grasping the condiment with your hand and bringing your arm towards you to place the condiment on the table. Now, imagine picking up a knife with your right hand. Move your arm to scoop condiment with the knife. Finally, picture bringing your arm towards you and spreading the condiment on the bun."

Putting Meat on the Bun

"Take a deep breath. Now that you have your bread cut and covered in condiment, imagine what kind of meat or substitute you would like on your sandwich. Now focus on reaching out your right arm to pick up pieces of meat one at a time and place them on your sandwich. Imagine how you would have to pinch your fingers on the slices to pick them up. Focus on how your arm moves through the air while you continually reach out to pick up more products, and the movement of your arm as you bend your elbow to place the products on the sandwich. Until you are happy with the final product."

Placing Final Toppings on the Sandwich

" Take a deep breath. Think about any last toppings that you might want to add to your favorite sandwich. Imagine yourself reaching out with your right arm to pick up your favorite toppings. Picture bringing your arm back into your body and placing the topping onto your sandwich. If you need a utensil, picture yourself picking it up with your right hand and then reaching your arm out in front of you to pick up the topping. Now focus on bringing the utensil back towards you to place the topping onto your sandwich."

Appendix V: Vegetarian Script

"Take a deep breath. Now that you have your bread cut and covered in condiment, imagine what kind of vegetables you would like on your sandwich. Focus on reaching out your right arm to pick up the vegetables one at a time and place them on your sandwich. Imagine how you would have to pinch your fingers in order to pick them up. Focus on how your arm moves through the air while you continually pick up more products, and the movement of your arm as you bend your elbow to place the products onto your sandwich, until you are happy with the final result."

Appendix VI: Source Nodes Coordinates

Node		Abbreviated Name	Hemi-sphere	X	Y	Z
Number	**Name**					
1	Anterior cingulate cortex	AntCC	MIDLINE	0	32	24
2	Posterior cingulate cortex	PosCC	MIDLINE	0	-32	24
3	Retrosplenial cingulate cortex	RsCC	MIDLINE	0	-48	12
4	Subgenual cingulate cortex	SubCC	MIDLINE	0	16	-8
5	Primary auditory cortex	A1	LEFT	-40	-14	4
6	Secondary auditory cortex	A2	LEFT	-60	-14	4
7	Frontal eye fields	FEF	LEFT	-36	8	56
8	Anterior insula	AntI	LEFT	-36	16	-4
9	Claustrum	Claus	LEFT	-36	-8	-4
10	Primary motor cortex	M1	LEFT	-24	-24	56
11	Inferior parietal cortex	IPC	LEFT	-44	-48	20
12	Angular gyrus	AG	LEFT	-44	-64	28
13	Precuneus	PreCun	LEFT	-8	-64	54
14	Superior parietal cortex	SPC	LEFT	-28	-56	54
15	Centrolateral prefrontal cortex	PFCCL	LEFT	-48	32	12
16	Dorsolateral prefrontal cortex	PFCDL	LEFT	-48	36	32
17	Dorsomedial prefrontal cortex	PFCDM	LEFT	-8	36	40
18	Medial prefrontal cortex	PFCMed	LEFT	-8	48	20
19	Orbitofrontal cortex	PFCORB	LEFT	-24	44	-20
20	Frontal polar prefrontal cortex	PFCFPol	LEFT	-24	64	4

Node		Abbreviated Name	Hemi-sphere	X	Y	Z
Number	**Name**					
21	Ventrolateral prefrontal cortex	PFCVL	LEFT	-48	32	-8
22	Parahippocampal cortex	ParHippC	LEFT	-28	-16	-16
23	Dorsolateral premotor cortex	PMCDL	LEFT	-28	0	60
24	Medial premotor cortex	PMCMed	LEFT	-4	0	60
25	Ventrolateral premotor cortex	PMCVL	LEFT	-44	4	24
26	Pulvinar	Pulvinar	LEFT	-16	-28	4
27	Primary somatosensory cortex	S1	LEFT	-40	-28	64
28	Secondary somatosensory cortex	S2	LEFT	-56	-16	16
29	Middle temporal cortex	TCMid	LEFT	-64	-24	-12
30	Inferior temporal cortex	TCI	LEFT	-64	-24	-24
31	Temporal pole	TempPol	LEFT	-52	12	-28
32	Superior temporal cortex	TCS	LEFT	-52	-4	-8
33	Ventral temporal cortex	TCV	LEFT	-32	-28	-28
34	Thalamus (ventral lateral nucleus)	Thal	LEFT	-8	-8	4
35	Primary visual cortex	V1	LEFT	-4	-84	-4
36	Secondary visual cortex	V2	LEFT	-4	-96	8
37	Cuneus	Cun	LEFT	-20	-88	20
38	Fusiform gyrus	FusiG	LEFT	-20	-84	-12
39	Primary auditory cortex	A1	RIGHT	40	-14	4
40	Secondary auditory cortex	A2	RIGHT	60	-14	4
41	Frontal eye fields	FEF	RIGHT	36	8	56

Node		Abbreviated Name	Hemi-sphere	X	Y	Z
Number	Name					
42	Anterior insula	AntI	RIGHT	36	16	-4
43	Claustrum	Claus	RIGHT	36	-8	-4
44	Primary motor cortex	M1	RIGHT	24	-24	56
45	Inferior parietal cortex	IPC	RIGHT	44	-48	20
46	Angular gyrus	AG	RIGHT	44	-64	28
47	Precuneus	PreCun	RIGHT	8	-64	54
48	Superior parietal cortex	SPC	RIGHT	28	-56	54
49	Centrolateral prefrontal cortex	PFCCL	RIGHT	48	32	12
50	Dorsolateral prefrontal cortex	PFCDL	RIGHT	48	36	32
51	Dorsomedial prefrontal cortex	PFCDM	RIGHT	8	36	40
52	Medial prefrontal cortex	PFCMed	RIGHT	8	48	20
53	Orbitofrontal cortex	PFCORB	RIGHT	24	44	-20
54	Frontal polar	PFCFPol	RIGHT	24	64	4
55	Ventrolateral prefrontal cortex	PFCVL	RIGHT	48	32	-8
56	Parahippocampal cortex	ParHippC	RIGHT	28	-16	-16
57	Dorsolateral premotor cortex	PMCDL	RIGHT	28	0	60
58	Medial premotor cortex	PMCMed	RIGHT	4	0	60
59	Ventrolateral premotor cortex	PMCVL	RIGHT	44	4	24
60	Pulvinar	Pulvinar	RIGHT	16	-28	4
61	Primary somatosensory cortex	S1	RIGHT	40	-28	64

Node		Abbreviated Name	Hemi-sphere	X	Y	Z
Number	**Name**					
62	Secondary somatosensory cortex	S2	RIGHT	56	-16	16
63	Middle temporal cortex	TCMid	RIGHT	64	-24	-12
64	Inferior temporal cortex	TCI	RIGHT	64	-24	-24
65	Temporal pole	TempPol	RIGHT	52	12	-28
66	Superior temporal cortex	TCS	RIGHT	52	-4	-8
67	Ventral temporal cortex	TCV	RIGHT	32	-28	-28
68	Thalamus (ventral lateral nucleus)	Thal	RIGHT	8	-8	4
69	Primary visual cortex	V1	RIGHT	4	-84	-4
70	Secondary visual cortex	V2	RIGHT	4	-96	8
71	Cuneus	Cun	RIGHT	20	-88	20
72	Fusiform gyrus	FusiG	RIGHT	20	-84	-12
73	Dentate Nucleus	Dentate	LEFT	-12	-52	-24
74	Posterior Lobe	PostLobe	LEFT	-30	-55	-49
75	Cruseus 1	CrusI	LEFT	-36	-46	-26
76	Cruseus 2	CrusII	LEFT	-45	-45	-32
77	Dentate Nucleus	Dentate	RIGHT	12	-52	-24
78	Posterior Lobe	PostLobe	RIGHT	30	-55	-49
79	Cruseus 1	CrusI	RIGHT	36	-46	-26
80	Cruseus 2	CrusII	RIGHT	45	-45	-32

Appendix VII: Motor Imagery Node Pairs

Significant Node Pairs During MI				
Node	*Hemi-sphere*	*Node*	*Hemi-sphere*	*BSR Value*
Posterior Cingulate Cortex	Midline	Contralateral Prefrontal Cortex	Left	-6.046923
Retrosplenial Cingulate Cortex	Midline	Superior Temporal Cortex	Right	-4.252636
Primary Auditory Cortex	Left	Thalamus	Left	-5.768384
Primary Auditory Cortex	Left	Contralateral Prefrontal Cortex	Right	-5.085583
Primary Auditory Cortex	Left	Dorsolateral Prefrontal Cortex	Right	-4.712359
Primary Auditory Cortex	Left	Ventrolateral Premotor Cortex	Right	-4.905731
Secondary Auditory Cortex	Left	Primary Sensory Cortex	Left	-4.707870
Anterior Insula	Left	CrusII	Right	-4.258146
Claustrum	Left	Secondary Auditory Cortex	Right	-4.485275
Primary Motor Cortex	Left	Parahippocampal Cortex	Right	-4.293309
Inferior Parietal Cortex	Left	Ventral Temporal Cortex	Right	-5.306369
Angular Gyrus	Left	Secondary Visual Cortex	Left	-4.854055
Angular Gyrus	Left	Angular Gyrus	Right	-4.567403
Precuneus	Left	Dorsolateral Premotor Cortex	Right	-4.786255
Precuneus	Left	CrusI	Right	-4.980391
Superior Parietal Cortex	Left	Medial Prefrontal Cortex	Right	-5.063730
Dorsomedial Prefrontal Cortex	Left	Anterior Insula	Right	-7.531295
Dorsomedial Prefrontal Cortex	Left	Dorsolateral Prefrontal Cortex	Right	-4.997683
Dorsomedial Prefrontal Cortex	Left	Pulvinar	Right	-4.204037
Medial Prefrontal Cortex	Left	Frontal Polar	Left	-4.228856
Frontal Polar	Left	Pulvinar	Left	-4.730337
Ventrolateral Prefrontal Cortex	Left	Precuneus	Right	-4.393868

Significant Node Pairs During MI				
Node	Hemi-sphere	Node	Hemi-sphere	BSR Value
Ventrolateral Prefrontal Cortex	Left	Posterior Lobe	Left	-4.492005
Parahippocampal Cortex	Left	Primary Visual Cortex	Left	-4.461650
Dorsolateral Premotor Cortex	Left	Middle Temporal Cortex	Right	-4.810990
Medial Premotor Cortex	Left	Superior Parietal Cortex	Right	-4.992370
Medial Premotor Cortex	Left	Ventrolateral Premotor Cortex	Right	-4.599886
Ventrolateral Premotor Cortex	Left	Fusiform Gyrus	Right	-4.760478
Pulvinar	Right	Medial Premotor Cortex	Right	-5.723614
Primary Sensory Cortex	Left	Frontal Eye Fields	Right	-4.632406
Primary Sensory Cortex	Left	Ventrolateral Prefrontal Cortex	Right	-4.318048
Inferior Temporal Cortex	Left	Inferior Temporal Cortex	Right	-4.525864
Temporal Pole	Left	Primary Auditory Cortex	Right	-7.565775
Temporal Pole	Left	Superior Temporal Cortex	Right	-4.643579
Superior Temoral Cortex	Left	Thalamus	Right	-4.972682
Ventral Temporal Cortex	Left	Parahippocampal Cortex	Right	-4.432128
Primary Visual Cortex	Left	Anterior Insula	Right	-5.838949
Primary Visual Cortex	Left	Posterior Lobe	Left	-4.507659
Primary Visual Cortex	Left	CrusI	Left	-4.174142
Cuneus	Left	CrusI	Left	-4.878358
Cuneus	Left	Posterior Lobe	Right	-4.665318
Fusiform Gyrus	Left	Claustrum	Right	-7.213448
Primary Auditory Cortex	Right	Dentate	Right	-5.067334
Secondary Auditory Cortex	Right	Dorsomedial Prefrontal Cortex	Right	-4.242876

Significant Node Pairs During MI				
Node	Hemi-sphere	Node	Hemi-sphere	BSR Value
Claustrum	Right	Posterior Lobe	Left	-4.459578
Claustrum	Right	Dentate	Right	-4.864610
Primary Motor Cortex	Right	Dorsolateral Prefrontal Cortex	Right	-4.439273
Inferior Parietal Cortex	Right	Parahippocampal Cortex	Right	-4.399391
Inferior Parietal Cortex	Right	Primary Visual Cortex	Right	-5.061074
Angular Gyrus	Right	CrusI	Left	-4.279803
Superior Parietal Cortex	Right	Medial Premotor Cortex	Right	-5.626406
Contralateral Prefrontal Cortex	Right	Primary Sensory Cortex	Right	-4.696419
Contralateral Prefrontal Cortex	Right	Inferior Temporal Cortex	Right	-4.572350
Dorsolateral Prefrontal Cortex	Right	Superior Temporal Cortex	Right	-6.576650
Dorsolateral Prefrontal Cortex	Right	Primary Visual Cortex	Right	-4.603279
Orbitofrontal Cortex	Right	Dentate – Left	Left	-4.233244
Primary Sensory Cortex	Right	Temporal Pole	Right	-4.624526
Superior Temporal Cortex	Right	Cuneus	Right	-7.010948
Secondary Visual Cortex	Right	Posterior Lobe	Right	-4.716611

**Appendix VIII: Motor Imagery Partial Least Square Results**
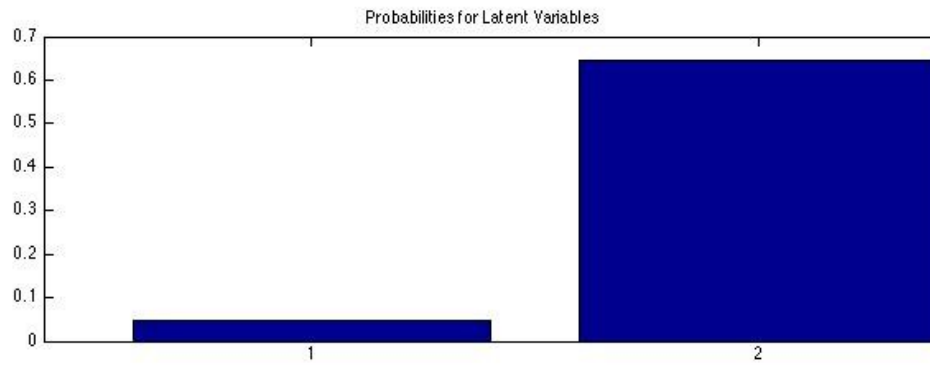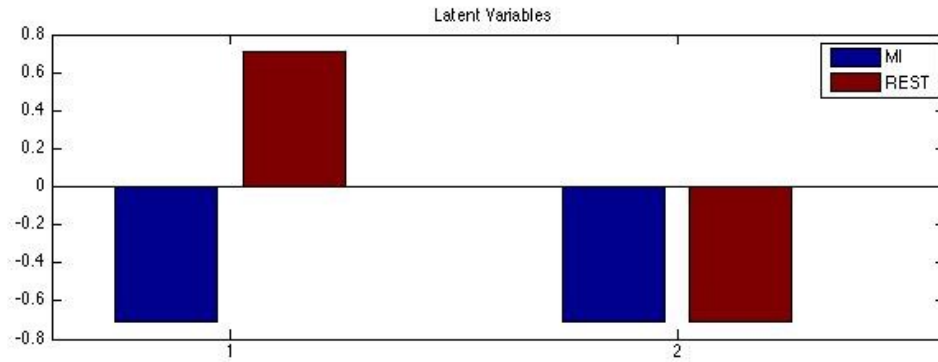
Appendix IX: Repetitive Task Practice Node Pairs

Significant Node Pairs During RTP				
Node	Hemi-sphere	Node	Hemi-sphere	BSR Value
Anterior Cingulate Cortex	Midline	Thalamus	Right	-2.566405
Posterior Cingulate Cortex	Midline	Ventral Temporal Cortex	Right	-2.546073
Retrosplenial Cingulate Cortex	Midline	Ventrolateral Premotor Cortex	Left	-2.869666
Retrosplenial Cingulate Cortex	Midline	Claustrum	Right	-2.542176
Subgenual Cingulate Cortex	Midline	Contralateral Prefrontal Cortex	Left	-2.627070
Subgenual Cingulate Cortex	Midline	Medial Premotor Cortex	Left	-2.834646
Secondary Auditory Cortex	Left	Dorsolateral Prefrontal Cortex	Left	-2.539283
Secondary Auditory Cortex	Left	Superior Parietal Cortex	Right	-2.560159
Frontal Eye Field	Left	Frontal Polar	Left	-2.570559
Anterior Insula	Left	Pulvinar	Right	-2.772830
Inferior Parietal Cortex	Left	Medial Prefrontal Cortex	Left	-2.541605
Inferior Parietal Cortex	Left	Dentate	Left	-2.987639
Superior Parietal Cortex	Left	Medial Prefrontal Cortex	Right	-2.546772
Contralateral Prefrontal Cortex	Left	Parahippocampal Cortex	Right	-2.741412
Contralateral Prefrontal Cortex	Left	Dentate	Right	-2.518140
Dorsomedial Prefrontal Cortex	Left	Dentate	Left	-2.558347
Medial Prefrontal Cortex	Left	Primary Motor Cortex	Right	-2.603501
Orbitofrontal	Left	CrusII	Right	-2.548665
Frontal Polar	Left	Inferior Parietal Cortex	Right	-2.527363
Frontal Polar	Left	Ventrolateral Prefrontal Cortex	Right	-2.966509
Ventrolateral Prefrontal Cortex	Left	Dentate	Left	-2.653000
Parahippocampal Cortex	Left	Dorsomedial Prefrontal Cortex	Right	-2.774712

Significant Node Pairs During RTP				
Node	*Hemi-sphere*	*Node*	*Hemi-sphere*	*BSR Value*
Medial Premotor Cortex	Left	Ventral Temporal Cortex	Right	-2.531021
Pulvinar	Left	Dorsolateral Prefrontal Cortex	Right	-2.625097
Secondary Sensory Cortex	Left	Orbitofrontal	Right	-2.517244
Secondary Sensory Cortex	Left	Dentate	Left	-2.537828
Temporal Pole	Left	Primary Visual Cortex	Right	-2.703849
Temporal Pole	Left	Dentate	Left	-2.555137
Superior Temporal Cortex	Left	Cuneus	Left	-2.765194
Superior Temporal Cortex	Left	Dorsolateral Prefrontal Cortex	Right	-3.081554
Primary Visual Cortex	Left	Claustrum	Right	-2.543950
Primary Visual Cortex	Left	Pulvinar	Right	-2.824881
Primary Visual Cortex	Left	Thalamus	Right	-2.551364
Cuneus	Left	Claustrum	Right	-2.615804
Cuneus	Left	Inferior Temoral Cortex	Right	-2.524728
Primary Auditory Cortex	Right	Secondary Visual Cortex	Right	-2.571236
Primary Auditory Cortex	Right	CrusI	Right	-2.795251
Secondary Auditory Cortex	Right	Parahippocampal Gyrus	Right	-2.660870
Secondary Auditory Cortex	Right	Ventral Temporal Cortex	Right	-2.576232
Secondary Auditory Cortex	Right	CrusI	Right	-2.685627
Frontal Eye Field	Right	Superior Parietal Cortex	Right	-2.738321
Claustrum	Right	Ventrolateral Prefrontal Cortex	Right	-2.562065
Claustrum	Right	Primary Visual Cortex	Right	-2.625470
Primary Motor Cortex	Right	Primary Visual Cortex	Right	-2.642186
Inferior Parietal Cortex	Right	Medial Prefrontal Cortex	Right	-2.517894

Significant Node Pairs During RTP				
Node	Hemi-sphere	Node	Hemi-sphere	BSR Value
Precuneus	Right	Fusiform Gyrus	Right	-2.540870
Dorsomedial Prefrontal Cortex	Right	Primary Sensory Cortex	Right	-2.569637
Ventrolateral Prefrontal Cortex	Right	Medial Premotor Cortex	Right	-2.590708
Parahippocampal Cortex	Right	Secondary Visual Cortex	Right	-2.853229
Medial Premotor Cortex	Right	Pulvinar	Right	-2.569368
Ventrolateral Premotor Cortex	Right	Pulvinar	Right	-2.545195
Pulvinar	Right	Ventral temporal Cortex	Right	-2.640145
Pulvinar	Right	Posterior Lobe of Cerebellum	Left	-2.804126
Temporal Pole	Right	CrusI	Right	-2.563048
Superior Temporal Cortex	Right	Dentate	Left	-2.594946
Thalamus	Right	Secondary Visual Cortex	Right	-2.761966
Thalamus	Right	Dentate	Right	-2.760648
Thalamus	Right	CrusI	Right	-2.520506

Appendix X: Repetitive Task Practice Partial Least Square Results
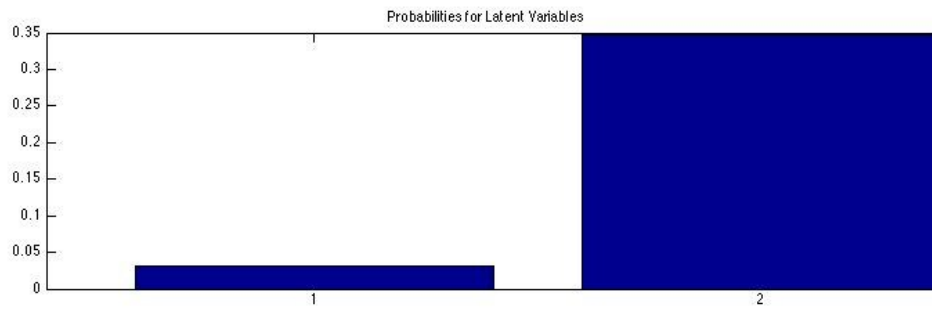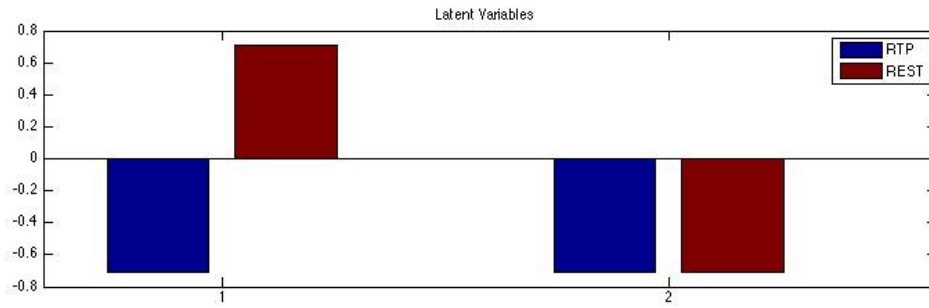
Appendix XI: Motor Imagery Node Degree

Node	Hemisphere	ND-MI
Contralateral Prefrontal Cortex	Left	6
Primary Sensory Cortex	Left	6
Dusiform Gyrus	Left	6
Medial Premotor Cortex	Right	6
Middle Temporal Cortex	Right	6
Medial Premotor Cortex	Left	5
Primary Auditory Cortex	Right	5
Secondary Visual Cortex	Right	5
CrusII	Right	5
Orbitofrontal	Left	4
Dorsolateral Premotor Cortex	Left	4
Secondary Sensory Cortex	Left	4
Cuneus	Right	4
Frontal Eye Field	Left	3
Claustrum	Left	3
Precuneus	Left	3
Dorsolateral Prefrontal Cortex	Left	3
Inferior Temporal Cortex	Left	3
Primary Visual Cortex	Left	3
Secondary Auditory Cortex	Right	3
Frontal Eye Field	Right	3
Medial Prefrontal Cortex	Right	3
Orbitofrontal	Right	3
Ventrolateral Prefrontal Cortex	Right	3
Parahippocampal Cortex	Right	3
Dorsolateral Premotor Cortex	Right	3
Ventrolateral Premotor Cortex	Right	3
Medial Prefrontal Cortex	Left	2
Primary Motor Cortex	Right	2
Inferior Parietal Cortex	Right	2
Inferior Temporal Cortex	Right	2
Superior Temporal Cortex	Right	2
Superior Parietal Cortex	Left	1
Ventrolateral Prefrontal Cortex	Left	1
Middle Temporal Cortex	Left	1
Primary Motor Cortex	Left	1
Precuneus	Right	1
Primary Sensory Cortex	Right	1

Appendix XII: Repetitive Task Practice Node Degree

Node	Hemisphere	ND-RTP
Dentate	Left	11
CrusI	Left	9
Ventral Temporal Cortex	Left	8
Secondary Auditory Cortex	Left	6
Dorsomedial Prefrontal Cortex	Left	6
Orbitofrontal	Left	6
Posterior Cingulate Cortex	Left	5
Secondary Visual Cortex	Left	5
Parahippocampal Cortex	Left	5
Secondary Sensory Cortex	Left	5
Anterior Insula	Left	4
Claustrum	Left	4
Medial Prefrontal Cortex	Left	4
Pulvinar	Left	4
Superior Temporal Cortex	Left	4
Thalamus	Left	4
Claustrum	Left	4
Dorsolateral Prefrontal Cortex	Left	4
Pulvinar	Right	4
Primary Sensory Cortex	Right	4
Superior Temporal Cortex	Right	4
Precuneus	Left	3
Primary Sensory Cortex	Left	3
Superior Parietal Cortex	Left	3
Inferior Temporal Cortex	Left	3
Precuneus	Right	3
Contralateral Prefrontal Cortex	Right	3
Temporal Pole	Right	3
Posterior Lobe of Cerebellum	Right	3
Frontal Eye Field	Left	2
Orbitofrontal	Left	2
Parahippocampal Cortex	Left	2
Dorsolateral Premotor Cortex	Left	2
Ventrolateral Premotor Cortex	Left	2
Middle Temporal Cortex	Left	2
Primary Visual Cortex	Left	2
Primary Auditory Cortex	Right	2
Frontal Eye Field	Right	2
Inferior Parietal Cortex	Right	2
Dorsomedial Prefrontal Cortex	Right	2
Inferior Parietal Cortex	Left	1
Dorsolateral Prefrontal Cortex	Left	1
Medial Premotor Cortex	Left	1

Node	Hemisphere	ND-RTP
Primary Motor Cortex	Right	1
Medial Premotor Cortex	Right	1
Inferior Temporal Cortex	Right	1
Primary Visual Cortex	Right	1

References

Ahmadlou, M., Adeli, H., & Adeli, A. (2012). Graph Theoretical Analysis of Organization of Functional Brain Networks in ADHD. *Clinical EEG and Neuroscience, 43*(1), 5-13. doi: 10.1177/1550059411428555

Arora, S., Aggarwal, R., Sirimanna, P., Moran, A., Grantcharov, T., Kneebone, R., . . . Darzi, A. (2011). Mental practice enhances surgical technical skills: a randomized controlled study. *Ann Surg, 253*(2), 265-270. doi: 10.1097/SLA.0b013e318207a789

Arya, K. N., Pandian, S., Verma, R., & Garg, R. K. (2011). Movement therapy induced neural reorganization and motor recovery in stroke: a review. *J Bodyw Mov Ther, 15*(4), 528-537. doi: 10.1016/j.jbmt.2011.01.023

Badia, S.B., Morgade, A.G., & Verschure, P.F.M.J. (2013). Using a hybrid brain computer interface and virtual reality system to monitor and promote cortical reorganization through motor activity and motor imagery training. *IEEE Transactions on Neural Systems and Rehabilitation Engineering, 21*(2), 174-181.

Bailet, S., Mosher, J.C., & Leahy, R.M. (2001). Electromagnetic Brain Mapping. *IEEE Signal Processing Magazine*, 14-30.

Bardouille, T., & Boe, S. (2012). State-related changes in MEG functional connectivity reveal the task-positive sensorimotor network. *PLoS One, 7*(10), e48682. doi: 10.1371/journal.pone.0048682

Bastian, A. J. (2006). Learning to predict the future: the cerebellum adapts feedforward movement control. *Curr Opin Neurobiol, 16*(6), 645-649. doi: 10.1016/j.conb.2006.08.016

Baugh, L. A., Lawrence, J. M., & Marotta, J. J. (2011). Novel claustrum activation observed during a visuomotor adaptation task using a viewing window paradigm. *Behav Brain Res, 223*(2), 395-402. doi: 10.1016/j.bbr.2011.05.009

Beauchamp, M.S., Lee, K.E., Argail, B.D., Martin, A. (2004). Integration of auditory and visual information about objects in superior temporal sulcus. *Neuron, 41*, 809-823.

Belin, P., Zatorre, R.J., & Ahad, P. (2002). Human temporal-lobe response to vocal sounds. *Cognitive Brain Research, 13*, 17-26.

Bernhardt, B. C., Chen, Z., He, Y., Evans, A. C., & Bernasconi, N. (2011). Graph-theoretical analysis reveals disrupted small-world organization of cortical thickness correlation networks in temporal lobe epilepsy. *Cereb Cortex, 21*(9), 2147-2157. doi: 10.1093/cercor/bhq291

Boe, S., Gionfriddo, A., Kraeutner, S., Tremblay, A., Little, G., & Bardouille, T. (2014). Laterality of brain activity during motor imagery is modulated by the provision of source level neurofeedback. *Neuroimage*. doi: 10.1016/j.neuroimage.2014.06.066

Boucard, A., Marchand, A., & Nogues, X. (2007). Reliability and validity of structural equation modeling applied to neuroimaging data: a simulation study. *J Neurosci Methods, 166*(2), 278-292. doi: 10.1016/j.jneumeth.2007.07.011

Braun, S., Kleynen, M., Schols, J., Schack, T., Beurskens, A., & Wade, D. (2008). Using mental practice in stroke rehabilitation: a framework. *Clin Rehabil, 22*(7), 579-591. doi: 10.1177/0269215508090066

Bremmer, F., Schlack, A., Shah, N.J., Zafiris, O., Kubischik, M., Hoffmann, K.P., Ziles, K., & Fink, G.R. (2001). Polymodal motion processing in posterior parietal and premotor cortex: A human fMRI study strongly implies equivalencies between humans and monkeys. *Neuron, 29*, 287-296.

Bullmore, E., & Sporns, O. (2009). Complex brain networks: graph theoretical analysis of structural and functional systems. *Nat Rev Neurosci, 10*(3), 186-198. doi: 10.1038/nrn2575

Buma, F. E., Lindeman, E., Ramsey, N. F., & Kwakkel, G. (2010). Functional neuroimaging studies of early upper limb recovery after stroke: a systematic review of the literature. *Neurorehabil Neural Repair, 24*(7), 589-608. doi: 10.1177/1545968310364058

Butler, A. J., & Page, S. J. (2006). Mental practice with motor imagery: evidence for motor recovery and cortical reorganization after stroke. *Arch Phys Med Rehabil, 87*(12 Suppl 2), S2-11. doi: 10.1016/j.apmr.2006.08.326

Butz, M., Worgotter, F., & van Ooyen, A. (2009). Activity-dependent structural plasticity. *Brain Res Rev, 60*(2), 287-305. doi: 10.1016/j.brainresrev.2008.12.023

Cao, C., & Slobounov, S. (2010). Alteration of cortical functional connectivity as a result of traumatic brain injury revealed by graph theory, ICA, and sLORETA analysis of EEG signals. *IEEE Transactions on Neural Systems and Rehabilitation Engineering, 18*(1), 11-19.

Carmichael, S. T. (2003). Plasticity of Cortical Projections after Stroke. *The Neuroscientist, 9*(1), 64-75. doi: 10.1177/1073858402239592

Carter, A. R., Shulman, G. L., & Corbetta, M. (2012). Why use a connectivity-based approach to study stroke and recovery of function? *Neuroimage, 62*(4), 2271-2280. doi: 10.1016/j.neuroimage.2012.02.070

Cavanna, A. E., & Trimble, M. R. (2006). The precuneus: a review of its functional anatomy and behavioural correlates. *Brain, 129*(Pt 3), 564-583. doi: 10.1093/brain/awl004

Chen, R., Gerloff, C., Hallett, M., & Cohen, L.G. (1997). Involvement of the ipsilateral motor cortex in finger movements of differentn complexities. *Ann Neurol, 41*, 247-254.

Ciccarelli, O., Toosy, A. T., Marsden, J. F., Wheeler-Kingshott, C. M., Sahyoun, C., Matthews, P. M., . . . Thompson, A. J. (2005). Identifying brain regions for integrative sensorimotor processing with ankle movements. *Experimental brain research. Experimentelle Hirnforschung. Experimentation cerebrale, 166*(1), 31-42. doi: 10.1007/s00221-005-2335-5

Classen, J., Gerloff, C., Honda, M., & Hallet, M. (1998). Integrative visuomotor behaviour is associated with interregionally coherent oscillations in the human brain. *J Neurophysiol, 79*, 1567-1573.

Cohen, D., & Cuffin, B. N. (1983). Demonstration of useful differences between magnetoencephalogram and electroencephalogram. *Electroencephalography and clinical neurophysiology, 56*(1), 38-51.

Cohen, D., & Halgren, E. (2003). Magnetoencephalography (Neuromagnetism). *Encyclopedia of Neuroscience*, 1-7.

Colebatch, J.G., Deiber, M.P., Passingham, R.E., Friston, K.J., & Frackowiak, R.S.J. (1991). Regional cerebral blood flow during voluntary arm and hand movements in human subjects. *Journal of Neuroscience, 65*(6), 1292-1401.

Conforto, A. B., Kaelin-Lang, A., & Cohen, L. G. (2002). Increase in hand muscle strength of stroke patients after somatosensory stimulation. *Annals of neurology*, *51*(1), 122-125.

Corbetta, M., & Shulman, G. L. (2002). Control of goal-directed and stimulus-driven attention in the brain. *Nat Rev Neurosci, 3*(3), 201-215. doi: 10.1038/nrn755

Craig, C. L., Marshall, A. L., Sjostrom, M., Bauman, A. E., Booth, M. L., Ainsworth, B. E., . . . Oja, P. (2003). International physical activity questionnaire: 12-country reliability and validity. *Med Sci Sports Exerc, 35*(8), 1381-1395. doi: 10.1249/01.MSS.0000078924.61453.FB

Cramer, S. C. (2004). Functional imaging in stroke recovery. *Stroke; a journal of cerebral circulation, 35*(11 Suppl 1), 2695-2698. doi: 10.1161/01.STR.0000143326.36847.b0

Cramer, S. C., Finklestein, S.P., Schaechter, J.D., Bush, G., & Rosen, B.R. (1999). Activation of distinct motor cortex regions during ipsilateral and contralateral finger movements. *J Neurophysiol, 81*(383-387).

Crick, F. C., & Koch, C. (2005). What is the function of the claustrum? *Philos Trans R Soc Lond B Biol Sci, 360*(1458), 1271-1279. doi: 10.1098/rstb.2005.1661

Crosbie, Jacqueline H., McDonough, Suzanne M., Gilmore, David H., & Wiggam, M. Ivan. (2004). The adjunctive role of mental practice in the rehabilitation of the upper limb after hemiplegic stroke: a pilot study. *Clin Rehabil, 18*(1), 60-68. doi: 10.1191/0269215504cr702oa

Cuffin, B.N., Schomer, D.L., Ives, S.J., & Blume, H. (2001). Experimental tests of EEG source localization accuracy in realistically shaped head models. *Clinical Neurophysiology, 112*, 2288-2292.

Culham, J. C., Cavina-Pratesi, C., & Singhal, A. (2006). The role of parietal cortex in visuomotor control: what have we learned from neuroimaging? *Neuropsychologia, 44*(13), 2668-2684. doi: 10.1016/j.neuropsychologia.2005.11.003

Culham, J. C., Danckert, S. L., DeSouza, J. F., Gati, J. S., Menon, R. S., & Goodale, M. A. (2003). Visually guided grasping produces fMRI activation in dorsal but not ventral stream brain areas. *Experimental brain research. Experimentelle Hirnforschung. Experimentation cerebrale, 153*(2), 180-189. doi: 10.1007/s00221-003-1591-5

Cunnington, R., Windischberger, C., Deecke, L., & Moser, E. (2002). The preparation and execution of self-initiated and externally-triggered movement: a study of event-related fMRI. *Neuroimage, 15*(2), 373-385. doi: 10.1006/nimg.2001.0976

De Vico Fallani, F., Pichiorri, F., Morone, G., Molinari, M., Babiloni, F., Cincotti, F., & Mattia, D. (2013). Multiscale topological properties of functional brain networks during motor imagery after stroke. *Neuroimage, 83*, 438-449. doi: 10.1016/j.neuroimage.2013.06.039

Debaere, F., Wenderoth, N., Sunaert, S., Van Hecke, P., & Swinnen, S. P. (2004). Cerebellar and premotor function in bimanual coordination: parametric neural responses to spatiotemporal complexity and cycling frequency. *Neuroimage, 21*(4), 1416-1427. doi: 10.1016/j.neuroimage.2003.12.011

Decety, J. (1996). The neurophysiological basis of motor imagery. *Behavioural Brain Research, 77*, 45-52.

Decety, J., & Jeannerod, M. (1996). Mentally simulated movements in virtual reality: does Fitt's law hold in motor imagery? *Behavioural Brain Research, 72*(127-134).

Dechent, P., Merboldt, K.D., & Frahm, J. (2004). Is the human primary motor cortex involved in motor imagery? *Cognitive Brain Research, 19*, 138-144. doi: 10.1016/j.cogbrainres.2004.05.001

10.1016/j.cogbrainres.2003.11.012

Destrebecqz, Arnaud, Peigneux, Philippe, Laureys, Steven, Degueldre, Christian, Del Fiore, Guy, Aerts, Joël, . . . Maquet, Pierre. (2003). Cerebral correlates of explicit sequence learning. *Cognitive Brain Research, 16*(3), 391-398. doi: 10.1016/s0926-6410(03)00053-3

Diaconescu, A.O., Alain, C., & McIntosh, A.R. (2011). The co-occurrence of multisensory facilitation and cross-modal conflict in the human brain. *J Neurophysiol, 106*, 2896-2909. doi: 10.1152/jn.00303.2011.-Perceptual

Dohle, C., Stephan, K. M., Valvoda, J. T., Hosseiny, O., Tellmann, L., Kuhlen, T., . . . Freund, H. J. (2011). Representation of virtual arm movements in precuneus. *Experimental brain research. Experimentelle Hirnforschung. Experimentation cerebrale, 208*(4), 543-555. doi: 10.1007/s00221-010-2503-0

Dosenbach, N. U., Fair, D. A., Miezin, F. M., Cohen, A. L., Wenger, K. K., Dosenbach, R. A., . . . Petersen, S. E. (2007). Distinct brain networks for adaptive and stable task control in humans. *Proc Natl Acad Sci U S A, 104*(26), 11073-11078. doi: 10.1073/pnas.0704320104

Dum, R. P., & Strick, P. L. (2005). Frontal lobe inputs to the digit representations of the motor areas on the lateral surface of the hemisphere. *J Neurosci, 25*(6), 1375-1386. doi: 10.1523/JNEUROSCI.3902-04.2005

Ehrsson, H. H., Geyer, S., & Naito, E. (2003). Imagery of voluntary movement of fingers, toes, and tongue activates corresponding body-part-specific motor representations. *J Neurophysiol, 90*(5), 3304-3316. doi: 10.1152/jn.01113.2002

Fassbender, C., Murphy, K., Foxe, J. J., Wylie, G. R., Javitt, D. C., Robertson, I. H., & Garavan, H. (2004). A topography of executive functions and their interactions revealed by functional magnetic resonance imaging. *Brain Res Cogn Brain Res, 20*(2), 132-143. doi: 10.1016/j.cogbrainres.2004.02.007

Ferraye, M. U., Debu, B., Heil, L., Carpenter, M., Bloem, B. R., & Toni, I. (2014). Using motor imagery to study the neural substrates of dynamic balance. *PLoS One, 9*(3), e91183. doi: 10.1371/journal.pone.0091183

Féry, Y. A. (2003). Differentiating visual and kinesthetic imagery in mental practice. *Canadian Journal of Experimental Psychology/Revue canadienne de psychologie expérimentale, 57*(1), 1.

Fleming, M. K., Stinear, C. M., & Byblow, W. D. (2010). Bilateral parietal cortex function during motor imagery. *Experimental brain research. Experimentelle Hirnforschung. Experimentation cerebrale, 201*(3), 499-508. doi: 10.1007/s00221-009-2062-4

Floyer-Lea, A., & Matthews, P. M. (2004). Changing brain networks for visuomotor control with increased movement automaticity. *J Neurophysiol, 92*(4), 2405-2412. doi: 10.1152/jn.01092.2003

French, B., Thomas, L. H., Leathley, M. J., Sutton, C. J., McAdam, J., Forster, A., . . . Watkins, C. L. (2009). Repetitive Task Training for Improving Functional Ability After Stroke. *Stroke, 40*(4), e98-e99. doi: 10.1161/strokeaha.108.519553

Friston, K. J. (2002). Bayesian estimation of dynamical systems: an application to fMRI. *Neuroimage, 16*(2), 513-530. doi: 10.1006/nimg.2001.1044

Friston, K. J., Harrison, L., & Penny, W. (2003). Dynamic causal modelling. *Neuroimage, 19*(4), 1273-1302. doi: 10.1016/s1053-8119(03)00202-7

Friston, K. J., Worsley, K.J., Frackowiak, R.S.J,, Mazziotta, J.C., & Evans, A.c. (1994). Assessng the significance of focal activations using their spatial extent. *Hum Brain Mapp, 1*, 210-220.

Fuchs, M., Kastner, J., Wagner, M., Hawes, S., Ebersole, J.S. (2002). A standardized boundary element method volume conductor model. *Clinical Neurophysiology, 113*, 702-712.

Fuchs, M., Wagner, M., Kohler, T., & Wischmann, H.A. (1999). Linear and nonlinear current density reconstructions. *Journal of Clinical Neurophysiology, 16*(3), 267-295.

Gao, Q., Duan, X., & Chen, H. (2011). Evaluation of effective connectivity of motor areas during motor imagery and execution using conditional Granger causality. *Neuroimage, 54*(2), 1280-1288. doi: 10.1016/j.neuroimage.2010.08.071

Garavan, H., Ross, T.J., & Stein, E.A. (1999). Right hemispheric dominance of inhibitory control: An event-related functional MRI study. *Proc Natl Acad Sci U S A, 96*, 8301-8306.

Gentili, R., Papaxanthis, C., & Pozzo, T. (2006). Improvement and generalization of arm motor performance through motor imagery practice. *Neuroscience, 137*(3), 761-772. doi: 10.1016/j.neuroscience.2005.10.013

Gerardin, E., Siringu, A., Lehericy, S., Poline, J.B., Gaymard, B., Marsault, C., Agid, Y., & Bihan, D.L. (2000). Partially overlapping neural networks for real and imagined hand movements. *Cereb Cortex, 10*(1093-1104).

Gerloff, C., Bushara, K., Sailer, A., Wassermann, E. M., Chen, R., Matsuoka, T., . . . Hallett, M. (2006). Multimodal imaging of brain reorganization in motor areas of the contralesional hemisphere of well recovered patients after capsular stroke. *Brain, 129*(Pt 3), 791-808. doi: 10.1093/brain/awh713

Gevins, A., Brickett, P., Costales, B., Le, J., & Reutter, B. (1990). Beyond topographic mapping: Towards functional-anatomical imaging with 124-channel EEGs and 3D MRIs. *Brain Topography, 3*(1), 53-64.

Gevins, A., Smith, M.E., McEvoy, L., & Yu, D. . (1997). High-resolution EEG mapping of cortical activation related to working memory: Effects of task difficulty, type of processing and practice. . *Cereb Cortex, 7*, 374-385.

Goldman-Rakic, P. S. (1987). Circuitry of primate prefrontal cortex and regulation of behavior by representational memory. *Comprehensive Physiology*.

Grafton, S. T. (2010). The cognitive neuroscience of prehension: recent developments. *Experimental brain research. Experimentelle Hirnforschung. Experimentation cerebrale, 204*(4), 475-491. doi: 10.1007/s00221-010-2315-2

Grafton, S.T., & Arbib, M.A. (1996). Localization of grasp representations in humans by positron emission tomography (observation compared with imagination). *Experimental brain research. Experimentelle Hirnforschung. Experimentation cerebrale, 112*, 103-111.

Grech, R., Cassar, T., Muscat, J., Camilleri, K. P., Fabri, S. G., Zervakis, M., . . . Vanrumste, B. (2008). Review on solving the inverse problem in EEG source analysis. *J Neuroeng Rehabil, 5*, 25. doi: 10.1186/1743-0003-5-25

Grefkes, C., Eickhoff, S. B., Nowak, D. A., Dafotakis, M., & Fink, G. R. (2008). Dynamic intra- and interhemispheric interactions during unilateral and bilateral hand movements assessed with fMRI and DCM. *Neuroimage, 41*(4), 1382-1394. doi: 10.1016/j.neuroimage.2008.03.048

Grefkes, C., & Fink, G. R. (2011). Reorganization of cerebral networks after stroke: new insights from neuroimaging with connectivity approaches. *Brain, 134*(Pt 5), 1264-1276. doi: 10.1093/brain/awr033

Gross, J., Hamalainen, M., Timmermann, L., Schnitzler, A., & Salmelin, R. (2001). Dynamic imaging of coherent sources: studying neural interactions in the human brain. *PNAS, 98*(2), 694-699.

Guillot, Aymeric, Genevois, Cyril, Desliens, Simon, Saieb, Sylvie, & Rogowski, Isabelle. (2012). Motor imagery and 'placebo-racket effects' in tennis serve performance. *Psychology of Sport and Exercise, 13*(5), 533-540. doi: 10.1016/j.psychsport.2012.03.002

Hagströmer, Maria, Oja, Pekka, & Sjöström, Michael. (2007). The International Physical Activity Questionnaire (IPAQ): a study of concurrent and construct validity. *Public Health Nutrition, 9*(06). doi: 10.1079/phn2005898

Hall, J.C. (2002). Imagery practice and the development of surgical skills. *The American Journal of Surgery, 184*, 465-470.

Hanakawa, T., Immisch, I., Toma, K., Dimyan, M. A., Van Gelderen, P., & Hallett, M. (2003). Functional properties of brain areas associated with motor execution and imagery. *J Neurophysiol, 89*(2), 989-1002. doi: 10.1152/jn.00132.2002

Hetu, S., Gregoire, M., Saimpont, A., Coll, M. P., Eugene, F., Michon, P. E., & Jackson, P. L. (2013). The neural network of motor imagery: an ALE meta-analysis. *Neurosci Biobehav Rev, 37*(5), 930-949. doi: 10.1016/j.neubiorev.2013.03.017

Hikosaka, O., Sakai, K., Miyauchi, S., Takino, R., Sasaki, Y., & Putz, B. (1996). Activation of human presupplementary motor area in learning of sequential procedures: A function MRI study. *J Neurophysiol, 76*(1), 617-622.

Hipp, J. F., Engel, A. K., & Siegel, M. (2011). Oscillatory synchronization in large-scale cortical networks predicts perception. *Neuron, 69*(2), 387-396. doi: 10.1016/j.neuron.2010.12.027

Hodics, T., Cohen, L. G., & Cramer, S. C. (2006). Functional imaging of intervention effects in stroke motor rehabilitation. *Arch Phys Med Rehabil, 87*(12 Suppl 2), S36-42. doi: 10.1016/j.apmr.2006.09.005

Holmes, Paul S., & Collins, David J. (2001). The PETTLEP Approach to Motor Imagery: A Functional Equivalence Model for Sport Psychologists. *Journal of Applied Sport Psychology, 13*(1), 60-83. doi: 10.1080/10413200109339004

Hwang, H. J., Kim, K. H., Jung, Y. J., Kim, D. W., Lee, Y. H., & Im, C. H. (2011). An EEG-based real-time cortical functional connectivity imaging system. *Med Biol Eng Comput, 49*(9), 985-995. doi: 10.1007/s11517-011-0791-6

Ishai, A. (2002). Visual Imagery of Famous Faces: Effects of Memory and Attention Revealed by fMRI. *Neuroimage, 17*(4), 1729-1741. doi: 10.1006/nimg.2002.1330

Jackson, P. L., Doyon, J., Richards, C. L., & Malouin, F. (2004). The efficacy of combined physical and mental practice in the learning of a foot-sequence task after stroke: a case report. *Neurorehabil Neural Repair, 18*(2), 106-111. doi: 10.1177/0888439004265249

Jackson, Philip L., Lafleur, Martin F., Malouin, Francine, Richards, Carol L., & Doyon, Julien. (2003). Functional cerebral reorganization following motor sequence learning through mental practice with motor imagery. *Neuroimage, 20*(2), 1171-1180. doi: 10.1016/s1053-8119(03)00369-0

Jankowska, E., & Edgley, S. A. (2006). How can corticospinal tract neurons contribute to ipsilateral movements? A question with implications for recovery of motor functions. *Neuroscientist, 12*(1), 67-79. doi: 10.1177/1073858405283392

Jeannerod, M. (2001). Neural simulation of action: a unifying mechanism for motor cognition. *Neuroimage, 14*(1 Pt 2), S103-109. doi: 10.1006/nimg.2001.0832

Jeannerod, M., & Frak, V. (1999). Mental imaging of motor activity in humans. *Current Opinion in Neurobiology, 9*, 735-739.

Jiang, T., He, Y., Zang, Y., & Weng, X. (2004). Modulation of functional connectivity during the resting state and the motor task. *Hum Brain Mapp, 22*(1), 63-71. doi: 10.1002/hbm.20012

Kalberlah, C., Villringer, A., & Pleger, B. (2013). Dynamic causal modeling suggests serial processing of tactile vibratory stimuli in the human somatosensory cortex-- an fMRI study. *Neuroimage, 74*, 164-171. doi: 10.1016/j.neuroimage.2013.02.018

Karnath, H. O., & Perenin, M. T. (2005). Cortical control of visually guided reaching: evidence from patients with optic ataxia. *Cereb Cortex, 15*(10), 1561-1569. doi: 10.1093/cercor/bhi034

Kasess, C. H., Windischberger, C., Cunnington, R., Lanzenberger, R., Pezawas, L., & Moser, E. (2008). The suppressive influence of SMA on M1 in motor imagery revealed by fMRI and dynamic causal modeling. *Neuroimage, 40*(2), 828-837. doi: 10.1016/j.neuroimage.2007.11.040

Kiebel, S. J., Garrido, M. I., & Friston, K. J. (2007). Dynamic causal modelling of evoked responses: the role of intrinsic connections. *Neuroimage, 36*(2), 332-345. doi: 10.1016/j.neuroimage.2007.02.046

Kilner, J.M., Paulignan, Y., & Boussaoud, D. (2004). Functional connectivity during real vs imagined visuomotor tasks: an EEG study. *NeuroReport, 15*(4), 637-642. doi: 10.1097/01.wnr.0000116965.73984.83

Kimberley, T. J., Lewis, S. M., Auerbach, E. J., Dorsey, L. L., Lojovich, J. M., & Carey, J. R. (2004). Electrical stimulation driving functional improvements and cortical changes in subjects with stroke. *Experimental brain research. Experimentelle Hirnforschung. Experimentation cerebrale, 154*(4), 450-460. doi: 10.1007/s00221-003-1695-y

Knight, R.T., Staines, W.R., Swick, D., Chao, L.L. (1999). Prefrontal cortex regulates inhibition and excitation in distributed neural networks. *Acta Psycholagica, 101*, 159-178.

Knyazeva, M.G., & Innocenti, G.M. (2001). EEG coherence studies in the normal brain and after early-onset cortical pathologies. *Brain Res Rev, 36*, 119-128.

Konishi, S., Nakajima, K., Uchida, I., Kikyo, H., Kameyama, M., & Miyashita, Y. (1999). Common inhibitory mechinism in human inferior prefrontal cortex revealed by event-related function MRI. *Brain, 122*, 981-991.

Kopp, B., Kunkel, A., Muhlnickel, W., Villringer, K., Taub, E., & Flor, H. (1999). Plasticity in the motor system related to theapy-induced improvement after stroke. *NeurorReport, 10*, 807-810.

Kosslyn, S.M., Ganis,G., & Thompson, W.L. (2001). Neural Foundations of Imagery. *Nature Reviews Neuroscience, 2*, 635-642.

Lacourse, M. G., Orr, E. L., Cramer, S. C., & Cohen, M. J. (2005). Brain activation during execution and motor imagery of novel and skilled sequential hand movements. *Neuroimage, 27*(3), 505-519. doi: 10.1016/j.neuroimage.2005.04.025

Lehn, H., Steffenach, H. A., van Strien, N. M., Veltman, D. J., Witter, M. P., & Haberg, A. K. (2009). A specific role of the human hippocampus in recall of temporal sequences. *J Neurosci, 29*(11), 3475-3484. doi: 10.1523/JNEUROSCI.5370-08.2009

Leung, H. C., & Cai, W. (2007). Common and differential ventrolateral prefrontal activity during inhibition of hand and eye movements. *J Neurosci, 27*(37), 9893-9900. doi: 10.1523/JNEUROSCI.2837-07.2007

Li, X., Ong, S.H., Pan, Y & Ang, K.K. . (2013). *Connectivity pattern modeling of motor imagery EEG.* Paper presented at the 2013 IEEE Symposium on Computational Intelligence, Cognitive Algorithms, Mind, and Brain.

Liepert, J., Miltner, W.H.R., Bauder, H., Sommer, M., Dettmers, C., Taub, E., & Weiller, C. (1998). Motor cortex plasticity during constraint-induced movement therapy in stroke patients. *Neuroscience Letters, 250*, 5-8.

Liu, Y., Liang, M., Zhou, Y., He, Y., Hao, Y., Song, M., . . . Jiang, T. (2008). Disrupted small-world networks in schizophrenia. *Brain, 131*(Pt 4), 945-961. doi: 10.1093/brain/awn018

Longhorne, P., Coupar, F., & Pollock, A. (2009). Motor recovery after stroke: A systematic review. *Lancet Neurol, 8*, 741-454.

Lorey, B., Pilgramm, S., Bischoff, M., Stark, R., Vaitl, D., Kindermann, S., . . . Zentgraf, K. (2011). Activation of the parieto-premotor network is associated with vivid motor imagery--a parametric FMRI study. *PLoS One, 6*(5), e20368. doi: 10.1371/journal.pone.0020368

Lorey, B., Pilgramm, S., Walter, B., Stark, R., Munzert, J., & Zentgraf, K. (2010). Your mind's hand: motor imagery of pointing movements with different accuracy. *Neuroimage, 49*(4), 3239-3247. doi: 10.1016/j.neuroimage.2009.11.038

Lou, H. C., Luber, B., Crupain, M., Keenan, J. P., Nowak, M., Kjaer, T. W., . . . Lisanby, S. H. (2004). Parietal cortex and representation of the mental Self. *Proc Natl Acad Sci U S A, 101*(17), 6827-6832. doi: 10.1073/pnas.0400049101

Luft, A. R., Smith, G. V., Forrester, L., Whitall, J., Macko, R. F., Hauser, T. K., . . . Hanley, D. F. (2002). Comparing brain activation associated with isolated upper and lower limb movement across corresponding joints. *Hum Brain Mapp, 17*(2), 131-140. doi: 10.1002/hbm.10058

Malouin, Francine, Richards, Carol L., Jackson, Philip L., Lafleur, Martin F., Durand, Anne, & Doyon, Julien. (2007). The Kinesthetic and Visual Imagery Questionnaire (KVIQ) for Assessing Motor Imagery in Persons with Physical Disabilities: A Reliability and Construct Validity Study. *Journal of Neurologic Physical Therapy, 31*(1), 20-29. doi: 10.1097/01.npt.0000260567.24122.64

Matsumoto, Riki, Ikeda, Akio, Ohara, Shinji, Matsuhashi, Masao, Baba, Kouichi, Yamane, Fumitaka, . . . Shibasaki, Hiroshi. (2003). Motor-related functional subdivisions of human lateral premotor cortex: epicortical recording in conditional visuomotor task. *Clinical Neurophysiology, 114*(6), 1102-1115. doi: 10.1016/s1388-2457(03)00065-8

McIntosh, A. R., & Lobaugh, N. J. (2004). Partial least squares analysis of neuroimaging data: applications and advances. *Neuroimage, 23 Suppl 1*, S250-263. doi: 10.1016/j.neuroimage.2004.07.020

Mechelli, A., Price, C. J., Friston, K. J., & Ishai, A. (2004). Where bottom-up meets top-down: neuronal interactions during perception and imagery. *Cereb Cortex, 14*(11), 1256-1265. doi: 10.1093/cercor/bhh087

Miall, R. C., & Reckess, G. Z. (2002). The cerebellum and the timing of coordinated eye and hand tracking. *Brain Cogn, 48*(1), 212-226. doi: 10.1006/brcg.2001.1314

Michel, C. M., Murray, M. M., Lantz, G., Gonzalez, S., Spinelli, L., & Grave de Peralta, R. (2004). EEG source imaging. *Clin Neurophysiol, 115*(10), 2195-2222. doi: 10.1016/j.clinph.2004.06.001

Micheloyannis, S., Pachou, E., Stam, C. J., Breakspear, M., Bitsios, P., Vourkas, M., . . . Zervakis, M. (2006). Small-world networks and disturbed functional connectivity in schizophrenia. *Schizophr Res, 87*(1-3), 60-66. doi: 10.1016/j.schres.2006.06.028

Miller, E.K., & Cohen, J.D. (2001). An integrative theory of prefrontal cortex function. *Annu Rev Neurosci, 24*, 167-202.

Milner, A. D., & Goodale, M. A. (2008). Two visual systems re-viewed. *Neuropsychologia, 46*(3), 774-785. doi: 10.1016/j.neuropsychologia.2007.10.005

Miyashita, Y. (1993). Inferior temporal cortex: Where visual perception meets memory. *Annu Rev Neurosci, 16*, 245-263.

Muehllehner, G., & Karp, J. S. (2006). Positron emission tomography. *Phys Med Biol, 51*(13), R117-137. doi: 10.1088/0031-9155/51/13/R08

Mulder, T. (2007). Motor imagery and action observation: cognitive tools for rehabilitation. *J Neural Transm, 114*(10), 1265-1278. doi: 10.1007/s00702-007-0763-z

Munzert, J., Lorey, B., & Zentgraf, K. (2009). Cognitive motor processes: the role of motor imagery in the study of motor representations. *Brain Res Rev, 60*(2), 306-326. doi: 10.1016/j.brainresrev.2008.12.024

Murase, N., Duque, J., Mazzocchio, R., & Cohen, L.G. (2004). Influece of interhemispheric interactions on motor function in chronic stroke. *Ann Neurol, 55*, 400-409.

Murias, M., Webb, S. J., Greenson, J., & Dawson, G. (2007). Resting state cortical connectivity reflected in EEG coherence in individuals with autism. *Biol Psychiatry, 62*(3), 270-273. doi: 10.1016/j.biopsych.2006.11.012

Murphy, T. H., & Corbett, D. (2009). Plasticity during stroke recovery: from synapse to behaviour. *Nat Rev Neurosci, 10*(12), 861-872. doi: 10.1038/nrn2735

Narayanan, N. S., & Laubach, M. (2006). Top-down control of motor cortex ensembles by dorsomedial prefrontal cortex. *Neuron, 52*(5), 921-931. doi: 10.1016/j.neuron.2006.10.021

Nunez, P.L., Srnivasan, R., Westdorp, A.F., Wijesinfhe, R.S., Tucker, D.M., Silberstein, R.B., & Cadusch, P.J. (1997). EEG coherency I: statistics, reference electrode, volume conduction, Laplacians, cortical imaging, and interpretation at multiple scales. *Electroencephalography and clinical Neurophysiology, 103*, 499-515.

O'Craven, K.M., & Kanwisher, N. (2006). Mental imagery of faces and places activates corresponding stimulus-specific brain regions. *Journal of Cognitive Neuroscience, 12*(6), 1013-1023.

Ogawa, S., Menon, R.S., Kim, S.G., & Ugurbil, K. (1998). On the characteristics of functional magnetic resonance imaging of the brain. *Annu Rev Biophys Biomol Struct, 27*, 447-474.

Oishi, K., Kasai, T., & Maeshima, T. (2000). Autonomic response specificity during motor imagery. *J Physiol Anthropol, 19*(6), 255-261.

Oldfield, R. C. (1971). The assessment and analysis of handedness: the Edinburgh inventory. *Neuropsychologia*, *9*(1), 97-113.

Padoa-Schioppa, C., Li, C. S., & Bizzi, E. (2004). Neuronal activity in the supplementary motor area of monkeys adapting to a new dynamic environment. *J Neurophysiol, 91*(1), 449-473. doi: 10.1152/jn.00876.2002

Page, S. J., Murray, C., Hermann, V., & Levine, P. (2011). Retention of motor changes in chronic stroke survivors who were administered mental practice. *Arch Phys Med Rehabil, 92*(11), 1741-1745. doi: 10.1016/j.apmr.2011.06.009

Page, S.J., Levine, P., Sisto, S.A., & Johnson, M.V. (2001). Mental practice combined with physical practce for upper-limb motor deficit in subacute stroke *Physical Therapy, 81*, 1455-1462.

Page, S.J., Szaflarski, J.P., Eliassen, J.C., Pan, H., & Cramer, C. . (2009). Cortical plasticity following motor skill learning during mental practice in stroke. *Neurorehabil Neural Repair, 23*(4), 382-388.

Pascual-Marqui, R.D. (2002). Standardized low resolution brain electromagnetic tomography (sLORETA): technical details. *Methods & Findings in Experimental & Clinical Pharmacology, 24D*, 5-12.

Paus, T. (1996). Location and function of the human frontal eye-field: A selective review. *Neuropsychologia, 34*(6), 475-483.

Penny, W. D., Stephan, K. E., Mechelli, A., & Friston, K. J. (2004). Comparing dynamic causal models. *Neuroimage, 22*(3), 1157-1172. doi: 10.1016/j.neuroimage.2004.03.026

Pfurtscheller, G., Brunner, C., Schlogl, A., & Lopes da Silva, F. H. (2006). Mu rhythm (de)synchronization and EEG single-trial classification of different motor imagery tasks. *Neuroimage, 31*(1), 153-159. doi: 10.1016/j.neuroimage.2005.12.003

Ponten, S. C., Bartolomei, F., & Stam, C. J. (2007). Small-world networks and epilepsy: graph theoretical analysis of intracerebrally recorded mesial temporal lobe seizures. *Clin Neurophysiol, 118*(4), 918-927. doi: 10.1016/j.clinph.2006.12.002

Pool, E. M., Rehme, A. K., Fink, G. R., Eickhoff, S. B., & Grefkes, C. (2013). Network dynamics engaged in the modulation of motor behavior in healthy subjects. *Neuroimage, 82*, 68-76. doi: 10.1016/j.neuroimage.2013.05.123

Porro, C.A., Cettolo, V., Francescato, M.P., & Beraldi, P. (2000). Ipsilateral involvement of primary motor cortex during motor imagery. *European Journal of Neuroscience, 12*, 3059-3063.

Ridding, M.C., & Rothwell, J.C. (1997). Stimulus/response curves as a method of measuring motor cortical excitability in man. *Electroencephalography and clinical Neurophysiology, 105*, 340-344.

Ringner, M. (2008). What is principal component analysis? *Nature Biotechnology, 26*(3).

Rizzolatti, G., Fadiga, L., Gallese, V., & Fogassi, L. (1996). Premotor and the recognition of motor actions. *Cognitive Brain Research, 3*, 131-141.

Rizzolatti, G., Fogassi, L., & Gallese, V. (2002). Motor and cognitive functions of the ventral premotor cortex. *Current Opinion in Neurobiology, 12*, 149-154.

Roebroeck, A., Formisano, E., & Goebel, R. (2005). Mapping directed influence over the brain using Granger causality and fMRI. *Neuroimage, 25*(1), 230-242. doi: 10.1016/j.neuroimage.2004.11.017

Rogers, R. G. (2006). Mental practice and acquisition of motor skills: examples from sports training and surgical education. *Obstet Gynecol Clin North Am, 33*(2), 297-304, ix. doi: 10.1016/j.ogc.2006.02.004

Roth, M., Decety, J., Raybaudi, M., Massarelli, R., Delon-Martin, C., Segebarth, C., ... & Jeannerod, M. (1996). Possible involvement of primary motor cortex in mentally simulated movement: a functional magnetic resonance imaging study. *Neuroreport, 7*(7), 1280-1284.

Roure, R., Collet, C., Deschaumes-Molinaro, C., Delhomme, G., Dittmar, A., & Vernet-Maury, E. (1999). Imagery quality estimated by autonomic response is correlated to sporting performance enhancement. *Physiology & Behaviour, 66*(1), 63-72.

Rubinov, M., & Sporns, O. (2010). Complex network measures of brain connectivity: uses and interpretations. *Neuroimage, 52*(3), 1059-1069. doi: 10.1016/j.neuroimage.2009.10.003

Sack, A. T., Jacobs, C., De Martino, F., Staeren, N., Goebel, R., & Formisano, E. (2008). Dynamic premotor-to-parietal interactions during spatial imagery. *J Neurosci, 28*(34), 8417-8429. doi: 10.1523/JNEUROSCI.2656-08.2008

Sanz-Arigita, E. J., Schoonheim, M. M., Damoiseaux, J. S., Rombouts, S. A., Maris, E., Barkhof, F., . . . Stam, C. J. (2010). Loss of 'small-world' networks in Alzheimer's disease: graph analysis of FMRI resting-state functional connectivity. *PLoS One, 5*(11), e13788. doi: 10.1371/journal.pone.0013788

Schoffelen, J. M., & Gross, J. (2009). Source connectivity analysis with MEG and EEG. *Hum Brain Mapp, 30*(6), 1857-1865. doi: 10.1002/hbm.20745

Schwartz, E.L., esimone, R., Albright, T.D., & Gross, C.G. (1983). Shape recognition and inferior temporal neurons. . *Proc. Natl. Acad. Sci. USA, 80*(5776-5778).

Sharma, N., Baron, J. C., & Rowe, J. B. (2009). Motor imagery after stroke: relating outcome to motor network connectivity. *Ann Neurol, 66*(5), 604-616. doi: 10.1002/ana.21810

Sharma, N., Pomeroy, V. M., & Baron, J. C. (2006). Motor imagery: a backdoor to the motor system after stroke? *Stroke, 37*(7), 1941-1952. doi: 10.1161/01.STR.0000226902.43357.fc

Shelton, T.O., & Mahoney, M.J. (1978). The content and effect of "psyching-up" strategies in weight lifters. *Cognitive Therapy and Research, 2*(3), 275-284.

Solodkin, A., Hlustik, P., Chen, E. E., & Small, S. L. (2004). Fine modulation in network activation during motor execution and motor imagery. *Cereb Cortex, 14*(11), 1246-1255. doi: 10.1093/cercor/bhh086

Sporns, O., Tononi, G., & Kotter, R. (2005). The human connectome: A structural description of the human brain. *PLoS Comput Biol, 1*(4), e42. doi: 10.1371/journal.pcbi.0010042

Stam, C. J. (2004). Functional connectivity patterns of human magnetoencephalographic recordings: a 'small-world' network? *Neuroscience Letters, 355*(1-2), 25-28. doi: 10.1016/j.neulet.2003.10.063

Stam, C. J., de Haan, W., Daffertshofer, A., Jones, B. F., Manshanden, I., van Cappellen van Walsum, A. M., . . . Scheltens, P. (2009). Graph theoretical analysis of magnetoencephalographic functional connectivity in Alzheimer's disease. *Brain, 132*(Pt 1), 213-224. doi: 10.1093/brain/awn262

Stinear, C. M., Byblow, W. D., Steyvers, M., Levin, O., & Swinnen, S. P. (2006). Kinesthetic, but not visual, motor imagery modulates corticomotor excitability. *Experimental brain research. Experimentelle Hirnforschung. Experimentation cerebrale, 168*(1-2), 157-164. doi: 10.1007/s00221-005-0078-y

Sudlow, C. L. M., & Warlow, C. P. (1997). Comparable Studies of the Incidence of Stroke and its pathological types Results from an international collaboration. *Stroke*, *28*(3), 491-499.

Sun, F. T., Miller, L. M., Rao, A. A., & D'Esposito, M. (2007). Functional connectivity of cortical networks involved in bimanual motor sequence learning. *Cereb Cortex, 17*(5), 1227-1234. doi: 10.1093/cercor/bhl033

Szava, S., Biscay, R., Galan, L., Bosch, J., Clark, I., & Jimenex, J.C. (1994). High resolution quanitative EEG analysis. *Brain Topography, 6*(3), 211-219.

Tanji, J., & Shima, K. (1994). Role for supplementary motor area cells in planning several movements aheas. *Nature, 371*, 413-416.

Thakor, N. V., & Tong, S. (2004). Advances in quantitative electroencephalogram analysis methods. *Annu Rev Biomed Eng, 6*, 453-495. doi: 10.1146/annurev.bioeng.5.040202.121601

Toni, I., Ramnani, N., Josephs, O., Ashburner, J., & Passingham, R. E. (2001). Learning arbitrary visuomotor associations: temporal dynamic of brain activity. *Neuroimage, 14*(5), 1048-1057. doi: 10.1006/nimg.2001.0894

Tonini, G., Sporns, O., & Edelman, G.M. . (1994). A measure for brain complexity: relating functional segregation and integration in the nervous system. *Proc. Natl. Acad. Sci. USA, 91*, 5033-5037.

Valencia, M., Martinerie, J., Dupont, S., & Chavez, M. (2008). Dynamic small-world behavior in functional brain networks unveiled by an event-related networks approach. *Physical Review E, 77*(5). doi: 10.1103/PhysRevE.77.050905

Vogeley, K., May, M., Falkai, P., Zilles, K., & Fink, G.R. (2004). Neural correlates of
first-person perspective as one constituent of human self-consiousness. *Journal of
Cognitive Neuroscience, 15*(5), 817-827.

Wagner, M., Fuchs, M., & Kastner, J. (2004). Evaluation of sLORETA in the presence of
noise and multiple sources. *Brain Topography, 16*(4), 277-280.

Wang, L., Yu, C., Chen, H., Qin, W., He, Y., Fan, F., . . . Zhu, C. (2010). Dynamic
functional reorganization of the motor execution network after stroke. *Brain,
133*(Pt 4), 1224-1238. doi: 10.1093/brain/awq043

Wang, L., Zhu, C., He, Y., Zang, Y., Cao, Q., Zhang, H., . . . Wang, Y. (2009). Altered
small-world brain functional networks in children with attention-
deficit/hyperactivity disorder. *Hum Brain Mapp, 30*(2), 638-649. doi:
10.1002/hbm.20530

Ward, N.S., Brown, M.M., & Frackowiak, R.S.J. (2003). Neural correlates of motor
recovery after stroke: A longitudinal fMRI study. *Brain, 126*, 2476-2496.

Wassermann, E. M., McShane, L. M., Hallett, M., & Cohen, L. G. (1992). Noninvasive
mapping of muscle representations in human motor cortex.
*Electroencephalography and Clinical Neurophysiology/Evoked Potentials
Section*, *85*(1), 1-8.

Watts, D.J., & Strogatz, S.H. (1998). Collective dynamics of 'small-world' networks.
Nature, 393, 440-442.

Wolbers, T., Wiener, J. M., Mallot, H. A., & Buchel, C. (2007). Differential recruitment
of the hippocampus, medial prefrontal cortex, and the human motion complex
during path integration in humans. *J Neurosci, 27*(35), 9408-9416. doi:
10.1523/JNEUROSCI.2146-07.2007

Woolsey CN, Erickson TC, Gilson WE. 1979. Localization in somatic
sensory and motor areas of human cerebral cortex as determined
by direct recording of evoked potentials and electrical stimulation.
J Neurosurg 51:476–506.

Yan, J., Sun, J., Guo, X., Jin, Z., Li, Y., Li, Z., & Tong, S. (2013). Motor imagery cognitive network after left ischemic stroke: study of the patients during mental rotation task. *PLoS One, 8*(10), 1-11. doi: 10.1371/journal.pone.0077325.t001

Yuan, H., Liu, T., Szarkowski, R., Rios, C., Ashe, J., & He, B. (2010). Negative covariation between task-related responses in alpha/beta-band activity and BOLD in human sensorimotor cortex: an EEG and fMRI study of motor imagery and movements. *Neuroimage, 49*(3), 2596-2606. doi: 10.1016/j.neuroimage.2009.10.028

Zeki, S., Watson, J.D.G., Lueck, C.J., Friston, K.J., Kennard, C., & Frackowiak, R.S.J. (1991). A direct demonstration of functional specialization inhuman visual cortex. *The Journal of Neuroscience, 11*(3), 641-649.